Chromatographic Separation and Stability Analysis of Small Interfering RNA and Lipid Vehicles Using Ion-Pair Reversed Phase Liquid Chromatography

A Thesis

Submitted to the Faculty

of

Drexel University

by

Li Li

In partial fulfillment of the

requirements for the degree

of

Doctor of Philosophy

December 2017

Dedications

This thesis is dedicated to my loving parents, Lanyin Cao and Yisong Li, for their unconditional love, support and encouragement.

Acknowledgements

I would like to thank my advisor Prof. Joe Foley for an incredible support of my study and research at Drexel. I am grateful for his patience, motivation, and immense knowledge in separation science. His encouragement and guidance helped me greatly throughout the research and the writing of this thesis.

I would also like to thank my research co-advisor, Dr. Roy Helmy, for his scientific guidance and for creating a supportive environment at Merck so I can focus and complete my Ph.D. study. I am very grateful that Dr. Helmy has taken time from his busy schedule to be my co-advisor, and without his help and encouragement, this would not have been possible.

I would like to thank my research committee members: Dr. Frank Ji (chair), Dr. Lynn Penn, Dr. Dan King, Dr. Peter Wade, and Dr. Ezra Wood. Special thanks to Dr. Mark Schure from the University of Delaware for serving in my research committee. Thank you all for your time and effort reviewing my work and thesis and for providing valuable comments. I also want to express my sincere appreciation to the faculty and staff of Drexel University Chemistry Department and my fellow graduate students for their support during my time at Drexel. Your friendship made this journey a truly memorable chapter of my life.

I want to express my most profound gratitude to my employer Merck for the financial support and lab resources during my study. I also want to thank my current and past mentors: Dr. Chris Welch, Dr. Tony Leone, Dr. Yun Mao, Dr. Mark Mowery and Dr. Peter Wuelfing, who have supported me to pursue my dream.

Finally, I want to thank my parents and siblings for always being there for me when I need the help to navigate through a challenging schedule. Special thanks to my husband Xiaoping and daughter Yuyan. Words cannot express how grateful I am to you all for the sacrifices that you've made on my behalf. Your unconditional love and support have been the constant driving force during this incredible journey.

Table of Contents

List of Tables

List of Schemes

List of Figures

List of Symbols

α selectivity
β ratio of V_m to V_s
γ tortuosity factor
γ_m tortuosity factor in the mobile phase
γ_s tortuosity factor in the stationary phase
ΔG Gibbs free energy
ΔH change in enthalpy
ΔS change in entropy
λ constant that is related to column packing structure
μm micrometer
σ standard deviation
σ^2 variance
ϕ volume fraction of organic solvent B

A eddy diffusion constant
Å angstrom
a_m activity of the solute in the mobile phase
a_s activity of the solute in the stationary phase
b gradient steepness
B longitudinal diffusion constant
C mobile phase plus stationary phase mass transfer
Cu^{2+} divalent copper ion
°C degree Celsius
dc column inner diameter
Dm solute diffusion coefficient in mobile phase
Ds solute diffusion coefficient in stationary phase
dp stationary phase particle diameter
F flow rate
Fe^{2+} iron divalent ion
H column plate height
H_2O_2 hydrogen peroxide
i.d. internal diameter
k retention factor
K the distribution constant for solute's inherent affinity for the stationary phase relative to the mobile phase
K_D distribution coefficient
k_w extrapolated value of retention factor (*k*) for 100% water mobile phase
L column length
log logarithm
M molarity
mAU milli-absorbance unit
mL milliliter

mm millimeter
mM millimolar
Mg^{2+} magnesium ion
MW molecular weight
N number of theoretical plates, or column efficiency
Na^{+} sodium ion
nL nanoliter
Nm number of moles of solute in mobile phase
Ns number of moles of solute in stationary phase
pA picoamp
pH -log of the hydrogen ion activity
pKa -log of the acid dissociation constant
R gas constant
Rs resolution
S a constant for a given solute
T temperature
t_G gradient time
tm the time solute spends in the mobile phase
t_R analyte retention time
μ mobile phase velocity
V_0 void volume
V_i volume of the pore system
V_m volume of the mobile phase
V_R retention volume
Vs volume of the stationary phase
w peak width

List of Abbreviations

ACN	acetonitrile
ACVA	4,4′-Azobis(4-cyanovaleric acid)
AD	adamantine
AGO 2	argonaute 2
AIBN	azobisisobutyronitrile
AMD	age-related macular degeneration
ApoB	apolipoprotein B
ASGPr	asialoglycoprotein receptor
BEH	ethylene bridged hybrid
BSO	buthionine sulfoximine
CAD	charged aerosol detection
CBA-DAH-R	cystaminebisacrylamide-diaminohexane
CD	cyclodextrin
CDP	cyclodextrin polymer
CE	capillary electrophoresis
CGE	capillary gel electrophoresis
CSH	charged surface hybrid
CZE	capillary zone electrophoresis
DAD	diode array detector
DAAA	diamylammonium acetate
DBAA	dibutylammonium acetate
DDPC	1,2-dipalmitoleoyl-sn-glycero-3-phosphocholine
DEAA	diethylamine
Dicer	also known as endoribonuclease Dicer or helicase with RNase motif
DLinDAP	1,2-Dilinoleoyl-3- dimethylaminopropane
DLinDMA	1,2-Dilinoleyloxy-3-dimethylaminopropane
DLin-K-DMA	2,2-Dilinoleyl-4-dimethylaminomethyl-[1,3]-dioxolane
DLin-KC2-DMA	2,2-Dilinoleyl-4-(2-dimethylaminoethyl)-[1,3]-dioxolane
DLin-KC3-DMA	2,2-Dilinoleyl-4-(3-dimethylaminopropyl)-[1,3]-dioxolane
DLin-KC4-DMA	2,2-Dilinoleyl-4-(4-dimethylaminobutyl)-[1,3]-dioxolane
DLPC	1,2-dilauroyl-sn-glycero-3-phosphocholine
DMMan-Mel	dimethylmaleic anhydride- melittin
DMPC	dimyristoleoyl phosphatidylcholine
DNA	deoxyribonucleic acid
DOPC	1,2-dioleoyl-*sn*-glycero-3-phosphocholine
DOTAP	1,2-dioleoyl-3-trimethylammonium propane
DPAA	dipropylammonium acetate
DPPC	dipalmitoylphosphatidylcholine
ds	double-stranded
DSC	differential scanning calorimetry

DSPC	1,2-distearoyl-sn-glycero-3-phosphatidylcholine
DTT	dithiothreitol
EAA	ethylamine
ELSD	evaporative light scattering detector
EOF	electroosmotic flow
GC	gas chromatography
Gen-Pak FAX	A type of anion-exchange column from Waters
GLcN	D-glucosamine
GLcNAc (or NAG)	N-acetyl-D-glucosamine
HCl	hydrochloric acid
HCV	hepatitis C virus
HEMA IEC BIO	A type of anion-exchange column from Alltech
HeLa	A type of tumor cell line
HFIP	hexafluoroisopropanol
HILIC	hydrophilic interaction liquid chromatography
HIV	human immunodeficiency virus
HPLC	high performance liquid chromatography
HSS	high strength silica
IEC	ion-exchange chromatography
IPA	isopropanol alcohol
IP-RPLC	ion-pair reversed phase liquid chromatography
IP-RP-HPLC	ion-pair reversed phase high performance liquid chromatography
IP-RP-UHPLC	ion-pair reversed phase ultra-high performance liquid chromatography
IV	intravenous
LC-ESI-MS	liquid chromatography-electrospray ionization-mass spectrometry
LNP	lipid nanoparticle
LOD	limit of detection
LOQ	limit of quantification
MeOH	methanol
MicroCal	microcalorimetry
MTT	3-(4,5-dimethylthiazol-2-yl)-2,5-diphenyltetrazolium bromide
mRNA	messenger ribonucleic acid
MS	mass spectrometry
MSD	Merck Sharp&Dohme
NAG	N-acetylglucosamine
NaOH	sodium hydroxide
NMR	nuclear magnetic resonance
NPLC	normal phase liquid chromatography
p53	protein 53 (a type of tumor protein)
PAGE	polyacrylamide gel electrophoresis
PARP	poly(adenosine diphosphate -ribose) polymerase
PBAVE	poly(butyl amino vinyl ether)

PC3	cancer 3 (a type of cell line)
PE	poly(ethylene)
PEG	polyethylene glycol
PEI	polyethylenimine
PEO	poly(ethylene oxide)
PI	phosphatidylinositol
PLK1	polo-like kinase 1
PLL	polyLysine
PS	monothiophosphate
PS2	dithiophosphate
PVP	polyvinylpyrrolidone
QPI	Quark Pharmaceuticals, Inc.
RI	reflective index
RP	reverse phase
RPLC	reverse-phase liquid chromatography
RISC	RNA-induced silencing complex
RNA	ribonucleic acid
RNAi	ribonucleic acid interference
RPLC	reversed phase liquid chromatography
RRM2	ribonucleoside-diphosphate reductase subunit M2
SAX	strong anion exchanger
SCX	strong cation exchanger
SEC	size exclusion chromatography
siRNA	small interfering ribonucleic acid
SNALP	stable nucleic acid lipid particle
TEA	triethylamine
TEAA	triethylammonium acetate
TEA-HFIP	triethylamine-hexafluoroisopropanol
TF	transferrin
THF	tetrahydrofuran
TKM	Tekmira (name of a biotech company)
TLC	thin layer chromatography
TMAA	tetramethylammonium acetate
TPP	thiamine pyrophosphate
TTR	transthyretin
UHPLC	ultra-high performance liquid chromatography
UV	ultraviolet
VEGF	vascular endothelial growth factor
WAX	weak anion exchanger
WCX	weak cation exchanger

Abstract

Chromatographic Separation and Stability Analysis of Small Interfering RNA and Lipid Vehicles using Ion-Pair Reversed Phase Liquid Chromatography
Li Li
Joe P. Foley, PhD
Roy Helmy, PhD

Chromatographic methods were developed capable of separating and quantitating siRNA, lipids, and their potential breakdown products due to oxidation or hydrolysis. Such methods are essential to developing lipid nanoparticles (LNPs) as a formulation delivery system for siRNAs. Separation of siRNAs was achieved using ion-pair reversed-phase liquid chromatography. Part 1 of the thesis describes the development of an ion-pair reversed-phase HPLC method for the separation of closely related stereoisomers of a chemically modified siRNA duplex. A systematic evaluation of key chromatographic parameters showed that a BEH C18 column with sub-2 μm particle size, coupled with the use of triethylammonium acetate as the ion-pair reagent and acetonitrile as the strong solvent of the hydro-organic mobile phase, achieved baseline resolution of siRNA stereoisomers and their desulfurization products. A high column temperature, creating a denaturing condition for siRNA, is critical to the separation of stereoisomers. An aprotic organic modifier, such as acetonitrile, can effectively disrupt the hydrogen bonding interaction between the duplex and enable the separation of stereoisomers by promoting hydrophobic interactions between the C18 stationary phase and the stereoisomers.

Part 2 of the thesis expands the utility of the ion-pair reversed-phase liquid chromatography to include a simultaneous separation of the main lipid components of an

LNP system. Ion-pair reversed-phase separation conditions were developed that can reduce the retention gap between siRNAs and lipids that have significant differences in their physical and chemical properties. Studies showed that a BEH phenyl column could significantly retain siRNA due to a combination of both hydrophobic and π - π interactions. In contrast, the lipids experienced a reduced retention with the phenyl column, a key advantage attributed to the presence of a short alkyl chain component in the stationary phase compared to octyl- or octadecyl-derivatized silica. While the ion-pair reagents had virtually no impact on the separation of the lipids, the retention times of the siRNAs showed a quantitative correlation with the structure of the ion-pair reagents in the mobile phase. The chromatographic separation conditions with a phenyl stationary phase, particularly with dibutylammonium acetate as the ion-pair reagent, markedly reduced the retention gap between the siRNAs and the lipids, achieving a baseline resolution of a complex matrix containing five siRNAs and six lipids in a 20-minute gradient elution method.

Finally, the ion-pair reversed-phase method was applied to the degradation products of a model siRNA system. Stress testing showed that the model siRNA developed minimal hydrolysis products at neutral pH. This indicated the importance of chemical modification at the 2'-position in the ribose unit of siRNA molecules. In contrast, the siRNA was prone to oxidation by hydrogen peroxide, with or without trace levels of a transition metal, and to oxidation by a radical initiator. Desulfurization and phosphodiester strand scission were the likely main degradation pathways contributing to the observed oxidative reactivity.

Chapter 1: Introduction to HPLC

1.1 A brief history of HPLC

Chromatography refers to a set of separation techniques where the components of a mixture are separated due to their different distribution coefficients between two immiscible phases. The term "chromatography" was first introduced in 1905 by a Russian botanist, Mikhail Tswett. He reported the separation of different plant pigments with glass columns packed with calcium carbonate. [1] Although Tswett is often considered as the father of modern chromatography, the concept of separating mixed components based on adsorption and desorption between two phases predated Tswett's discovery. A survey of earlier literature by Herbert Weil and Trevor Williams [2] showed that, as early as 1897, D.T. Day had demonstrated the fractionation of hydrocarbon in petroleum based on a differential adsorption process in packed columns. [3]

After Tswett's initial discovery of chromatography, his work faded into obscurity until early in 1940 when Martin and Synge introduced partition chromatography. Martin and Synge also developed the theory pertaining to liquid chromatography and correctly predicted that separation efficiency could significantly improve with small packing particles under high pressure. [4,5] Martin and Synge's seminal work ushered in the dawn of modern liquid chromatography, and the remarkable contributions earned them the Nobel Prize in Chemistry in 1952.

Following the ground-breaking work by Martin and Synge, Calvin Giddings [6] and Josef Huber [7] further proved in theory that LC could achieve high efficiency with columns packed with particles of less than 150 μm, when operated at high pressure to increase mobile phase linear velocity. In the late 1960s, significant progress was made to

translate the theoretical potential of LC into practical applications. Jack Kirkland and Csaba Horvath applied pellicular stationary phase (with 40 μm in diameter) for liquid chromatography, [8,9] achieving comparable efficiency as gas chromatography. This work marked the true beginning of modern liquid chromatography. The first commercial HPLC system was introduced in 1968 by Waters [10], and the technique emerged as an essential analytical tool around 1972 when columns packed with less than < 30 μm became available. [11,12] The speed and efficiency of HPLC system continued to improve with the introduction of even smaller particles,[13] which ultimately led to the development of UHPLC system. [14]

As researchers explored packing materials with very small particles, they began to encounter the pressure-induced heat formation in the mobile phase, causing additional band broadening, which imposed an upper limit on the particle size and pressure for HPLC separation. [15,16] This technical issue was resolved by Jorgensen, who applied capillary HPLC column for ultra-pressure separation, where the heat transfer is more efficient than in the conventional column. [17] Ultra-high performance separation was finally achieved with the introduction of sub-2 μm particles in columns with a narrow outer diameter, coupled with an improvement in HPLC hardware to minimize extra-column band broadening.[18] Extra-column band broadening is all the processes outside the column that increase the width of chromatographic peaks. The first commercial UHPLC system was introduced in 2004, which marked another important milestone since the initial discovery of "chromatography" almost a century ago. [19]

1.2 HPLC theory and principles

1.2.1 Key factors impacting chromatographic resolution

The purpose of a separation is to resolve some or all of the components from each other in a matrix. The separation of two bands can be modulated by changing the experimental conditions. The resolution (Rs) is often used to describe the extent of the separation between two species 1 and 2, and it is related to three chromatographic parameters, the retention factor (k), selectivity (α) and plate number (N). To establish the relationship between Rs and k, α and N, we first define the resolution of two solute zones, which is expressed in Eqn. (1.1)

$$\mathrm{Rs} = \frac{2(t_{R2} - t_{R1})}{(w_1 + w_2)} \tag{1.1}$$

where t_R is the retention time and w is the width of each peak. The retention time (t_R) is the amount of time a compound spends on the column after it has been injected. The peak width is associated with the extent of a solute-zone, which is also related to the plate number as defined in (1.2). σ is the standard deviation of the solute zone and can be measured from the peak width at baseline ($w = 4\sigma$), assuming a Gaussian distribution

$$\mathrm{N} = \frac{t_{R2}}{\sigma^2} \tag{1.2}$$

The retention factor measures the amount of time the solute spends in the stationary phase compared with time spent in the mobile phase and is expressed by Eqn. (1.3), where t_0 is the retention time of non-retaining species. The retention factor can also be expressed as a mass-based equilibrium constant and can thus be seen to be independent of

column length, radius and flow rate (Eqn. 1.4). N_S and N_M refer to the number of moles of the solute in the stationary phase and mobile phase, respectively.

$$k = \frac{t_R - t_0}{t_0} \tag{1.3}$$

$$k = \frac{N_S}{N_M} \tag{1.4}$$

The selectivity (α) is the ratio of the retention factors of two solutes, as defined in Eqn. (1.5). The selectivity or relative spacing of the two analytes can be varied by changing the stationary and mobile phases.

$$\alpha = \frac{k_2}{k_1} \tag{1.5}$$

Lastly, the resolution (Rs) can be expressed in Eqn. (1.6) [20] with N, k and α as key variables.

$$Rs = \frac{N^{1/2}}{4}(\alpha\text{-}1)\left(\frac{k_1}{1+k_{avg}}\right) \tag{1.6}$$

The equation shows that separation resolution is impacted by plate number (N), the selectivity factor and retention factor. Partial derivatives of the resolution equation further revealed that the impact of the three fundamental variables on resolution decreases in the following order: selectivity > retention factor > plate number. This order suggests that for any separation method development, one should begin with the selection of column type and mobile phase composition, which has a direct impact on selectivity. The next step involves the optimization of the retention factor with adjustment of the mobile phase composition as a function of time. Lastly, the plate number can be improved by optimizing the flow rate, particle size, and the column dimensions.

1.2.2 Fundamental principles of band broadening and zone separation

Equation (1.6) [20] shows the relationship between resolution (Rs) and key chromatographic parameters, thus providing a general rule of thumb for HPLC method development. To systematically improve separation speed and efficiency, we need to understand band broadening and zone separation at a molecular level. A well-established theory exists that relates band broadening and zone separation to fundamental parameters, such as molecular diffusion coefficient, the partition coefficients of the analytes between the two phases, and the physical properties of the packing material in the column (particle size, porosity, etc.).

1.2.2.1 Column contributions to band dispersions and Van Deemter equation

As an analyte travels through a packed column, multiple sources contributed to band broadening, including eddying (A), i.e., a bulk diffusion by mean of multiple paths taken by the solute, longitudinal dispersion (B) and resistance to mass transfer (C) in both the mobile and stationary phases. [6,21,22] For a uniformly packed column, the variance due to multiple paths taken by the solute is described as in (1.7).

$$\sigma_A^2 = 2\lambda d_p L \qquad (1.7)$$

where λ is a constant (0.5 to 1) that is related to the packing structure, d_p is particle diameter, and L is the column length. Large and irregular particles will cause significant band broadening.

The random motion of molecules along the separation axis in the mobile and stationary phases also leads to band broadening; this is called longitudinal diffusion. The variance due to diffusion in the mobile phase and stationary phases is calculated as follows:

$$\sigma_{B}{}^{2}{}_{M} = \frac{2\gamma_M D_M L}{u} \quad (1.8)$$

$$\sigma_{B}{}^{2}{}_{S} = \frac{2\gamma_S D_S k L}{u} \quad (1.9)$$

where D_M and D_S are the bulk diffusivity coefficients in the mobile phase and stationary phase, respectively. γ_M and γ_S stand for the tortuosity factors in the mobile and stationary phases, respectively. u is the linear velocity of the mobile phase. The equation (1.9) suggests that the variance contribution to band broadening in stationary phase increases with retention factor as the analyte will spend more time diffusing in the column. This explains why late eluting peaks tend to be broader than the earlier eluters.

As an analyte migrates through a packed column in a stream of the mobile phase, the solute tends to remain in its transport path due to inertial forces, or its resistance to mass transfer. The flow pattern in a packed column invariably is parabolic, meaning flow in the center of the channel tends to move faster than flow closer to the channel boundary due to reduced frictional force as the boundary is approaching. The resistance to mass transfer, coupled with a differential flow rate across the column radius, leads to zone broadening during separation. For laminar flow in a packed column, the variance contribution to band broadening in mobile phase can be described as:

$$\sigma_{c}{}^{2} = \frac{k^2 d_p{}^2 L u}{100(1+k^2)D_M} \quad (1.10)$$

For a given linear velocity, broadening due to resistance to mass transfer is more significant for liquid chromatography than in gas chromatography since the D term is in the denominator and it is higher in the gas phase than in the liquid phase. Typically, however, the reduced linear velocities, i.e., the linear velocities relative to the

column/particle dimensions are similar, and in those instances the relative contribution to resistance to mass transfer to overall band broadening in GC and LC are comparable. The total variance contribution to band broadening that occurs within the column is

$$\sigma_{total}^2 = \sigma_A^2 + \sigma_B^2{}_M + \sigma_B^2{}_S + \sigma_C^2{}_S \quad (1.11)$$

Equation (1.12) can be further simplified based on equations (1.2) and (1.7) to (1.11).

$$H = A + B/u + Cu \quad (1.12)$$

where H is the plate height, the column length divided by theoretical plate number (N). The A term represents the eddy diffusion, and B and C terms are related to longitudinal diffusion and resistance to mass transfer, respectively, in both mobile phase and stationary phases.

Equation (1.12), also called the van Deemter equation, shows the change of plate height as a function of the linear velocity of the mobile phase. For a given mobile phase composition and stationary phase, the resolving power is at maximum for a column at an optimum linear velocity

$$u_{opt} = (B/C)^{1/2} \quad (1.13)$$

The van Deemter equation also highlights a significant impact of particle size on plate height. As the particle size decreases, the minimum plate height occurs at a higher velocity. This sets up the theoretical foundation for UHPLC technique where the resolving power is improved with sub-2 μm particles under high pressure.

1.2.2.2 Fundamental principles of solute-zone separation

In addition to the influence of theoretical plate number (N), retention factor and selectivity also impact the resolution (R_s). The thermodynamic information provides a mechanistic framework for the molecular interaction between the solute and the mobile

phase and stationary phase, which are related intrinsically to retention factor and selectivity. In chromatography, the free energy associated with partitioning of the solute between the mobile phase and the stationary phase is related to molar enthalpy (H) and entropy (S). The enthalpy is attributed to the molecular interaction between the solute and the two phases, and entropy is related to the disorder of the system. The free energy is also related to the thermodynamic equilibrium constant for the solute, which is partitioning between the two phases, as shown in eqn. (1.14). [23]

$$\text{Ln K} = \frac{-\Delta G}{RT} = \frac{-\Delta H}{RT} + \frac{\Delta S}{R} \qquad (1.14)$$

The equilibrium constant K is the ratio of solute activity in the mobile phase and stationary phase, which is related to the retention factor via eqn. (1.15).

$$\text{k} = \frac{K}{\beta} = \left(\frac{a_S}{a_M}\right)\left(\frac{V_S}{V_M}\right) \qquad (1.15)$$

where a_S and a_M are the respective activities of the solute in the stationary phase and mobile phase, and β is the ratio of the volumes of the mobile phase (V_m) and the stationary phase (V_s). Eqn. (1.14) can be written as eqn. (1.16) which relates the retention factor to the thermodynamic parameter of the partitioning process.

$$\text{Ln k} = \frac{-\Delta H}{RT} + \frac{\Delta S}{R} - \ln\beta \qquad (1.16)$$

1.3 HPLC methodology

There are several separation techniques within the framework of HPLC. Most of the methods explored the fundamental physical and chemical differences between the molecules.

1.3.1 Normal-phase liquid chromatography

In normal phase liquid chromatography (NPLC), the stationary phase is more polar than the mobile phase. The stationary phase can be unmodified polar inorganic adsorbents, such as silica, alumina, or zirconia, or a bonded phase on a silica support. The mobile phase is a mixture of non-polar organic solvents, like hexane, heptane plus isopropanol alcohol (IPA), without water. The main retention mechanism is an adsorption/desorption process, where the adsorption sites are the silanol groups on unmodified silica or polar groups, such as cyano, amino, or diol for bonded silica. The retention behavior is governed by the Soczewinski equation (1.13) [24]

$$\text{Log } k = C - N \log X_B \qquad (1.13)$$

where C and N are constants for a given analyte and X_B is mole fraction of B solvent in the mobile phase. N also represents the number of polar groups in the analyte. Regardless of the mobile phase or stationary selected, the retention time of normal phase separation always increases as the mobile phase polarity decreases. For a given separation condition, the retention time increases as the polarity of the analytes increases.

Although NPLC is less popular than reversed-phase liquid chromatography (RPLC), it finds important applications in separating very polar analytes, such as carbohydrates, where retention and resolution on a reversed-phase column are challenging to achieve. Normal phase separation often achieves superior separation of positional isomers and diastereomers.[25,26,27,28]

1.3.2 Reversed-phase liquid chromatography

Majority of the chromatography separation relies on the reversed-phase methodology, making this technique by far the most important of all. Reverse-phase

liquid chromatography (RPLC) is often the first choice for normal samples. The separation technique applies to a broad range of sample matrices, including polar and non-polar small molecules, achiral isomers, chiral isomers, and biomolecules. The mobile phase, consisting of a mixture of water and organic solvents of different polarity, is more polar than the stationary phase, typically a silica support modified with C8 or C18. The separation of a mixture of solutes is based on the partition mechanism.[29, 30, 31] As the solutes migrate through the reversed-phase column, the non-polar samples will preferentially partition into the hydrophobic stationary phase as opposed to the mobile phase; therefore the non-polar solutes are retained more strongly on the column. For a given mobile phase condition, the analytes will be separated based on their hydrophobicity.

Key experimental factors impacting RPLC retention include the mobile phase, the stationary phase, and the temperature. In terms of mobile phase, solvent strength profoundly influences the retention of the analyte. At a first approximation, log k has a linear relationship with the percentage of mobile phase B (the strong solvent), as shown in Eqn. (1.14). [32]

$$\log k = \log k_W - S\phi_B \qquad (1.14)$$

Where k_w is a theoretical value of k when the mobile phase is 100% water, S is a constant and ϕ_B is the volume fraction of the mobile phase B. Common organic solvents used for RPLC separation include methanol (MeOH), acetonitrile (ACN), tetrahydrofuran (THF) and 2-propanol. These solvents are all somewhat polar. The solvent strength (or hydrophobicity) increases in the order of MeOH < ACN < THF < 2-propanol, with 2-propanol being the most hydrophobic. [33,34] RPLC column is another variable controlling

the retention of the analytes. Most of RPLC separations use silica-based columns to which a hydrocarbon is bonded. The chemistry and concentration of the bonded phase, as well as the surface area all impact the retention characteristics of the analytes. For non-polar and non-ionic species, the retention increases in the following order for bonded-phase silica column: Cyano < C4 < C8 < C18. [35,36]

1.3.3 Ion-pair chromatography

Ion-pair chromatography refers to a separation technique that uses organic or inorganic ionic additives, introduced into the mobile phase to achieve adequate retention of charged analytes (Figure 1.1). As the mobile phase runs through the column, the concentration of the ion-pair reagent will reach equilibrium between the stationary phase and the mobile phase. Two co-existing mechanisms contribute to the retention of the ionic solutes. The first is the formation of an ion-pair in solution, followed by partitioning of the ion-pair into the stationary phase. The ion-pair reagent can also partition directly into the stationary phase, forming a dynamic ion-exchange stationary phase to interact with the free ionic solutes via charge-charge interaction. [37,38]

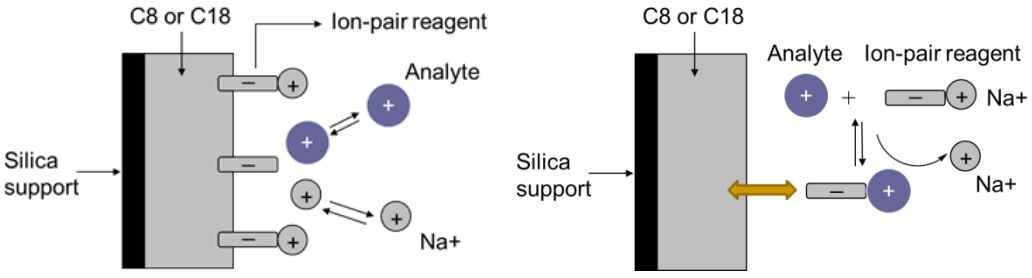

(a) (b)

Figure 1.1 Schematic diagram of ion-pair chromatography retention
(a) Retention of a positively charged analyte via charge-charge interaction with ion-pair reagent partitioned into station phase.
(b) Retention of ion-paired complex via partition into stationary phase

The manipulation of ion-pair chromatography shares many features with reversed-phase separation techniques, including the selection of mobile phase and stationary phase. The only difference is that ion-pair chromatography incorporates ionizable or permanently charged additives in the mobile phase. Similar to reversed-phase chromatography, the retention in ion-pair chromatography is impacted by mobile phase composition, such as the solvent strength and pH of the mobile phase, and the chemistry of the bonded phase. [39] In addition, the types of ion-pair reagents, as well as their concentrations, have a significant impact on the retention time of the analytes. For an ion-pair reverse-phase separation, the retention time of the analyte tends to increase with increasing hydrophobicity of the ion-pair reagent. For a given type of ion-pair reagent, an increase in the concentration leads to a longer retention time for the analyte until it reaches a plateau due to saturation of the stationary phase with the ion-pair reagent. Since an ion-exchange process is part of the retention mechanism for ion-pair chromatography, a high concentration of ion-pair reagent can reduce the retention time, and this is due to the competition of the counter ion (of the ion-pair reagent) with the analytes for interaction with the column.

1.3.4 Ion-exchange chromatography

Ion-exchange chromatography (IEC) is a branch of separation techniques that find most applications in the life sciences, such as the separation of biomolecules, including carbohydrates, amino acids, peptides and most importantly, oligonucleotides. IEC is also useful in separating small and highly charged cations or anions. IEC separations are performed on columns that are functionalized with cation or anion exchangers via covalent bonds. Figures 1.2 and 1.3 show typical cation and anion exchange functional

groups. The mobile phase typically consists of water, buffer, and inorganic salt. Retention is based on competition between the sample ions and mobile phase counterions (the dissociated product from the salt) for interaction with the stationary phase. Retention time in IEC can be varied by the type of the counterion and its concentration, as well as the pH and solvent strength of the mobile phase. Different types of counterions have different charge densities that can impact the binding affinity to the ion exchange functional groups. Counterions with a higher charge are more effective in displacing the analyte than those with a lower charge, leading to a shorter retention. The relative ability of an ion to displace the analytes and to provide smaller values of retention factor *k* is in the following order:

Anion exchanger: $F^- < OH^- <$ acetate$^-$ $< Cl^- < SCN^- < Br^- < NO_3^- < I^-$ >oxalate $^{-2} < SO_2^{-2} <$ citrate^{-3}

Cation exchanger: $Li^+ < H^+ < Na^+ < NH_4^+ < K^+ < Rb^+ < Cs^+ < Ag^+ < Mg^{2+} < Zn^{2+} < Co^{2+} < Cu^{2+} < Cd^{2+} < Ni^{2+} < Ca^{2+} < Pb^{2+} < Ba^{2+}$

The retention factor is related to the concentration of counterion via Eqn (1.15). [40, 41]

$$\log k = a - m\log C \qquad (1.15)$$

where a and m are constant for a given analyte, m is related to an absolute charge of the analyte, and C is the concentration of the counterion. Other factors, including the ionic strength and pH of the mobile phase, also impact retention. In general, as the ionic strength increases, the interaction between analyte and ion exchange functional group in the stationary phase is weakened, resulting in less retention. As expected, the impact of pH on retention in IEC is associated with the pKa(s) of the analyte, if any, and the trend is opposite to that of RPLC due to different retention mechanism.

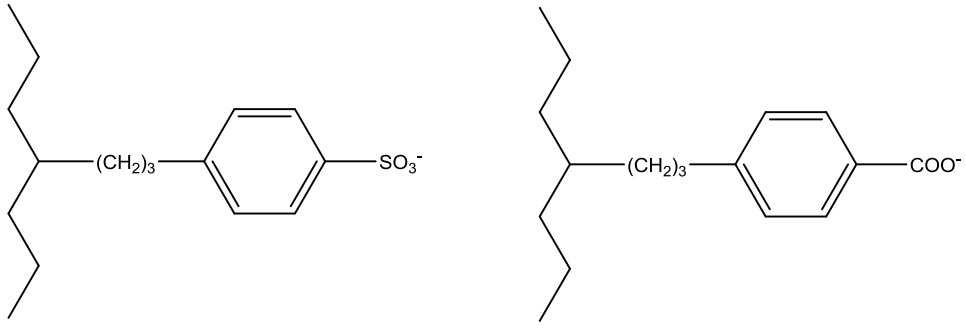

(a) SCX (b) WCX

Figure 1.2 Cation-exchange functional groups
(a): SCX = strong cation exchange; (b): WCX = weak cation exchange

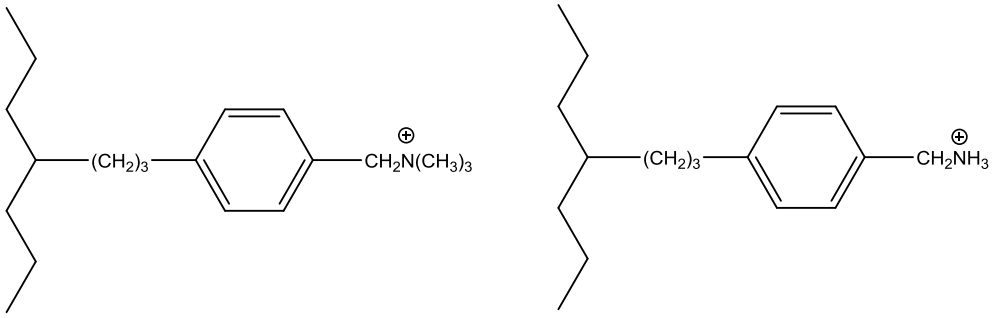

(a) SAX (b) WAX

Figure 1.3 Anion-exchange functional groups
(a): SAX = strong anion exchange; (b): WAX = weak anion exchange

1.3.5 Size exclusion chromatography

Size exclusion chromatography (SEC) separates molecules based on size and shape, making this technique the simplest form of chromatography. The separation is performed on a passive stationary phase with porous particles, including inorganic silica or polymeric organic material. The retention mechanism is a permeation process where the hydrodynamic radius of the molecule governs the extent of permeation into the pore

of the packing material. Large molecules will spend less time inside the pores of the packaging material, therefore eluting with a smaller volume of the mobile phase. In contrast, molecules of a smaller size can freely diffuse in and out the pores, exhibiting a greater retention volume. The SEC partition coefficient is proportional to the fraction of the intra-particle (pore) volume that is accessible to the solute, as shown in Eqn. (1.16). [42]

$$K_D = \frac{V_R - V_0}{V_i} \tag{1.16}$$

Where V_R, V_0, and V_i are the retention volume of the analyte of interest, the interstitial volume, and the intra-particle volume, respectively. The partition coefficient ranges from 0 to 1 with zero representing the solutes that can freely access the entire pore volume of the stationary phase, while a retention factor of unity refers to analytes that are too large and have no access to the intraparticle pore structure, being completely excluded from the pores.

The main application of SEC is to measure the molecular weight distribution of the solute. For an analyte with a partition coefficient between 0 and 1, the elution volume has a linear relationship to the molecular weight (Eqn. 1.17).

$$\mathrm{LogM} = m\left(\frac{V_R - V_0}{V_i}\right) + b \tag{1.17}$$

Since retention time in SEC is influenced by the hydrodynamic radius of the analyte, the technique is an important tool to study physical aggregation of the biomolecules, such as proteins and peptides. [43] Other applications include the determination of nanoparticle size and shape. [44]

List of References

1. M.S. Tswett, On a new category of adsorption phenomena and on its application to biochemical analysis, Proceedings of the Warsaw Society of Naturalists. 14(6) (1905) 20–39.

2. H. Weil, T.I. Williams, History of chromatography, Nature. 166 (1950) 1000-1001.

3. D.T. Day, A suggestion as to the origin of pennsylvania petroleum, Proc. Amer. Phil. Soc. 36(154) (1897) 112-115.

4. A.J.P. Martin, R.L.M. Synge, Separation of the higher monoamino-acids by counter-current liquid-liquid extraction: the amino-acid composition of wool, Biochem. J. 35(1-2) (1941) 91-121.

5. A.J.P. Martin, R.L.M. Synge, A new form of chromatogram employing two liquid phases: 1. A theory of chromatography, 2. Application to the micro-determination of the higher monoamino-acids in proteins, Biochem. J. 35(12) (1941) 1358-1368.

6. J.C. Giddings, Dynamics of chromatography, Marcel Dekker, New York, 1965.

7. J.F.K Huber, High efficiency, high speed liquid chromatography in columns, J. Chromatogr. Sci. 7 (1969) 85-90.

8. C. Horvath, B.A. Preiss, S.R. Lipsky, Fast liquid chromatography: an investigation of operating parameters and the separation of nucleotides on pellicular ion exchangers, Anal. Chem. 39 (1967)1422-1428.

9. J.J. Kirkland, Controlled surface porosity supports for high speed gas and liquid chromatography, Anal. Chem. 41 (1969) 218-220.

10. L.S. Ettre, Jim Waters: The development of GPC and the first HPLC Instruments, LC/GC North America, 23(8) (2005) 752-761.

11. J.J. Kirkland, High speed liquid-partition chromatography with chemically bonded organic stationary phases, J. Chromatogr. Sci. 9 (1971) 206-214.

12. R.E. Majors, High performance liquid chromatography on small particle silica gel, Anal. Chem. 44 (1971) 1722-1726.

13. R. Endele, I. Halász, K. Unger, Influence of the particle size (5-35 μm) of spherical silica on column efficiencies in high-pressure liquid chromatography, J. Chromatogr. Sci. 99 (1974) 377-393. .

14. M. Swartz, UPLC™: An introduction and review, J. Liq. Chromatogr. Relat. Technol. 28 (2005) 1253-1263.

15. M. Martin, C. Eon, G. Guiochon, Study of the pertinence of pressure in liquid chromatography III. A practical method for choosing the experimental conditions in liquid chromatography, J. Chromatogr. 110 (1975) 213-232.

16. I. Halász, R. Endele, J. Asshauer, Ultimate limits in high-pressure liquid chromatography, J. Chromatogr. 112 (1975) 37-60.

17. J.E. MacNair, K.C Lewis, J.W. Jorgenson, Ultrahigh-pressure reversed-phase liquid chromatography in packed capillary columns, Anal. Chem. 69 (1997) 983-989.

18. J.R. Mazzeo, U.D. Neue, M. Kele, R.S. Plumb, A new separation technique takes advantage of sub-2-μm porous particles, Anal. Chem. 77(23) (2005) 460 A–467.

19. M. Swartz, Ultra performance liquid chromatography: Tomorrow's HPLC technology today, LabPlus Int. 18(3) (2004) 6-9.

20. J.P. Foley, Resolution equations for column chromatography, Analyst. 116 (1991) 1275-1279.

21. M.J.E. Golay, D.A. Desty (Ed.), Gas chromatography, Academic Press, New York, 1958, p. 36.

22. J.J. Van Deemter, F.J. Zuiderweg, A. Klinkenberg, Longitudinal diffusion and resistance to mass transfer as causes of nonideality in chromatography, Chem. Eng. Sci. 5 (1956) 271-289.

23. J.R. Conder, C.L. Young, Physicochemical measurement by gas chromatography, Wiley, New York, 1979.

24. E. Soczewinski, Solvent composition effects in thin-layer chromatography systems of the type silica gel-electron donor solvent, Anal. Chem. 41 (1969) 179-182.

25. S.L. Maslen, F. Goubet, A. Adam, P. Dupreeb, E. Stephens, Structure elucidation of arabinoxylan isomers by normal phase HPLC–MALDI-TOF/TOF-MS/MS, Carbohydr. Res. 342 (2007) 724–735.

26. A.K. Eldin, S. Görgen, J. Pettersson, A.M. Lampi, Normal-phase high-performance liquid chromatography of tocopherols and tocotrienols: Comparison of different chromatographic columns, J. Chromatogr. A 881 (2000) 217–227.

27. R.N. Rao, B. Shankaraiah, M.S. Sunder, Separation and determination of λ-Cyhalothrin by normal phase-liquid chromatography using a CN column, Anal. Sci. 20 (2004) 1745-1748.

28. C. Hegyi, E. Olah, J. Fekete, Separation of cypermethrin diastereomers by normal phase liquid chromatography, J. Liq. Chromatogr. Relat. Technol. 29 (2006) 2835–2851.

29. P.W. Carr, D.E. Martire, L.R. Snyder, eds., Retention in Reversed-Phase HPLC, J. Chromatogr. Vol. 656, 1993.

30. L.C. Tan, P.W. Carr, Revisionist look at solvophobic driving forces in reversed-phase liquid chromatography: II. Partitioning vs. adsorption mechanism in monomeric alkyl bonded phase supports, J. Chromatogr. A 775 (1997) 1-12.

31. A. Ailaya, C. Horváth, Retention in reversed-phase chromatography: partition or adsorption? J. Chromatogr. A 829 (1998) 1-27.

32. L.R. Snyder, M.A. Quarry, Computer simulation in HPLC method development: reducing the error of predicted retention times, J. Liq. Chromatogr. 10 (1987) 1789-1820.

33. P.J. Schoenmakers, H.A.H. Billiet, L. de Galan, Influence of organic modifiers on the retention behavior in reversed-phase liquid chromatography and its consequences for gradient elution, J. Chromatogr. 185 (1979) 179-195.

34. P.J. Schoenmakers, H.A.H. Billiet, L. de Galan, Systematic study of ternary solvent behavior in reversed- phase liquid chromatography, J. Chromatogr. 218 (1979) 261-284.

35. P.E. Antle, A.P. Goldberg, L.R. Synder, Characterization of silica-based reversed-phase columns with respect to retention selectivity: Solvophobic effects, J. Chromatogr. 321 (1985) 1-32.

36. J.J. DeStefano, J.A. Lewis, L.R. Synder, Reverse phase high performance liquid chromatography based on column selectivity, LCGC, 10 (1992) 130.

37. B.A. Bidlingmeyer, S.N. Deming, W.P Jr. Price, B. Sachok, M. Petrusek, Retention mechanism for reversed-phase ion-pair liquid chromatography, J. Chromatogr, 186 (1979) 419-434.

38. W.R. Melander, C. Horvath, Mechanistic study of ion pair reversed-phase chromatography, J. Chromatogr, 201 (1979) 211-224.

39. C.M. Riley, E. Tomlinson, T.M. Jefferies, Functional group behavior in ion-pair reversed-phase high-performance liquid chromatography using surface active pairing ions, J. Chromatogr. A 185 (1979) 197-224.

40. Y. Baba, Computer-assisted retention prediction system for inorganic cyclic polyphosphates and its application to optimization of gradients in anion-exchange chromatography, J. Chromatogr. 550 (1991) 5-14.

41. J.E. Madden, P.R. Haddad, Critical comparison of retention models for the optimisation of the separation of anions in ion chromatography II. Suppressed anion chromatography using carbonate eluents, J. Chromatogr. A 850 (1999) 29–41.

42. M. Potschka, Mechanism of size-exclusion chromatography I. Role of convection and obstructed diffusion in size-exclusion chromatography, J. Chromatogr. A 648 (1993) 41-69.

43. P. Hong, S. Koza, E.S.P. Bouvier, Size-exclusion chromatography for the analysis of protein biotherapeutics and their aggregates, J. Liq. Chromatogr. Relat. Technol., 35 (2012) 2923–2950.

44. G.T. Wei, F.K. Liu, C.R.C. Wang, Shape separation of nanometer gold particles by size-exclusion chromatography, Anal. Chem.71 (1999) 2085-2091.

Chapter 2: Overview of small interfering RNA-based therapy, delivery technology and analytical characterization of lipid nanoparticle formulations

2.1 RNA interference: mechanism of action and biologic significance

RNA interference (RNAi) is a naturally occurring biological event in a cell's cytoplasm where double-stranded (ds) RNA interferes with the expression of a specific gene. It was first discovered by Fire and Mello in their seminal work to study the effect of exogenous ds-RNA on Unv-22 gene (encoded for myofilament protein) expression in C. elegans.[1] The gene-silencing effect of small interfering RNA (siRNA) was further demonstrated in mammalian cells using synthetic siRNA (21 to 23 mers, **Figure 2.1**). [2] RNA interference (**Figure 2.2**) begins with the breakdown of a long double-stranded RNA molecule by an enzyme called Dicer, forming a 21- to 23-mer small interfering RNA. The short strand RNA binds RNA-induced silencing complex (RISC) and splits itself into single strands. Following the cleavage of the sensing RNA single strand, the antisense RNA will selectively bind and degrade mRNA with a complementary sequence, achieving a gene silencing effect that can last for days to weeks. RNA interference is an important biological process that allows cells to fight against viral attack or gene mutation. The RNA interference (RNAi) mechanism is also implicated for controlling protein level in cells responding to various external stimuli.[3]

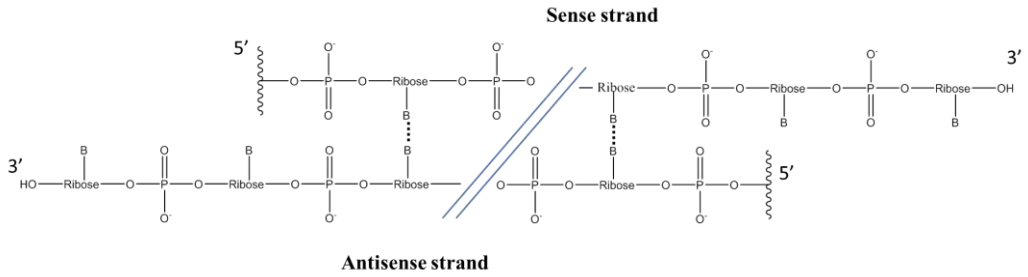

Figure 2.1 A generalized structure of a siRNA drug with the ribose sugars, phosphodiester bonds and bases (B).

The phenomenon of RNA interference represents a fundamental tool to study gene function, and more importantly, it offers a novel approach to develop new therapeutics for treating a variety of diseases. siRNA-based therapeutics have several advantages compared to gene therapy or protein or small molecule-based drugs due to its direct interference with protein translation, avoiding gene altering events that could occur with DNA-based drugs. siRNA acts on mRNA, hence suppressing certain harmful proteins before they are made in the body. Furthermore, siRNA is easy to design and can engage a broader range of disease targets than traditional therapeutics. [4]

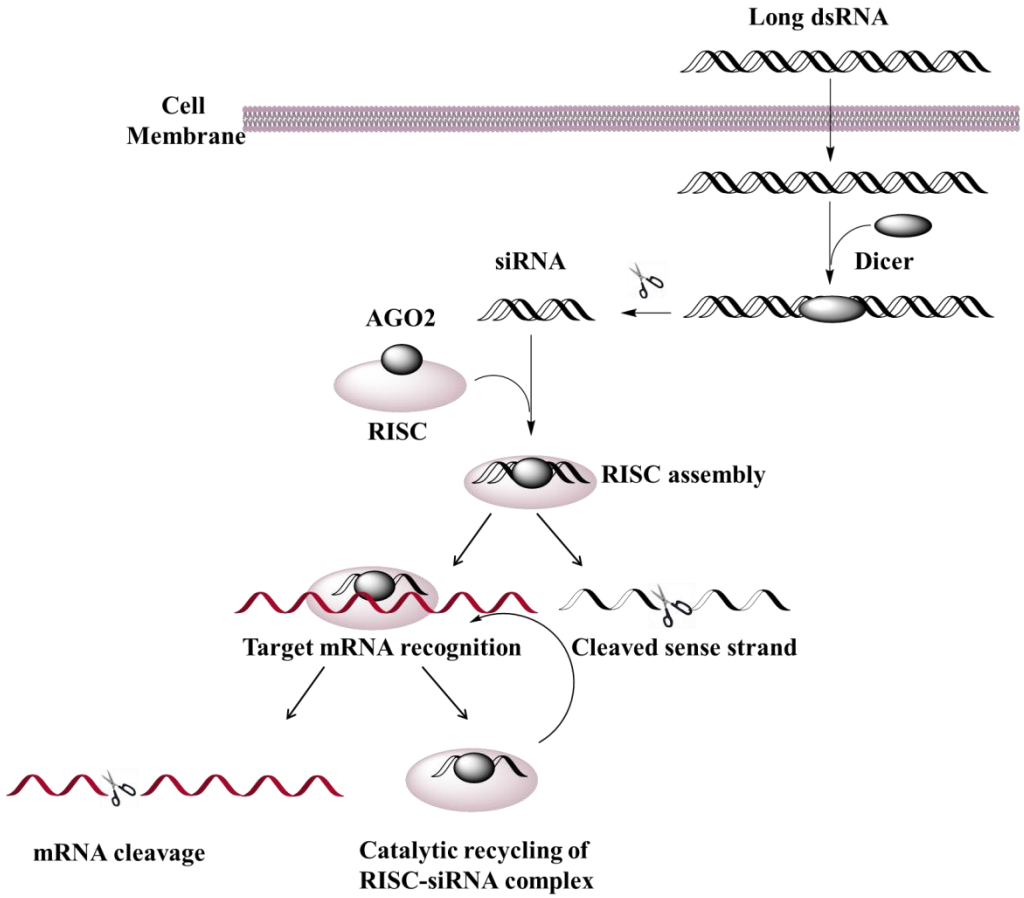

Figure 2.2 The mechanism of RNA interference

RNAi machinery has provided new opportunities for treating diseases with significant unmet medical needs, such as cancer, autoimmune disorders, and viral infections. The genetic nature of cancer implies that siRNAs, with complementary sequences to cancer genes, can directly target the tumor cells. siRNA sequences loaded in lipid- or polymer-based nanocarriers showed early promise in suppressing the target genes associated with breast cancer, cervical cancer, liver cancer, lung cancer and prostate cancer. [4] Autoimmune disorders, such as rheumatic diseases, have complex pathogeneses, and the identification of the underlying genes responsible for inflammation and structure damage yielded promising siRNA therapeutic candidates. [5] RNAi-based

therapy is also uniquely suited to combat viral infections. Standard treatment for HIV and hepatitis C virus often involves a cocktail of multiple drugs, and strict adherence to dosing regimen is vital to combat drug resistance due to viral mutation. [6,7] siRNAs targeting several gene products can reduce such mutations with a single injection. The therapeutic effect can last for weeks and months owing to the catalytic nature of gene suppression by siRNA. [8]

Since the inception of siRNA-based biomedical research, there have been over 50 clinical trials executed that focus on the safety and efficacy of more than 20 different siRNA sequences in humans. [9,10,11,12, 13] Early trials primarily relied on local delivery of siRNA to target tissues/organs. The first siRNA clinical trial commenced in 2004 to test the safety and efficacy of Bevasiranib (a siRNA targeting vascular endothelial growth factor (VEGF) to inhibit retinal neovascularization) in age-related macular degeneration (AMD) patients. The study was sponsored by Opko Health Inc., and it met primary goals for phase I and II. The program was later terminated in phase III due to poor efficacy. [12] Quark Pharmaceuticals conducted the first clinical trial of QPI-1002 (I5NP), an uncoated siRNA, which targeted pro-apoptotic protein p53 in patients undergoing kidney transplantation. A delivery vehicle is not needed since uncoated RNA is often accumulated in the kidney, the target organ for this therapy. QPI-1002 (I5NP) is safe and well tolerated in patients, and it achieved sustained p53 suppression. A phase II study is ongoing with results pending. In 2008, Calando Pharmaceuticals initiated a phase I trial, which demonstrated for the first time the systemic delivery of siRNA (CALAA-01) via IV injection of siRNA containing nanocarriers. CALAA-01 was intended for treating melanoma and specifically targeted ribonuclease reductase. The study was later

terminated due to findings related to safety. [14] PRO-040201 (TKM-ApoB) was developed by Tekmira Pharmaceuticals using SNALP (stable nucleic acid lipid particle) delivery technology. The drug was tested in patients with hypercholesterolemia and achieved a good safety profile. Unfortunately, the development was later terminated due to an immune response likely triggered by the siRNA. [9] Despite setbacks in the earlier trials, several siRNA-based drug candidates have advanced into phase II/III. ALN-TTR02 (Patisiran) was developed by Alnylam Pharmaceuticals for treating TTR-mediated amyloidosis. Based on encouraging phase I data in patients with transthyretin amyloidosis, the drug candidate is currently being evaluated in phase II/III for its long-term safety and tolerability in a broader patient population. TKM-PLK1 by Tekmira Pharmaceuticals, targeting polo-like kinase-1, is also being evaluated in Phase II trials for treating the solid tumor in the liver.

2.2 siRNA delivery platforms

With a properly designed siRNA sequence, RNAi machinery can be exploited to silence any gene in the body, opening a new frontier for developing personalized medicines. Although developing siRNA into clinically viable therapeutics is promising, significant challenges remain. Due to their size and negative charge, siRNAs cannot easily pass through a cell's membrane. Therefore, the safe and effective delivery of siRNA has been the biggest challenge for RNAi technology in addition to the toxicities related to off-target gene-silencing effects. [15,16] Local delivery of naked siRNA is possible for tissues that are external, such as ocular, pulmonary, colonic, epidermal, etc. [9, 12] For broad applications, a systemic delivery of siRNA is critically needed as many target tissues can only be accessed via the bloodstream. There are multiple challenges to

achieving the systemic delivery of siRNA. [17, 18] First is the enzymatic degradation of siRNA by endogenous nucleases. [19] The structural integrity of siRNA largely relies on chemical modification with protective groups or physical encapsulation using macromolecules, such as lipid or polymer. In addition to maintaining chemical stability post-injection, the siRNA complex must navigate in the circulatory system without premature clearance due to kidney filtration, aggregation with serum proteins, and uptake by phagocytes. Encapsulation of siRNA in lipid or polymer nanocarriers with engineering control of the size, shape, and surface charge significantly prolongs the half-life of siRNA in blood. The next challenge for siRNA delivery is permeation through the cell membrane, which proceeds through receptor-mediated endocytosis. Endocytosis is a cellular process where the cells absorb molecules or substances from outside the cell by engulfing it with the cell membrane. The process of endocytosis forms a membrane-bound vesicle, also known as an endosome, inside the cell. The size of the endosome varies according to the cell type. For example, in HeLa cells, endosomes are approximately 500 nm in diameter when fully mature. [20] Once inside the cell, the intact siRNA is liberated from the delivery cargo and released into the cytoplasm to invoke its gene-silencing function. Accomplishing this complex sequence of events requires the elegant design of an integrated delivery system, which includes the carriers (lipids or polymers), cell targeting ligands, and shielding ligands to avoid off-target interactions. [21, 22] Many delivery systems have been explored in the past two decades, including siRNA-containing lipid nanoparticles, siRNA polymer conjugate, or siRNA single chemical entities. [23, 24, 25]

2.2.1 Lipid-based delivery systems

In an aqueous environment, lipids have the tendency to form unilamellar or multilamellar liposomes, where the lipid bilayers form a sphere with an aqueous core. The liposome-based technology was first reported 30 years ago for the delivery of DNA and RNA.[26, 27] The technology was later adopted for siRNA delivery with some modifications due to differences between DNA and siRNA in size, charge, and site of action. **Figure 2.3** shows a typical structure of a siRNA-containing lipid nanoparticle (LNP), with the particle sizes less than 100 nm. The LNP is also referred as a unilamellar vesicle that is composed of a lipid bilayer. siRNA is encapsulated in lipid bilayers, which consist mostly of cholesterol and cationic lipids. The lipid bilayers also contain as a minor component, the PEGylated short-chain lipid, which is decorated on the bilayer surface. The LNP enters the cell in a two-step process: a receptor (anchored on PEG tip) – mediated endocytosis, followed by endosome escape and release of siRNA into the cytoplasm. The primary mechanism for cell uptake of a liposome is the fusion of a multilamellar lipoplex with the cell membrane as shown in **Figure 2.4**. The cationic lipids are the most important components of LNPs for modulating the cell uptake of siRNA. They directly influence siRNA encapsulation efficiency and the particle size and surface charge of LNPs, which are critical parameters for siRNA delivery to cell cytoplasm.[28] The unsaturated hydrocarbon chain in the lipids, as well as the pH-dependent charge density of the lipid's headgroup, is responsible for the escape of siRNA from the endosome (or the rupture of endosome membrane). The PEG group decorated on the LNP surface can mitigate the absorption of serum proteins, which can deactivate cell penetration of LNP. The PEG group also improves the LNP's physical stability in

systemic circulation upon IV injection, preventing particle aggregation in plasma. Lastly, the PEG moiety can help LNPs to evade the immune system and avoid premature uptake by phagocytes. [29, 30]

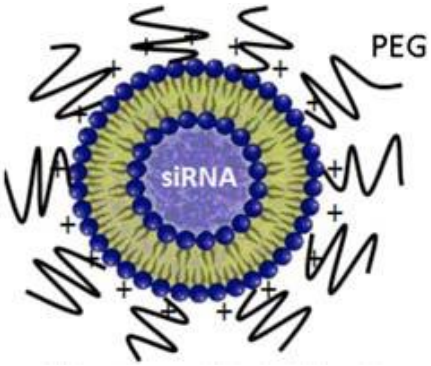

Figure 2.3 siRNA-containing lipid nanoparticles with surface modification with PEG polymers

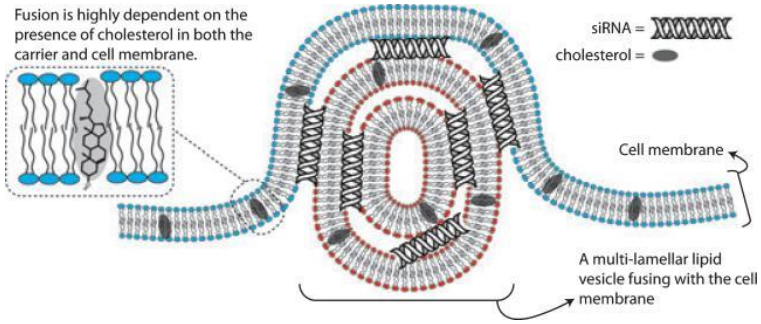

Figure 2.4 Schematic representation of the fusion of a multilamellar small interfering RNA lipoplex with the cell membrane. The positively charged lipid bilayer adsorbs to the negatively charged surface of the cell, resulting in either an endocytosis process or by fusion of the lipoplex with the cell membrane, thereby releasing the nucleic payload into the cytosol. During the process, the lipid membrane is stressed and lipids are freed to the intracellular and extracellular compartments. [25]

2.2.1.1 Cationic lipids as carriers for siRNA delivery

The majority of siRNA delivery vehicles employ cationic lipids as the carriers. Cationic lipids were originally used in stable nucleic acid lipid particle (SNALP)

formulations for DNA and RNA delivery in the 1980s. [16] The cationic lipid associates with negatively charged siRNA through electrostatic interactions, forming a complex known as lipoplex. The lipoplex has a multilamellar structure with positively charged lipid bilayers separated by negatively charged siRNA sheets. Studies have shown that cationic lipids, such as DOTAP (1,2-dioleoyl-3-trimethylammonium propane), can effectively encapsulate siRNA, forming liposomes that can interact with a negatively charged cell membrane to deliver siRNA into the cytoplasm. [31] The high permeability of liposomes through the cell membrane using early-generation cationic lipids did not translate into a high percentage of gene knockdowns due to poor endosome escape of the siRNA. [32] A combinatorial library of lipid-like molecules was generated for the systematic evaluation of siRNA delivery efficiency. [33] The screening efforts identified several novel cationic lipids capable of promoting the efficient delivery of siRNA both *in vitro* and *in vivo*. A rational design of cationic lipids was proposed by Semple and his team based on the hypothesis that the structure of a cationic lipid impacts its interaction with naturally occurring anionic phospholipids in the endosomal membrane. [28] An ion-pair event triggers the formation of a non-bilayer structure, a precursor for membrane disruption and endosome escape. The structure and activity of a series of cationic lipids (**Figure 2.5**) were investigated to understand the impact of the alkyl chain, linker, and headgroup on siRNA delivery and efficacy. The best-performing lipid was Dlin-KC2-DMA, i.e., the LNP on which it was based showed superior efficacy in both rodents and non-human primates.

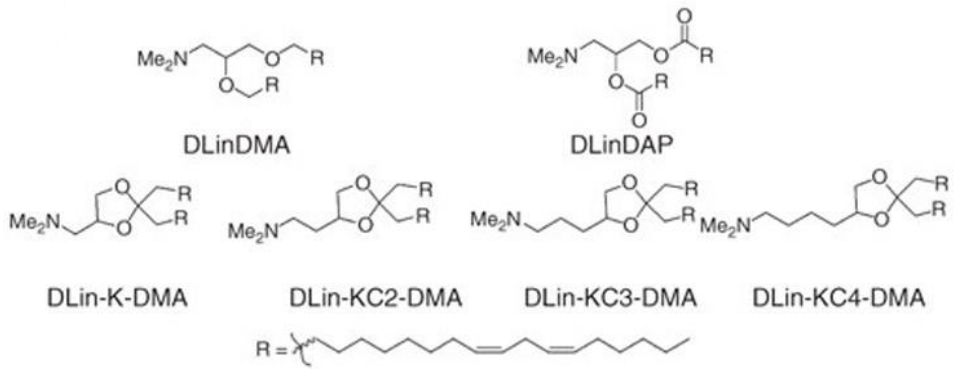

Figure 2.5 Structure of cationic lipids used for siRNA delivery. [28]

2.2.1.2 Anionic lipids as carriers for siRNA delivery

Although most lipid-based delivery systems used cationic lipids as the carrier, studies showed that anionic lipids could be used stand-alone or in combination with cationic lipids to address specific issues associated with the delivery of siRNA or DNA. For example, DNA encapsulated in a cationic-based SNALP formulation can undergo deactivation by polyanions present in tumor fluid, such as hyaluronic acid. The delivery issue was resolved by complexing DNA with a polylysine to impart a net positive charge on the particle surface, followed by treatment with anionic lipids to increase the transfection of DNA to target tumor cell. [34] In another study, an LNP constructed with an anionic lipid, dilinoleylmethyl-4-dimethylaminobutyrate (DLin-MC3-DMA), showed substantially improved siRNA delivery and gene knockdown for the treatment of liver disease. [8] LNPs constructed with anionic lipids are expected to have an improved safety profile relative to LNPs constructed with cationic lipids due to the lack of positive charge. For example, cationic lipids have been implicated for non-specific interaction with negatively charged cellular components, including opsonins, serum proteins, and enzymes. [35] This non-specific interaction can interfere with ion-channel activities.

Anionic lipids provided a safe alternative to cationic lipids used mostly in SNALP formulations. Development efforts for the anionic lipid-based delivery system have been focused primarily on increasing encapsulation efficiency achieved by charge repulsion between carrier and siRNA. A bridging agent is often incorporated to promote the association between carrier and siRNA.

2.2.2 Polymer-based delivery systems

Polymer-based delivery systems include two major categories, where the distinction lies in the nature of the linkage between the polymer carrier and siRNA. The first type is the nanoparticle-based system, where the polymer and siRNA form nano-aggregates through electrostatic interaction and other non-covalent bonds, while the second type is an integrated system, where the polymer, siRNA, and various other functional moieties are brought together through reversible covalent bonds.

2.2.2.1 Nanoparticle-based polymer delivery systems [36, 37,38]

The nanoparticle-based polymer delivery platform utilizes cationic polymers as carriers to form a complex with negatively charged siRNA through electrostatic interaction. The complexation process effectively contracts the siRNA to prevent its hydrolytic degradation and to facilitate cell-uptake through endocytosis. In addition to polymers, these delivery systems often contain other components to minimize off-target effects and to improve cell-targeting efficiency. The safe and effective delivery via polymer-siRNA nanoparticles relies on the particle size, its physical stability during extracellular circulation, cellular uptake via endocytosis and efficient release of siRNA from the complex through polymer biodegradation. The polymer includes naturally

occurring polycations (e.g., atelocollagen and chitosan) that are biocompatible and biodegradable as well as the synthetic ones (e.g., polyethylenimine).

2.2.2.1.1 Natural polymers as carriers for siRNA delivery

Natural polymers were among the early candidates explored for siRNA delivery owing to their biocompatible and biodegradable nature. Chitosan is one of the most studied natural polymers for cellular delivery. It is a copolymer consisting of GLcNAc (N-acetyl-D-glucosamine) and GLcN (D-glucosamine) building blocks (**Figure 2.6**). The co-polymer carries positive charges under acidic or neutral environment. The decomposition product incurs no toxicity *in vivo* which makes it a good polymer carrier candidate for siRNA.[39] The thiamine pyrophosphate (TPP) salt of chitosan forms stable nanoparticles with siRNA, effectively shielding siRNA from chemical degradation and promoting efficient cellular uptake of the siRNA. The delivery efficiency depends on the molecular weight of the polymer and the surface charge of polymer – siRNA complex, controlled by the ratio of chitosan-TPP and siRNA. A polymer with a greater positive charge density promotes a stable complex formation. The gene-silencing percentage reached a maximum with the lowest particle size of the complex. The chitosan salt based delivery system demonstrated no sign of cytotoxicity based on an MTT (3-(4, 5-dimethylthiazol-2-yl)-2,5-diphenyltetrazolium bromide) assay, and the cell viability is ~ 90% of those untreated cell lines.[40]

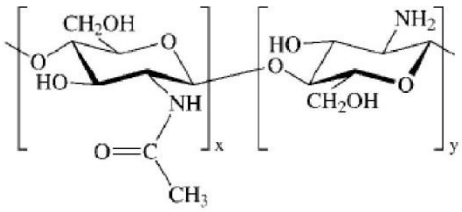

Figure 2.6 Chemical structure of natural copolymer chitosan

Atelocollagen is another natural polymer that was explored for gene and/or siRNA delivery. [41] This natural polymer is prepared by enzymatic digestion of type I collagen of calf derma to remove telopeptides, known to cause an immune response. The delivery formulation is typically a simple binary mixture containing polymer and siRNA. In vivo gene knockdown achieved with this approach is promising, and the mice that received an intravenous injection of natural polymer atelocollagen and siRNA mixture showed an 80 to 90% reduction in bone tumor metathesis. [42]

2.2.2.1.2 Synthetic polymers as carriers for siRNA delivery

In addition to natural, biodegradable polymers, synthetic polymers were also extensively evaluated as potential carriers for siRNA delivery. The system design focuses on rationale selection of the shielding ligands, preventing non-specific interaction between nanoparticles and extracellular proteins, and the cell targeting ligands, enabling effective cell uptake to the cytoplasm.

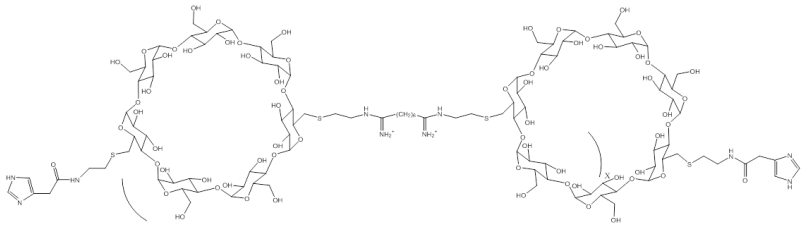

CD-containing linear polymer (CDP)

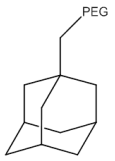

PEG-Adamantane (PEG-AD)

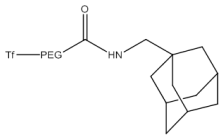

Transferrin-PEG-Adamantane (Tf-PEG-AD)

Figure 2.7 Components of Cyclodextrin (CD)-based nanoparticles for siRNA delivery [44]

Cyclodextrin (CD) is a cyclic oligomer with glucose as a building block. It is a pharmaceutical excipient commonly used to enhance solubilization of poorly soluble drug in parenteral formulations. The solubilization enhancement is associated with the cavity within the CD that allows host-guest interaction (or complexation). CD is safe and well tolerated for human use and a good candidate for gene delivery. [43] A three-component system (**Figure 2.7**), consisting of CD-containing linear polymer (CDP), PEG- adamantane (AD) and AD-PEG-TF (transferrin), was developed for siRNA delivery. [44] The CD-containing polymer (carrying polycations) forms nanoparticles with siRNA via electrostatic interaction regardless of the size and type of siRNA. The polymer serves as a physical barrier to prevent chemical degradation of siRNA. The CD on the polymer backbone also provides host sites for attaching PEG and PEG-TF functional groups with the AD as the anchor. The PEG group functions as a stability enhancer to prevent nanoparticle aggregation, while the AD-PEG-TF structural moiety

decorated on the polymer surface enhances the cell uptake, with TF serving as the cell targeting ligand. Finally, the polymer backbone is linked to amine-containing chemical groups that were designed to facilitate the release of siRNA from the endosome to the cytoplasm.

Key variables dictating the delivery properties include the type of CD and charged groups on the polymer backbone, as well as the distance between the CD and the charged groups. A longer distance between CD and the charge center renders a low toxicity but a low binding affinity with siRNA. Among various positively charged groups (e.g., amidine, quaternary amine and secondary amine) evaluated on the polymer backbone, amidine stands out as the best. The formulation preparation is simple and involves mixing a naked siRNA from one vial with a pre-mixed CD-containing polymer, AD-PEG, and AD-PEG-TF constituents into buffer solution before use. The final mixture yields a stable nanoparticle with a diameter of ~ 70 nm. The CD-based delivery platform with siRNA designed for RRM2 (ribonucleoside-diphosphate reductase subunit M2) gene knockdown showed significant suppression of the RRM2 protein. It was safe and well tolerated based on non-human primate and mice models. The formulation is currently being evaluated for safety in an early human clinical trial for treating cancer. [44]

Polyethylenimine (PEI) is another popular synthetic polymer often used for DNA or siRNA delivery. [45] It has a high density of positive charges on the polymer backbone under physiologic pH due to the protonated amino groups. The positive charges in PEI enable the formation of stable non-covalent complexes with the negatively-charged siRNA. A linear PEI with MW of 22 kDa achieved the efficient delivery of siRNA with minimal cytotoxicity. Further studies indicated that the delivery efficiency of the PEI

system depends highly on the molecular weight and configuration (linear or branched) of the polymer and the mass ratio between PEI and siRNA.[46] The chemical modification of PEI with PEG groups improves the transfection efficiency of siRNA while reducing the potential toxicity. The underlying mechanism is that the non-ionic PEG group can reduce the potential non-specific interaction between the positive polyplex and extracellular matrix, including proteins. In addition, the amino groups on PEI are implicated in the so-called "proton sponge effect", [47] where they serve as a low pH buffer system in the endocytosis/liposomal system, increasing the osmotic pressure and eventually leading to the breakage of the endosome membrane to release the siRNA to the cytoplasm. PEI is a non-biodegradable polymer, so the safety profile is less ideal due to the accumulation of large MW polymer in cells.

Bioreducible polymers, such as poly (disulfide amine), were recently reported as an effective carrier to deliver siRNA. [48] These polymers were prepared through copolymerization of low molecular weight cationic monomers containing disulfide groups as a reducible linkage. Compared to non-degradable polymers, such as PEI, the bioreducible-based polymer delivery platform would be more biocompatible, intrinsically safe and less toxic. An arginine-conjugated poly(cystaminebisacrylamide-diaminohexane) (i.e., poly (CBA-DAH-R)) was developed for VEGF gene-silencing siRNA delivery. The polymer forms 200-nm particles after complexing with siRNA; maximal physical stability of the nanoparticles is achieved at mass ratios from 20 to 1 between polymer and siRNA. The reducible property of the polymer carrier was confirmed by the absence of nanoparticles in a solution of dithiothreitol (or DTT)), where DTT mimics a reductive environment. The degradation of the polymer by DTT disrupted

the polymer-siRNA complex. An in vitro cytotoxicity assay suggested that the system with poly (disulfide amine) carrier exhibits ~ 100% cell viability while the PEI polymer results in only 40% relative cell viability. In vitro transfection efficiency is ~ 80% in human prostate carcinoma PC-3 cell line, and the high cell uptake indeed correlated with significantly suppressed gene expression. The high gene knockdown efficiency associated with poly(disulfide) is attributed to the ability of the disulfide bond in the polymer backbone that can be reduced easily. The importance of reductive cleavage of the disulfide bond was confirmed with confocal fluorescence microscopy; the cell lines treated with buthionine sulfoximine (BSO), a reagent that can increase the intracellular reducing potential, showed a marked decrease in the localization of siRNA in the cytoplasm.

For a nanoparticle-based siRNA delivery system, the polymer choice is typically constrained to polycations, where the backbone contains positively charged amine groups. With technology advancement in polymer engineering, it is possible to chemically modify neutral polymers for potential use as siRNA delivery vehicle. Poly(ethylene oxide) (PEO) and polyester (PE) have been extensively used as vehicles for oral drug delivery, thus, their safety and toxicity are well characterized. The copolymers of PEO and PE, grafted with a short cationic moiety, were recently developed as safe and effective siRNA carriers with promising in vitro results. The systems demonstrated efficient cell uptake as well as in vitro gene knockdown encoded for P-glycoprotein. [49]

2.2.2.2 Covalent bond based delivery system: dynamic polyconjugate[50]

A polyconjugate is a complex formed between a synthetic polymer and a biological molecule, such as siRNA. In contrast to the polymer-based nanocarrier delivery systems, where the positively charged polymers form complexes with siRNA through electrostatic interactions, the dynamic polymer conjugates chemically link all functional groups together through reversible covalent bonding. The key to the polyconjugate delivery system is to maintain the integrity of the chemical bonds before delivering siRNA to the target cells. However, once inside the cell the covalent bonds need to self-dissociate to release siRNA to the cytoplasm.

2.2.2.2.1 Polyvinylether-based polyconjugate

The first polyconjugate achieving such a task was reported by Rozema and co-workers. [51] The negatively charged, non-aggregating siRNA polyconjugate comprised reversible linkages attaching three main structural motifs onto the polymer backbone - poly(butyl amino vinyl ether) (PBAVE). The key functional moieties include siRNA, PEG (the shielding group) and N-acetylglucosamine (NAG, the cell-targeting group). The disulfide bond links siRNA to the polymer backbone, and the PEG and NAG groups are attached to the polymer through reversible modification with maleic anhydride derivatives. Polyconjugate enters the hepatocytes through ASGPr-mediated endocytosis. The low pH environment of the endosome cleaves the acid-labile maleate bond, releasing the PEG and NAG groups. The de-protected free amine groups can disrupt the endosome membrane, releasing the polymer-siRNA conjugate into the cytoplasm. The disulfide bond linking siRNA and the polymer will be subsequently oxidized in the cytoplasm, resulting in the release of the free siRNA in the cell. (**Figure 2.8**)

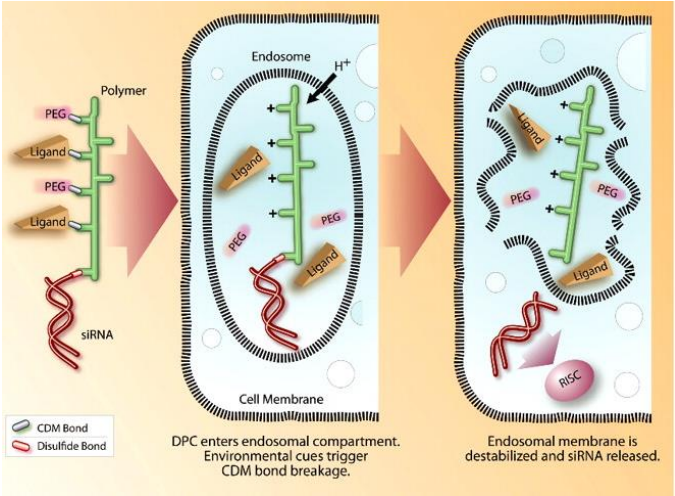

Figure 2.8 Cell uptake of siRNA-polymer conjugate [51]

Both PEG and NAG groups are important for effective siRNA delivery. The dissociation of the PEG group from the polyconjugate in the endosome is the critical step for an effective gene knockdown. When a PEG group was permanently linked to the polymer backbone, the polyconjugate was found to become completely inactive. The NAG functional group is also critical to siRNA cell uptake. The hepatocyte uptake of siRNA was significantly reduced when NAG was replaced with glucose in the polyconjugate assembly, confirming NAG as cell targeting ligand for the liver. The non-covalent bonded polyconjugate, where siRNA and polymer were assembled through electrostatic interactions, showed a marked decrease in siRNA accumulation in the liver, underscoring the importance of covalent bonding between siRNA and polymer backbone. Dynamic polyconjugates delivered siRNA effectively to liver cells for both *in-vitro* and *in-vivo* models. Significant gene knockdown was demonstrated for apoB and PARP genes with maximum efficiency of 80 to 90% at 2.5 mg/kg dose. The time duration of

gene knockdowns is satisfactory. The dose level tested is well tolerated, and no toxicity was indicated based on several safety biomarkers. The apoB gene silencing with siRNA polyconjugates effectively elicits a reduction in apoB gene expression and cholesterol level in serum as well as an impairment of triglyceride transport from the liver. However, the fatty liver induced by the gene knockdown and its potential acute effect in humans should be further investigated prior to advancing apoB siRNA as a viable therapeutic agent.

The siRNA polyconjugates offer a promising delivery platform for gene-based therapeutic applications with high potency and low toxicity. The reversible covalent bonds used in linking siRNA, cell targeting ligand, and shielding ligand provide added flexibility for targeting variety cell types. The key advantage over the nanoparticle-based delivery platforms includes minimal accumulation in off-target cells. The smaller particle size of the polyconjugate (~ 10 nm), compared to the nanoparticle delivery system (~100 nm), eliminates the potential activation of immune cells, resulting in near elimination of toxicity effects.

2.2.2.2.2 PolyLycine-based polyconjugate [52]

A polymer conjugate containing a polylysine (PLL) backbone bonded with PEG and 2,3-dimethylmaleicanhydride (DMMan)-masked-melittin (Mel) was recently reported as a potential delivery platform for siRNA therapeutic. The integrated siRNA-containing polyconjugate was constructed by means of a three-step synthesis. The first step involves the coupling reaction between PEG and the PLL polymer backbone. Then a pH-labile DMMan-masked melittin group is attached to the modified PLL through a disulfide bond. Lastly, the siRNA was incorporated into the delivery cargo (e.g., PEG-

PLL-DMMan-Mel) through a reducible covalent bond. Similar to the PBAVE-based system, the PEG group functioned as the shielding agent, and the methylmaleic anhydride-masked melittin is the endosomolytic agent, facilitating the escape of siRNA under weakly acidic endosomal environment. The polyconjugate system forms nanoparticles with sizes ranging from 80 to 300 nm, significantly larger than the PBAVE system discussed previously. The in vitro gene-silence efficiency was evaluated in cultured Neuro2A cells having stable luciferase expression. The gene-knockdown is ~ 80% at low doses (0.125 μg to 0.25 μg). Despite promising *in vitro* efficacy, the *in vivo* toxicity studies suggested unusually high toxicity based on a rat model. Further optimization of this delivery platform is needed for therapeutic applications.

2.2.3 Summary of siRNA delivery platforms

Among the various systems discussed above, siRNA-containing lipid nanoparticle (LNP) remains the most advanced delivery platform being tested in human clinical trials. The development of LNP systems requires the characterization of several critically important quality attributes, among which is the chemical stability of key constituents in the LNPs. The remaining part of the introductory chapter will highlight the challenges and opportunities associated with analytical method development for quantitating the siRNA, lipids and their related species. Separation techniques, such as HPLC and CE, coupled with various types of detectors—UV, MS, ELSD, and CAD, will be discussed with respect to their potential utility in addressing the analytical challenges.

2.3 Overview of analytical separation and stability characterization of LNP

2.3.1 Chemical degradation of RNA and lipids in LNP

A fully assembled LNP typically contains siRNA, cationic lipids, PEG-containing short-chain lipids, and cholesterol. Chemical stability of the LNP is a key consideration during formulation development. Evaluation of the stability performance of an LNP system entails the quantitation of active components, including siRNA and lipids, and their respective breakdown products due to degradation. Quantitation of each component in LNP is important for verifying a target potency of siRNA and the desired lipid composition for achievement of optimum physical properties, such as particle size, surface charge, etc. The analysis and control of low-level breakdown products from siRNA and lipids ensures that patients are not exposed to potentially harmful species. This analysis and control is also a mandate from regulatory agencies before a new therapeutic can be tested in clinical trials.

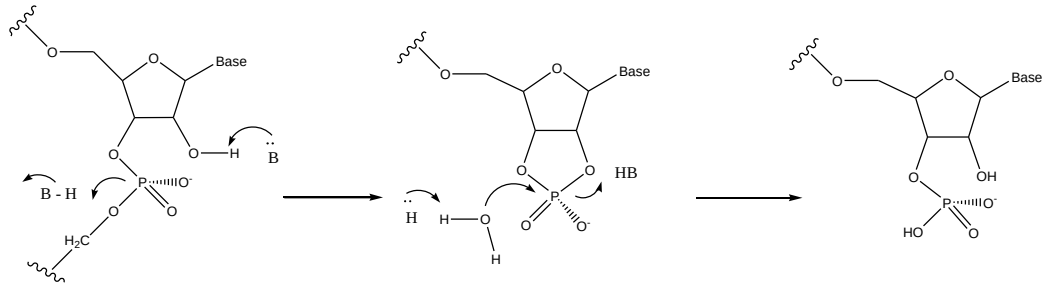

Scheme 2.1 Base-catalyzed intramolecular hydrolysis of the phosphodiester bond in RNA. (B denotes a Bronsted base.) [53]

Both siRNA and lipids in LNP have the potential to form low-level degradation products due to hydrolysis and/or oxidation. RNA is a complex molecular assembly,

consisting of a long chain of nucleotides. Each nucleotide contains a nitrogenous base, a ribose sugar, and a phosphate. The sugar-phosphate backbone of a native RNA molecule is subject to hydrolytic degradation. The hydrolysis is accelerated by both acid and base. [53] **Scheme 2.1** shows a base-catalyzed intramolecular hydrolysis of the phosphodiester bond in RNA. The bond cleavage proceeds with the displacement of a 5'-linked nucleoside by a nucleophilic 2'-oxyanion group (e.g., the deprotonated 2'-OH), forming 2',3'-cyclic phosphate, which can rapidly hydrolyze to generate the end products. In an acidic environment, the 2',3'-cyclic phosphate intermediate can undergo pseudorotation forming an isomer of the starting RNA, in addition to the 3'-5' phosphodiester bond breakage. [54]

Synthetic siRNA must be chemically modified to improve in vivo serum stability[55]; for this, the phosphodiester linkage is modified by phosphorothioate substitution. In addition, the replacement of a hydroxyl group at the 2' position with - OMe or -F also stabilizes the RNA (**Figure 2.9**). Despite the chemical modification, the hydrolytic degradation of a fully modified siRNA can still occur in an actual LNP system. In addition to hydrolysis, the phosphorothioate group (**Scheme 2.2**) and the nitrogenous bases in siRNA can undergo oxidation (**Scheme 2.3**). [56]

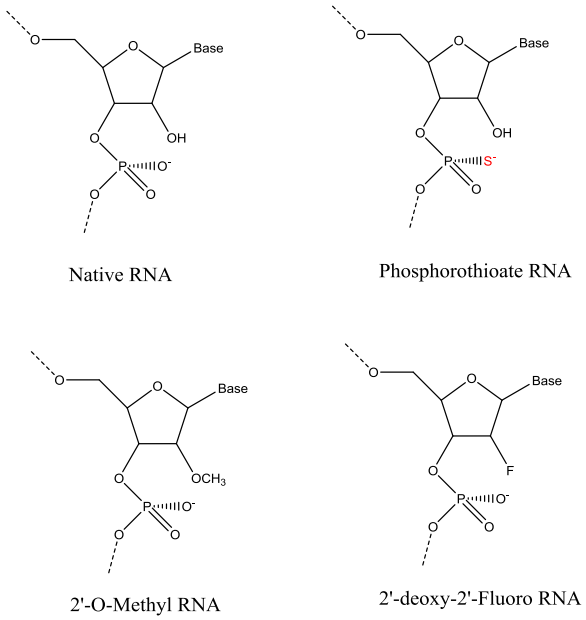

Figure 2.9 Chemical modification of RNA to improve chemical stability [55]

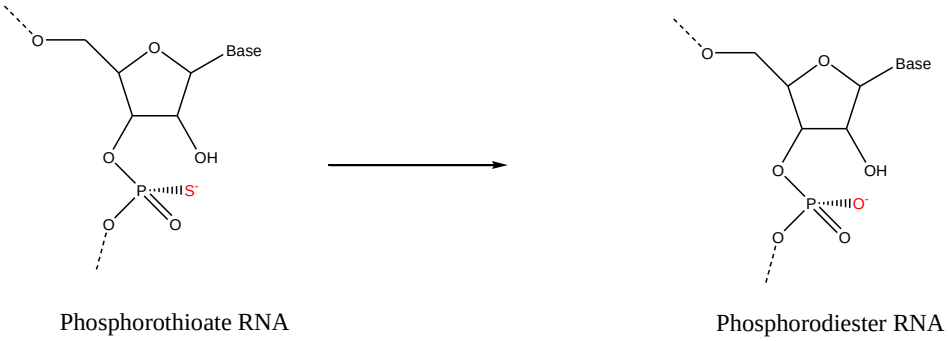

Scheme 2.2 Oxidation of phosphorothioate RNA to phosphodiester RNA[55]

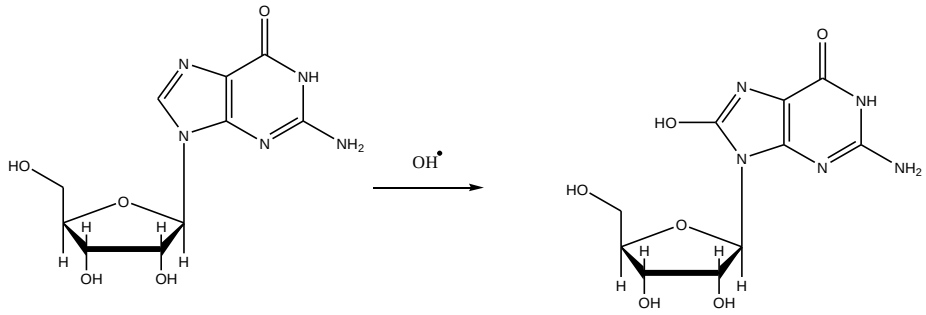

Scheme 2.3 Oxidation of nitrogenous base – Guanine [53]

The chemical stability of lipids varies significantly, depending on their structure. Like siRNA, the lipids are prone to hydrolysis or oxidation. Free radical-mediated auto-oxidation is typical for lipids with unsaturated alkyl chains.[57] **Scheme 2.4** shows an example of autoxidation of a lipid with two double bonds. The reactive peroxide intermediate can further engage secondary degradation, forming complex final products, including unsaturated aldehydes, di- and epoxy-aldehydes, lactones, furans, ketones, and oxo and hydroxyl acids, etc. Lipids containing ester groups (e.g., dipalmitoyl-phosphatidylcholine (DPPC)) are prone to hydrolysis, resulting in the formation of fatty acids and the lyso form of the parent lipid (**Scheme 2.5**).

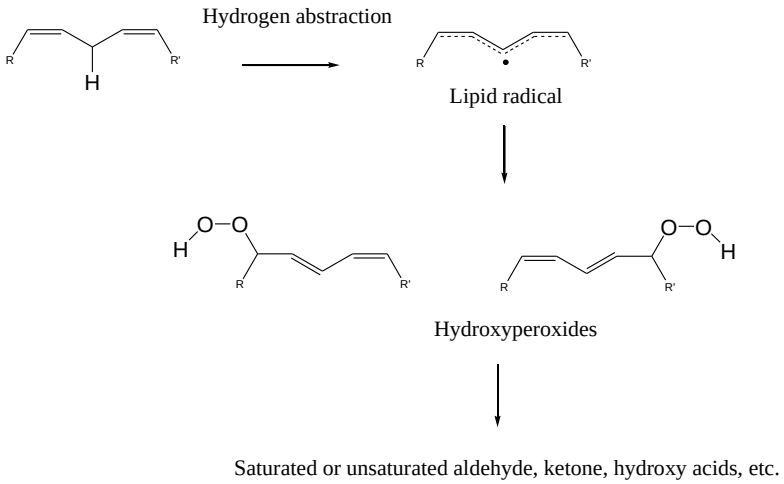

Scheme 2.4 Autoxidation of unsaturated lipids [56]

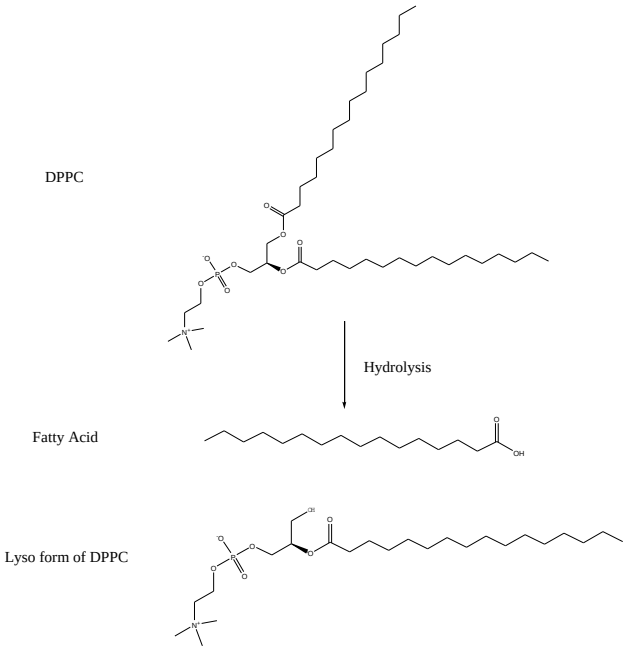

Scheme 2.5 Hydrolysis of dipalmitoylphosphatidylcholine (DPPC).

2.3.2 Overview of separation techniques for oligonucleotides

Many separation techniques have been explored in the past for the analysis of oligonucleotides. These include polyacrylamide gel electrophoresis (PAGE), capillary

gel electrophoresis (CGE), anion-exchange chromatography, and ion-pair reversed-phase liquid chromatography (IP-RPLC). The techniques developed for oligonucleotides, in theory, are applicable for the analysis of siRNA and their potential degradation products in LNPs. The separation method should afford sufficient selectivity between siRNA and its potential hydrolytic breakdown products, which often differ by one or two nucleotides from the parent molecule. Furthermore, the method should enable the separation of siRNA with a phosphorothioate linkage from its potential oxidation product (i.e., siRNA with a phosphodiester linkage). High performance liquid chromatography (HPLC) is an ideal technique to fulfill this need. With the introduction of sub- 2μm particles in column with a narrower outer diameter, coupled with significant improvement in instrument hardware, HPLC has superior separation efficiency, excellent accuracy, and precision. The technique encompasses a broad range of separation modes including normal phase, reverse phase, ion-exchange, ion-pair chromatography, etc. Due to the extreme polarity of oligonucleotides (RNA or DNA), an early study suggested that separation using conventional reversed-phase HPLC would be challenging. [58] Anion exchange chromatography has the potential to provide adequate resolution for RNA analysis due to charge interaction between RNA with negative charges and anionic exchangers on the stationary phase. [59, 60,61] IP-RPLC also provides adequate separation for oligonucleotides due to a retention mechanism that is similar to ion exchange chromatography. [62,63,64]

Capillary electrophoresis (CE) is another attractive technique for siRNA analysis, largely due to its ultra-high separation efficiency, fast analysis time and its charge-to-frictional-drag-ratio based separation mechanism that is compatible with negatively charged siRNA analytes. Since the differences in charge-to-frictional-drag ratios for

different RNA molecules diminish rapidly as the number of nucleotides exceeds 10, the separation of a typical sample of siRNA (21 to 23 mers) would require capillary gel electrophoresis (CGE), where the polymer network in the gel provides separation for large oligonucleotides. The differential migration in CGE is based on both charge and molecular size.[65]

The detection of siRNA is relatively straightforward since one of the building blocks of siRNA, the nucleoside, exhibits a large molar absorptivity in the UV region, making the diode array absorbance detector an excellent choice for detection. Further structural elucidation of potential degradation products would require the use of in-line mass spectrometry following the LC separation. Liquid chromatography electrospray ionization mass spectrometry (LC-ESI-MS) is a standard technique in the pharmaceutical industry for quantifying the active drug and its metabolite(s) in biological fluids. Its application to oligonucleotides is promising but not without challenges, such as the (i) limited ionization efficiency and signal suppression due to significant adduct formation with sodium or potassium cations; and (ii) potential inconsistency of chromatographic resolution and mass detection in terms of mobile phase selection.[66]

2.3.2.1 Ion-pair reversed-phase liquid chromatography

Ion-pair reversed-phase liquid chromatography (IP-RPLC) is an extension of traditional RPLC. Both techniques share some common features, including the hydrophobic organic mobile phases and nonpolar stationary phases that are employed. The key difference between them is the inclusion of small organic salts (e.g., sodium hexane sulfonate or tetrabutylammonium acetate) in the mobile phase for IP-RPLC. The hydrophobic portion of ion-pair reagent adsorbs onto the C18 phase of the column,

providing a dynamic ion-exchange phase for the retention of analytes with opposite charges. The overall retention in IP-RPLC is related to charge and hydrophobicity of the analyte. The separation selectivity can be tuned by varying the identity and/or concentration of the ion-pair agent, the pH of the mobile phase, and the identity and/or percentage of organic solvent in the mobile phase. Like regular RPLC, the stationary phase can significantly impact the selectivity in IP-RPLC.

The separation mechanism of oligonucleotides in IP-RPLC was systematically studied by comparing the retention time of an array of homo-oligonucleotides (< 40 mers) and various oligonucleotides with a minor structural difference on two types of stationary phases, the Clarity Oligo-RP and Synergi Polar RP. In addition to the hydrophobic interactions, the studies suggested that dipolar and π- π interactions also contributed significantly to retention. Columns that can provide these additional interactions provided a better resolution between oligonucleotides that differ by one base pair or by one nucleotide unit. [67]

An IP-RPLC method was developed to quantify and characterize the antisense oligonucleotides, their impurities, and major metabolites. [64] The separation was performed on a capillary HPLC system with a Terra MS C18 column packed with 2.5-µm porous sorbent. The small particle size improves the separation efficiency by reducing band broadening due to eddying or resistance to mass transfer. **Figure 2.10** compares a typical chromatogram of a mixture of 7- to 30-mer oligonucleotides on RP-HPLC with a typical chromatogram of the same mixture on CGE. The separation is highly dependent upon the selection of ion-pair reagent. **Figure 2.11** compares the separation of 25-mer phosphorothioate oligonucleotide by means of the triethylammonium acetate (TEAA)

ion-pair system with that by means of triethylamine-hexafluoroisopropanol (TEA-HFIP). The former system showed no resolution of individual oligomers, while the latter system demonstrates baseline resolution. An increase in TEA concentration further improves the separation. The superior resolution achieved with TEA-HFIP is attributed to a reduction of the impact of the oligonucleotide's hydrophobicity on retention, a reduction that appears to be crucial to a successful separation. The mobile phase composition not only impacts the separation, but it also significantly influences the mass spectrometry signal used as one means of the detection. TEAA at 100 mM concentration significantly suppresses the ionization efficiency of the oligonucleotides. The best signal-to-noise ratio for MS was achieved with TEA-HFIP.

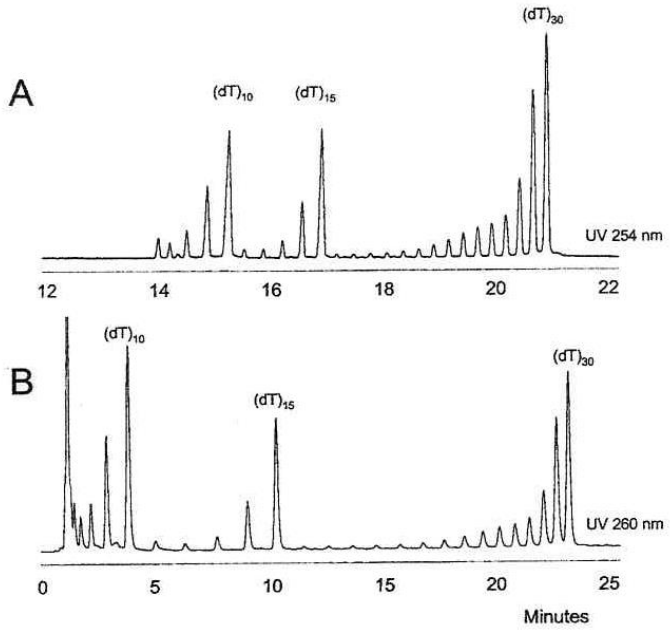

Figure 2.10 Separation of 30-mer homooligodeoxythymidines on A: ion-pair reversed-phase LC; and B: capillary gel electrophoresis. [64]

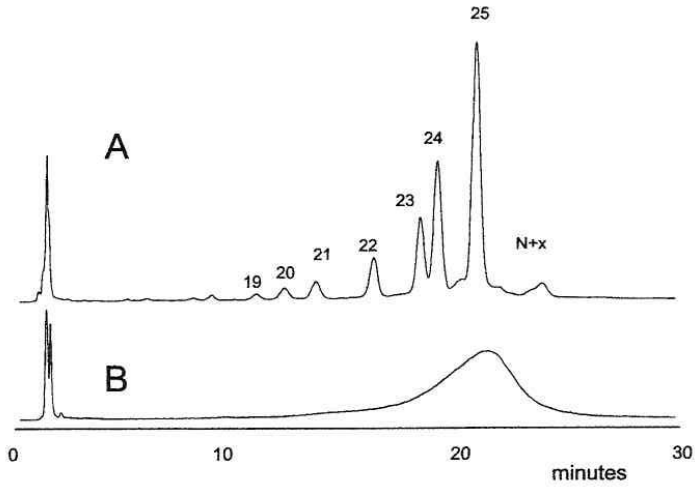

Figure 2.11 Impact of ion-pair reagent on the separation of phosporothioate oligonucleotides (19- to 25-mer); A: TEAA; B: TEA-HFIP [64]

The ion-pair RPLC was also employed for the analysis and purification of siRNA. The oligonucleotides were separated using an X-Bridge C18 column. The mobile phase components consisted of aqueous 0.1 M TEAA (pH 7) and 80/20 aqueous 0.1 M TEAA/ACN. A gradient elution method was developed to separate the target siRNA duplex from its synthetic impurities - potential mismatched duplexes arising from the annealing of a mixture of a full-length upper strand and its complementary truncated lower strand. [68]

2.3.2.2 Ion-exchange chromatography

Ion-exchange chromatography (IEC) has some similarity to IP-RPLC in terms of the retention mechanism. Their key difference lies in the nature of the association between ion exchangers and column stationary phase support. For IEC the ion exchangers are covalently bonded to the column stationary phase. Quaternary ammonium and sulfonate groups are characterized as strong ion exchangers. The

selectivity in IEC can be optimized through changes in pH, salt or buffer type, stationary phase, and mobile phase composition.

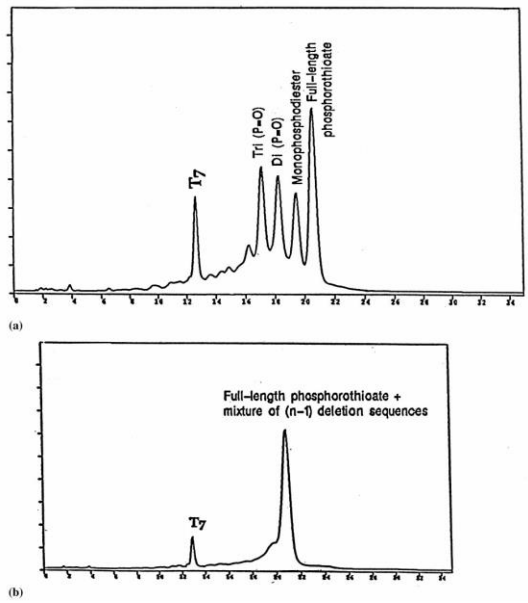

Figure 2.12 Anion exchange chromatograms of (a) a mixture containing full-length, fully thioated, 20-base oligonucleotide, 5'-GCC CAA GCT GGC ATC CGT CA-3', and its mono-, di-, and triphosphodiester analogs and (b) 1:1 solution of full-length 5%-GCC CAA GCT GGC ATC CGT CA-3% sequence and a mixture of its (*n*-1) deletion sequences. [69]

Anion exchange chromatography demonstrated an effective separation for oligonucleotides (20 bp) with fully thioated phosphorothioate linkages and its structural analogs with mono-, di-, or tri-phosphodiester substitution (**Figure 2.12**). The separation was performed on a GEN-PAK FAX or a HEMA IEC BIO column, which contains diethylaminoethyl cellulose or hydroxyethyl methylamine as the stationary phase. Gradient elution was employed, with the mobile phase containing pH 8 Tris buffer as solvent A and IPA or MeOH as solvent B. However, the method was not able to differentiate full-length oligonucleotides from their n - 1 single deletion impurities.

Complementary to ion exchange chromatography, CGE provides excellent selectivity for an oligonucleotide and its n - 1 single deletion, but it fails to achieve adequate separation for oligonucleotides with the same length and sequence but with minor differences in the number of diester groups. [69] Later, Yang and coworkers reported a strong anion exchange chromatography method (Mono Q column) for separating structural analogs of 14-mer oligonucleotides.[70] The stationary phase is composed of a quaternary amine bound to polystyrene-divinyl benzene beads, exhibiting a strong interaction with the negatively charged oligonucleotides. An acceptable resolution was achieved for oligonucleotides with phosphodiester groups as compared with those having single substitution with monothiophosphate (PS) and dithiophosphate (PS2). In this study, the type of counter ions (Cl^- vs SCN^-) and their concentration had a significant impact on the selectivity. The results also suggested that retention is linearly related to the number of sulfur groups in the oligonucleotide.

The key challenge with anion exchange chromatography is to improve the resolution of oligonucleotides that differ only by one nucleotide, which could be the case for siRNAs that undergo hydrolytic degradation (causing single deletion). New stationary phase chemistry has the potential to improve the resolution of ion exchange chromatography. In a recent study, a monolithic capillary column incorporating poly (N,N,N-triethylammonium-2-hydroxypropyl-methacrylate-co-divinylbenzene) as the stationary phase was prepared for separation of oligonucleotides. The column provided the baseline separation of oligonucleotides with 12 to 18 base pairs. [71] (**Figure 2.13**)

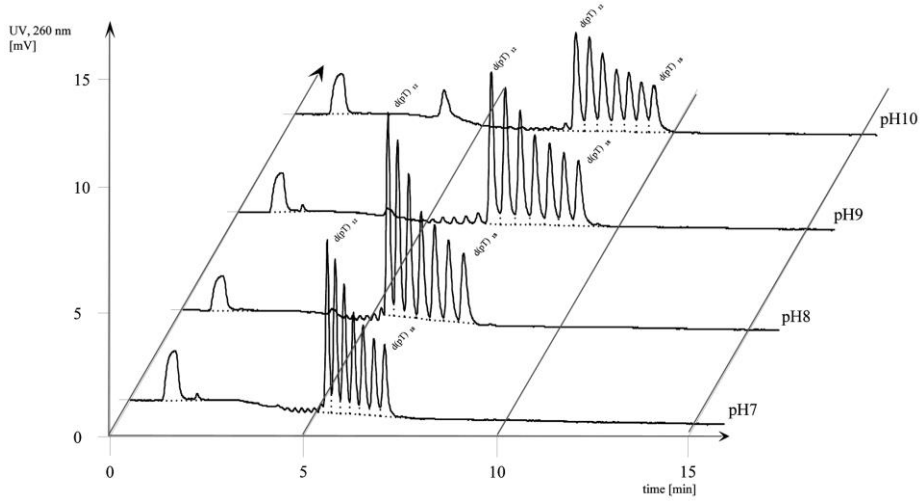

Figure 2.13 Effect of mobile pH on the separation of d(pT)12 -18 using N,N,N-triethylammonium-2-hydroxypropyl-methacrylate-co-divinylbenzene as stationary phase.[71]

2.3.2.3 Capillary electrophoresis

Capillary electrophoresis is a separation technique where the analytes are separated based on a difference in electrophoretic migration velocity (e.g., capillary zone electrophoresis). The electrophoretic migration velocity is linearly proportional to the electrophoretic mobility, which in turn is related to charge and size of the analyte. The migration velocity of the analyte in a capillary also depends on the rate of electroosmotic flow (EOF). When an electric field is applied across the capillary filled with slightly acidic to strongly basic buffers, negative charges are formed in the inner surface of the silica capillary as result of deprotonation of silanol groups. Hydrated cations in a buffer solution associate with negatively charged silanol groups, creating an electrical double layer. When an electric voltage is applied across the capillary, the positive ions in the diffuse region of the electric double layer will migrate toward the anode, pulling water along and creating a bulk electroosmotic flow. The velocity of the liquid in a narrow tube is nearly uniform across the inner diameter of the capillary resulting in a plug flow,

which is in direct contrast to the parabolic flow exhibited in the pumped flow of a packed HPLC column.

Many separation modes have been developed in past decades using CE for various applications. Those include capillary zone electrophoresis (CZE), capillary isoelectric focusing, and capillary gel electrophoresis (CGE). CGE is mostly used for bimolecular analysis due to the added retention mechanism related to the size and conformational feature of the analytes. CGE is a slight variation from CZE, where the separation is performed in a polymer matrix filled with buffer. The porous network of the polymer gel will hinder the migration of the analytes to different extents depending on their frictional drag (related to molecular size), which has proven to be useful for DNA and RNA analysis.

As mentioned previously, CGE is not suitable for separating oligonucleotides with minor structural differences in the ribose-phosphate linkage (phosphorothioate *vs* phosphodiester), but it does provide superior resolution for oligonucleotides that differ by only one nucleotide. The first comprehensive study on RNA separation by means of CGE was reported by Skeidsvoll and Ueland in 1996. The results suggested that the type of gel polymer, gel concentration, electrical field strength, and temperature are the key variables impacting the separation of RNA with a different number of base pairs. RNAs with base pairs ranging from 100 to 6000 were well separated under an electric field of 200 V/cm in a separation medium consisting of tris-borate, urea and 0.3% HPMC. [72] In another example, baseline resolution was achieved for a mixture of six phosphorothioate oligonucleotides (16 to 21 mers) differing in length by one nucleotide (**Figure 2.14**). [73]

The separation was performed with a gel matrix and elution buffer consisting of 10% micro-gel in the tris-borate buffer at pH 9.

Most CGE methods were developed for analyzing single-stranded oligonucleotides. For duplex RNA or DNA, the samples are typically denatured first (into separate strands) prior to analysis. However, the direct analysis of double-stranded oligonucleotides has occasionally been attempted. The results suggested that duplex nucleotides tend to denature on the column, resulting in the formation of two complementary single strands during the separation. Further study suggested that low-level metal ions (e.g., Na^{+} or Mg^{2+}) in the separation buffer can stabilize the duplex and suppress the on-column formation of single-stranded oligonucleotides. However, the resolution of duplex oligonucleotides from their analogs with n - 1 nucleotide is much poorer than that of single-stranded oligonucleotides.[74]

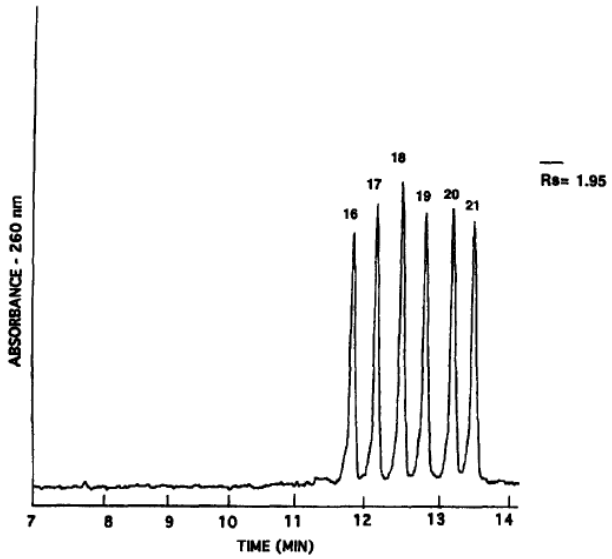

Figure 2.14 Electropherogram of a mixture of six phosphorothioate oligonucleotides (16-21 mers) differing in length by one nucleotide. (Electrophoresis was conducted with an electrokinetic injection at -8 kV for 5 s, and a constant running voltage of -22 kV was used.) [73]

2.3.3 Overview of lipid separation and analysis

Lipids are in a class of biomolecules covering a wide range of chemical structures. The structural diversity is essential to their biological functions. Aside from composing the membrane bilayer, lipids also provide an energy source for metabolism and participate in metabolic processes, including signal transduction, secretion, and protein trafficking. [75,76] The comprehensive analysis of lipid species, their related networks, as well as their metabolic pathways at the molecular level, has evolved into an exciting research field – known as lipidomics – more than 14 years ago. [77,78] Separation techniques, coupled with powerful structure characterization tools, such as mass spectrometry or NMR, are at the forefront in addressing fundamental questions around the biological roles of lipids in human health and disease.[79, 80, 81]

Prior to the development of HPLC techniques, lipids were analyzed by means of GC, but thermal degradation concerns during the sample introduction process limit this approach for broad applications. [82] Although there are some reports on the use of capillary electrophoresis for lipid analysis, [83] its predominant use of aqueous separation media prevents its application to the analysis of non-polar lipids, which have solubility issues in aqueous media. As a product of the earlier efforts towards the development of liquid chromatography, thin-layer chromatography (TLC) has been used quite extensively for lipid analysis because of its simplicity and high-throughput. The refined version of high-performance TLC is a valuable tool for the analysis of different classes of lipids. Among all the separation techniques, HPLC is often the method of choice for total lipid analysis. Two common separation modes are normal phase HPLC and reversed phase HPLC. [84,85] Normal phase HPLC separates lipids based on an

adsorption/desorption process, where the interaction between hydrophilic moiety in the lipid (e.g., the polar head-group) and the polar stationary phase dominates the retention mechanism. The separation of the lipids in NP-HPLC is more selective for structural differences between lipid classes than within a lipid class. **Figure 2.15** shows the separation of representative lipid classes by means of normal phase chromatography. [86]

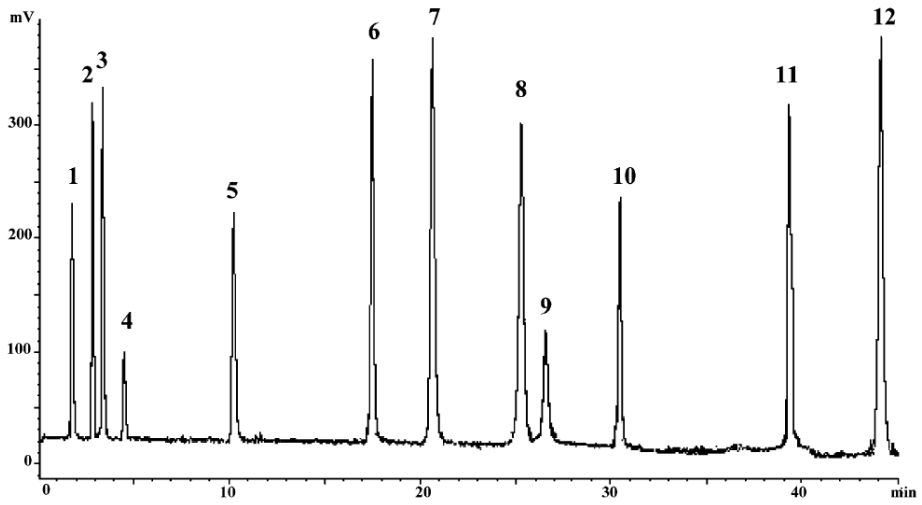

Figure 2.15 Separation of lipid classes representatives (1) PAR (paraffin, liquid), (2) WE (*n*-hexyldecyl palmitate), (3) CE (cholesteryl palmitate), (4) FAME (stearic acid methyl ester), (5) TAG (glycerol tripalmitate), (6) FOH (hexadecyl alcohol), (7) FFA (stearic acid), (8) CHOL (cholesterol), (9) 1,3-DAG (glycerol-1,3-dipalmitate), (10) 1,2-DAG (glycerol-1,2-dipalmitate), (11) MAG (glycerol monopalmitate) and (12) FAA (erucylamide) [86]

For reversed-phase HPLC, the lipids are separated based on overall polarity, the degree of saturation in the alkyl chain, and the chain length, thus providing a greater selectivity for lipids of different structure within classes than the normal phase separation mode provides. Both isocratic and gradient mobile phase conditions with reversed-phase HPLC were reported for the separation and analysis of lipids in relatively simple sample

matrices. For example, an isocratic HPLC method was developed for the analysis of cholesterol, 1,2-dioleoyl-*sn*-glycero-3-phosphocholine (DOPC), and degradation products of DOPC, including oleic acid and lysophosphatidylcholine. [87] The separation was accomplished in 20 minutes with satisfactory resolution on a Basil BDS C8 column. The mobile phase was comprised of pH 2.7 phosphate buffer and MeOH at a 15:85 volume ratio. The validation was excellent with respect to specificity, linearity, and recovery and precision. Zhong et al. reported the analysis of cationic liposomes with RPLC coupled to an evaporative light scattering detector (ELSD). A gradient method was developed that provided an excellent separation of 1,2-dioleoyl-3-trimethylammonium propane (DOTAP), 1,2-distearoyl-sn-glycero-3-phosphatidylcholine (DSPC), DPPC, and cholesterol within 15 minutes (**Figure 2.16**). The method was also capable of separating lipid degradation products, including the fatty acids and the lyso forms of lipids (i.e., the remaining part of the lipid after the loss of an acyl group from the sn - 1 position of the parent lipid). Since DPPC and DSPC have very weak UV absorption, the principal means of detection was an ELSD. A limit of quantification (LOQ) of 0.3 µg was demonstrated with the nebulizer and evaporator temperature of the ELSD set at 50^{o}C and 75 ^{o}C, respectively. The N_2 gas flow was set at 1.5 ml/min. [88]

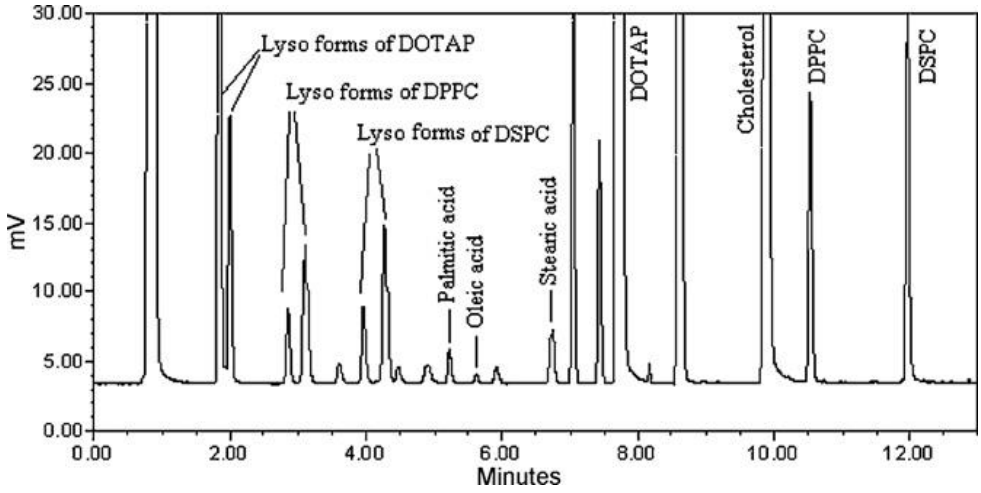

Figure 2.16 Example chromatogram of forced degradation of a lipid mixture using 0.1N HCl at room temperature for 4 days. [88]

Most of the bonds in lipids are C-C and C-H bonds, resulting in very weak UV chromophores and thus poor sensitivity with a UV absorbance detector. Universal detectors, such as the evaporative light scattering detector (ELSD) [89] and the charged aerosol detector (CAD), [90] are often the detector of choice for routine analysis of lipids. The key advantage of ELSD is the universal signal response as a function of analyte concentration, regardless of the spectral properties. There are three steps involved in ELSD operation, the nebulization of the eluent from the mobile phase, the evaporation of residual solvent and quantitation of non-volatile dried particles based on light scattering technique. The signal response is highly dependent upon the distribution and average value of the droplet size in the nebulization, which in turn depends on (i) the flow rate of the mobile phase, (ii) the nebulization gas, and (iii) the mobile phase composition. The key limitation of the ELSD is its relatively high limit of quantitation (LOQ, ~ 0.1 µg) and narrow dynamic range (2-3 orders of magnitude). Also, this detector has little tolerance to buffer salt, and the mobile phase has to be volatile.

Another alternative to the UV absorbance detector is the charged aerosol detector (CAD), which was introduced commercially in 2005. It has many features in common with the ELSD but a markedly improved limit of quantification (low ng to high ug) and a wider dynamic range (four orders of magnitude). A minor drawback for both ELSD and CAD is the slightly non-linear relationship between the analytical signal and analyte concentration. The operational principles for CAD are similar to ELSD in the nebulization and evaporation steps. The key distinction lies in the last step where the CAD transfers charge to the dried sample particles with N_2 gas that has passed a high-voltage platinum wire. The resulting charged particles are then measured by an electrometer. The CAD also demonstrates better reproducibility than ELSD.

2.4 Research objectives and rationales

Lipid nanoparticle (LNP) has emerged as a promising delivery vehicle for siRNA therapeutics that can potentially overcome the barriers to drug delivery. The development of a safe and efficacious LNP formulation is labor-intensive. The process involves the characterization of several critically important quality attributes, among which is the chemical stability of key constituents in the LNP systems. This research focused on three objectives aiming to address the challenges associated with stability characterization of the LNP systems. The first objective was to develop a separation method that can monitor the stereoisomers of a chemically modified siRNA and their potential oxidation products. Various chemical modifications are often made to synthetic RNA to prevent hydrolysis by endonucleases. The phosphorothioate modification is commonly used to improve siRNA stability. The phosphorothioate linkages introduce

additional chiral centers to siRNA, forming multiple stereoisomers that have different biological activities. A separation method capable of resolving siRNA stereoisomers can be a valuable tool to study the structure and gene-silencing activity relationship of the stereoisomers. Furthermore, the method can be used to characterize the chemical stability of the siRNA stereoisomers. The siRNA with phosphorothioate modification can undergo desulfurization in the presence of oxidants, where the sulfur atom is replaced by an oxygen atom. Desulfurization reaction is detrimental to siRNA stability due to hydrolysis and should be closely monitored and controlled in the formulation. Separation of closely related siRNA stereoisomers is a well-noted challenge in the field of separation science. This research attempted to bridge the gap in the literature by studying key chromatographic parameters central to the separation of siRNA stereoisomers by means of ion-pair reversed-phase HPLC.

The second objective of the research was to develop an integrated separation methodology that can quantify siRNA, lipids, and their potential degradation products. Such enabling separation method can significantly increase the speed and throughput during the pre-clinical evaluation of LNPs, where a large array of formulations containing multiple siRNAs and lipids are routinely analyzed to support various *in vivo* studies. To ensure a universal use of the proposed separation method for an LNP system where multiple siRNAs and lipids might co-exist, we deliberately selected a series of siRNAs with different sequences and chemical modifications as well as a range of lipids with different chain lengths and head groups for the study. While there is a significant literature presence concerning the separation of RNA or lipids in their respective sample

matrix, to the best of our knowledge, there is no prior work on the simultaneous separation of siRNAs, lipids, and their related impurities.

Lastly, the research aimed to map out the main degradation pathways for a chemically modified siRNA by means of forced stress testing. Forced stress testing is a useful tool that can predict a stability problem during formulation development. Few studies have been reported in the literature to use this predictive tool to study the stability performance of a chemically modified siRNA. Here we systematically evaluated the stability attributes of a model siRNA under various stress conditions. The goal was to provide a mechanistic understanding of siRNA degradation chemistry and a scientific framework for a rational selection of the key functional excipients for the LNP formulation.

Among the various separation techniques reviewed in Chapter 2, we selected ion-pair reversed-phase liquid chromatography (IP-RPLC) as the method of choice for our research. The selection was based on a careful comparison of the advantages and disadvantages of the main techniques for RNA and lipid analysis. Ion exchange chromatography (IEC), IP-RPLC, and capillary gel electrophoresis (CGE) are attractive techniques that have been used widely for RNA analysis. For IEC, the separation is based on differential electrostatic affinities of the negatively charged RNAs for the positively charged stationary phase. The main advantage of the technique is its ability to separate RNA and its common N-x deletions, where N represents the number of base pairs in the parent RNA and x stands the number of the base pairs removed from the parent strand. The technique is also capable of separating RNA with phosphodiester (PS) linkages from that with phosphorothioate (PO) linkages, where the structural difference

between the samples can be a single atom: sulfur instead of oxygen. The change of one atom on such a large molecule can still create enough difference in charge to allow separation by anion exchange chromatography. The disadvantage of IEC is that the technique is not very selective for RNAs that are the same length but have different base pairs. In addition, the mobile phase for IEC contains a high concentration of non-volatile inorganic salts, which is not compatible with a mass spectrometer and requires an additional interface between the LC and the MS detector to remove the salts (i.e., a desalting step).

The separation in CGE is primarily based on the length of the oligonucleotide strand. The electrophoretic mobility of the analyte is also influenced by the type and concentration of the polymer gel. The key advantage for CGE is its extraordinary resolving power, which allows the separation of the RNAs based on size and charge. Similar to IEC, the technique lacks the selectivity in separating RNAs that have the same length but minor difference in base pairs. The technique can be interfaced with a mass spectrometer, but it requires significant efforts to remove the high concentration of non-volatile salts and buffers that are typically used for the separation.

IP-RPLC separates RNA based on both electrostatic and hydrophobic interactions between the analytes and the stationary phase. The technique offers many advantages in RNA separation that are similar to IEC. Like IEC, IP-RPLC separates RNA based on the length of the strand, providing an excellent selectivity for RNA and its N-x deletion products. IP-RPLC is also capable of separating RNAs with PO and PS linkages, which is similar to IEC. What differentiates IP-RPLC from IEC is its ability to separate RNA from its potential impurities that have the same length as the parent strand but with

different base pairs. Furthermore, IP-RPLC can employ volatile ion-pair reagents, and thus can be directly interfaced to a mass spectrometer for structural characterization.

Among the three techniques discussed so far, ion-pair reversed-phase HPLC emerged as a lead option for RNA analysis owing to its dual retention mechanism and has the potential to separate RNA and its closely related degradation products. Furthermore, it is likely the only technique suitable for separating both RNAs and lipids. The extremely hydrophobic nature of the lipids makes their separation difficult with IEC or CGE; both are mostly aqueous-based separation techniques.

List of References

1. A. Fire, S. Xu, M.K. Montgomery, S.A. Kostas, S.E. Driver, C.C. Mello, Potent and specific genetic interference by double-stranded RNA in Caenorhabditis elegans, Nature. 391 (1998) 806-811.

2. S.M. Elbashir, J. Harborth, W. Lendeckel, A.Yalcon, K.Weber, T. Tuschl, Duplexes of 21-nucleotide RNAs mediated RNA interference in cultured mammalian cells, Nature. 411 (2001) 494-498.

3. G. Meister, T. Tuschl, Mechanism of gene silencing by double-stranded RNA, Nature. 431 (2004) 343-349.

4. Y.K. Oh, T.G. Park, siRNA delivery systems for cancer treatment, Adv. Drug Delivery Rev. 61 (2009) 850-862.

5. F. Apparailly, C. Jorgensen, siRNA-based therapeutic approaches for rheumatic diseases, Nat. Rev. Rheumato. 9 (2013) 56-62.

6. J.B. Nachega, J.J. Parienti, O.A. Uthman, R. Gross, D.W. Dowdy, P.E. Sax, J.E. Gallant, M.J. Mugavero, E.J. Mills, T.P. Giordano, Lower pill burden and once-daily antiretroviral treatment regimens for HIV Infection: A meta-analysis of randomized controlled trials, Clin. Infect. Dis. 58(9) (2014)1297-1307.

7. J.G. McHutchison, M. Manns, K. Patel, T. Poynard, K.L. Lindsay, C. Trepo, J. Dienstag, W.M. Lee, C. Mak, J.J. Garaud, A.K. Albrecht, Adherence to combination therapy enhances sustained response in genotype-1–infected patients with chronic hepatitis C, Gastroenterol. 123 (2002) 1061–1069.

8. T. Coelho, D. Adams, A. Silva, P. Lozeron, P.N. Hawkins, T. Mant, J. Perez, et al., Safety and efficacy of RNAi therapy for transthyretin amyloidosis, N. Engl. J. Med. 369 (2013) 819-829.

9. J.C. Burnett, J.J. Rossi, RNA-based therapeutics: current progress and future prospects, Chem. Bio. 19 (2012) 60-71.

10. J.C. Burnett, J.J. Rossi, K. Tiemann, Current progress of siRNA/shRNA therapeutics in clinical trials, Biotechnol. J. 6(9) (2011) 1130–1146.

11. A. Wittrup, J. Lieberman, Knocking down disease: a progress report on siRNA therapeutics, Nat. Rev. Genet. 16(9) (2015) 543-552.

12. G. Ozcan, B. Ozpolat, R.L. Coleman, A.K. Sood, G. Lopez-Berestein, Preclinical and clinical development of siRNA-based therapeutics, Adv. Drug Deliv. Rev. 87 (2015) 108-119.

13. T.S. Zatsepin, Y.V. Kotelevtsev, V. Koteliansky, Lipid nanoparticles for targeted siRNA delivery-going from bench to bedside, Int. J. Nanomed. 11 (2016) 3077-3086.

14. J.E. Zuckerman, I. Gritli, A. Tolcher, J.D. Heidel, D. Lim, R. Morgan, B. Chmielowski, A. Ribas, M.E. Davis, Y. Yen, Correlating animal and human phase Ia/Ib clinical data with CALAA-01, a targeted, polymer-based nanoparticle containing siRNA, Proc. Nalt. Acad. Sci. 111(31) (2014) 11449-11454.

15. R. Kanasty, J.R. Dorkin, A. Vegas, D. Anderson. Delivery materials for siRNA therapeutics, Nat. Mater. 12 (2013) 967-977.

16. K.A. Whitehead, R. Langer, D.G. Anderson, Knocking down barriers: advances in siRNA delivery, Nat. Rev. Drug Discov. 8 (2009) 129-138.

17. J. Wang, Z. Lu, M.G. Wientjes, J.L.S. Au, Delivery of siRNA therapeutics: barriers and carriers, AAPS J. 12(4) (2010) 492-502.

18. K. Tatiparti, S. Sau, S.K. Kashaw, A.K. Lyer, siRNA delivery strategies: a comprehensive review of recent developments, Nanomaterials. 7(4) 2017 77-94.

19. J.M. Layzer, A.P. Mccaffrey, A.K. Tanner, Z. Huang, M.A. Kay, B.A. Sullenger, In vivo activity of nuclease-resistant siRNAs, RNA. 10 (2004) 766–771.

20. I.G. Ganley, K. Carroll, L. Bittova, S. Pfeffer, Rab9 GTPase regulates late endosome size and requires effector interaction for its stability, Mol. Biol. Cell, 15 (2004) 5420–5430.

21. K. Gao, L. Huang, Nonviral methods for siRNA delivery, Mol. Pharm. 6(3) (2009) 651-658.

22. S. Zhang, B. Zhao, H. Zhao, B. Wang, Cationic lipids and polymers mediated vector for delivery of siRNA, J. Control. Release. 123(1) (2007) 1-10.

23. L. Li, Y. Shen, Overcoming obstacles to develop effective and safe siRNA therapeutics, Expert Opin. Biol. Ther. 9(5) (2009) 609-619.

24. S.Y. Wu, N.A.J. McMillan, Lipidic systems for In Vivo siRNA Delivery, AAPS J. 11(4) (2009) 639-652.

25. A. Schroedet, C.G. Levins, C. Cortez, R. Langer, D.G. Anderson, Lipid-based nanptherapeutics for siRNA delivery, J. Intern Med. 267(1) (2010) 9-21.

26. P.L. Felgner, T.R. Gadek, M. Holm, R. Roman, H.A. Chan, M. Wenz, J.P. Northrop, G.M. Ringold, M. Danielsen, Lipofection: a highly efficient, lipid-mediated DNA transfection procedure, Proc. Natl. Acad. Sci. 84 (1987) 7413-7417.

27. R.W. Malone, P.L. Felgner, I.M. Verma, Cationic liposome-mediated RNA transfection, Proc. Natl. Acad. Sc. 86 (1989) 6077-6081.

28. S.C. Semple, A. Akinc, J. Chen, A.P. Sandhu1, B.L. Mui, C.K. Cho, D.W.Y. Sah, D. Stebbing, et al. Rational design of cationic lipids for siRNA delivery, Nat. Biotechnol. 28(2) (2010) 172-176.

29. D.T. Augustea, K. Furmanb, A. Wongc, J. Fullera, S.P. Armesd, T. J. Deminge, R. Langer, Triggered release of siRNA from poly(ethylene glycol)-protected, pH-dependent liposome, J. Control. Release. 139 (2008) 266-274.

30. M.S. Martina, V. Nicolas, C. Wilhelm, C. Ménager, G. Barratt, S. Lesieur, The in vitro kinetics of the interactions between PEGylated magnetic-fluid-loaded liposomes and microphages, Biomaterials. 28 (2007) 4143-4153.

31. S. Martino, I.D. Girolamo, R. Tiribuzi, F. D'Angelo, A. Datti, A. Orlacchio, Efficient siRNA delivery by the cationic liposome DOTAP in human hematopoietic stem cells differentiating into dendritic cells, J. Biomed Biotechnol. 2009 (2009) 410260-410267.

32. S. Spagnou, A.D. Miller, M. Keller, Lipidic carriers of siRNA: differences in the formulation, cellular uptake, and delivery with plasmid DNA, Biochemistry. 43 (2004) 13348-13356.

33. A. Akinc, A. Zumbuehl, M. Goldberg, E.S. Leshchiner, V. Busini, N. Hossain, S.A. Bacallado, D.N. Nguyen, *et al.* A combinatorial library of lipid-like materials for delivery of RNAi therapeutics, Nat. Biotechnol. 26 (2008) 561–569.

34. R.J. Lee, L. Huang, Folate-targeted, anionic liposome-entrapped polylysine-condensed DNA for tumor cell-specific gene transfer, J. Biol. Chem. 271 (1996) 8481-8487.

35. O. Zelphati, L.S. Uyechi, L.G. Barron, F.C. Szoka Jr., Effect of serum components on the physico-chemical properties of cationic lipid/oligonucleotide complexes and on their interactions with cells, Biochim. Biophys. Acta. 1390 (1998) 119–133.

36. D.J. Gary, N. Puri, Y.Y Won, Polymer-based siRNA delivery: perspectives on the fundamental and phenomenological distinctions from polymer-based DNA delivery, J. Control. Release. 121 (2007) 64–73.

37. W.J. Kim, S.W. Kim, Efficient siRNA delivery with non-viral polymeric vehicles, Pharm. Res. 269 (3) (2009) 657-666.

38. K. Chaturvedi, K. Ganguly, A.R. Kulkarni, V.H. Kulkarni, M.N. Nadagouda, W.E. Rudzinski, T. M. Aminabhavi, Cyclodextrin-based siRNA delivery nanocarriers: a state-of-the-art review, Expert Opin. Drug Deliv. 8(11) (2011) 1455-1468.

39. H. Katas, H.C. Alpar, Development and characterization of chitosan nanoparticles for siRNA, J. Control Release. 115(2) (2006) 216-225.

40. T. Rojanarata, P. Opanasopit, T. Ngawhirunpat, U. Ruktanonchai, Chitosan-thiamine pyrophosphate as a novel carrier for siRNA delivery, Pharm. Res. 25(12) (2008) 2807-2814.

41. Y. Minakuchi, F. Takeshita, N. Kosaka, H. Sasaki, Y. Yamamoto, M. Kouno, K. Honma, S. Nagahara, K. Hanai, M. Terada, T. Ochiya, Atelocollagen-mediated synthetic small interference for effective gene silencing in vitro and in vivo, Nucleic Acids Res. 32(13) (2004) 1-7.

42. F. Takeshita, Y. Minakuchi, S. Nagahara, K. Honma, H. Sasaki, K. Hirai, T. Teratani, N. Namatame, Y. Yamamoto, K. Hanai, T. Kato, A. Sano, T. Ochiya, Efficient delivery of small

interfering RNA to bone-metastatic tumors by using atelocollagen in vivo, Proc. Natl. Acad. Sci. 102(34) (2005) 12177–12182.

43. J.D. Heidel, Linear cyclodextrin-containing polymers and their use as delivery agents, Expert Opin. Drug Deliv. 3(5) (2006) 642-646.

44. E. Davis, The first targeted delivery of siRNA in humans via a self-assembling, cyclodextrin polymer-based nanoparticle: from concept to clinic, Mol. Pharm. 6(3) (2009) 659–668.

45. S. Werth, B. Urban-Klein, L. Dai, S. Höbel, M. Grzelinski, U. Bakowsky, F. Czubayko, A. Aigner, A low molecular weight fraction of polyethylenimine (PEI) displays increased tranfection efficiency of DNA and siRNA in fresh and lyophilized complexes, J. Control. Release. 112 (2006) 257-270.

46. B. Urban-Klein, S. Werth, S. Abuharbeid, F. Czubayko, A. Aigner, RNAi-mediated gene-targeting through systemic application of polyethylenimine (PEI)-complexed siRNA in vivo, Gene Ther.12 (2005) 461–466.

47. O. Boussif, F. Lezoualc'h, M.A. Zanta, M.D. Mergny, D. Scherman, B. Demeneix, J.P. Behr, A versatile vector for gene and oligonucleotide transfer into cells in culture and in vivo: polyethylenimine, Proc. Natl. Acad. Sci. 92(16) (1995) 7297-7301.

48. S.H. Kim, J.H. Jeong, T. Kim, S.W. Kim, D.A. Bull, VEGF siRNA delivery system using arginine-grafted bioreducible poly(disulfide amine), Mol. Pharm. 6(3) (2009) 718–726.

49. X.B. Xiong, H. Uludağ, A. Lavasanifar, Biodegradable amphiphilic poly(ethylene oxide)-block-polyesters with grafted polyamines as supramolecular nanocarriers for efficient siRNA delivery, Biomaterials. 30(2) (2009) 242-253.

50. J.A. Wolff, D.B. Rozema, Breaking the bonds: non-viral vectors become chemically dynamic, Mol. Ther. 16(1) (2007) 8–15.

51. D.B. Rozema, D.L. Lewis, D.H. Wakefield, S.C. Wong, J.J. Klein, P.L. Roesch, S.L. Bertin, T.W. Reppen, Q. Chu, A.V. Blokhin, J.E. Hagstrom, J.A. Wolff, Dynamic PolyConjugates for targeted in vivo delivery of siRNA to hepatocytes, Proc. Natl. Acad. Sci. 104(32) (2007) 12982-12987.

52. M. Meyer, C. Dohmen, A. Philipp, D. Kiener, G. Maiwald, C. Scheu, M. Ogris, E. Wagner, Synthesis and biological evaluation of a bioresponsive and endosomolytic siRNA−polymer conjugate, Mol. Pharm. 6(3) (2009) 752–762.

53. D. Pogochi, C. Shoneich, Chemical stability of nucleic acid–derived drugs, J. Pharm. Sci. 89(4) (2000) 443-455.

54. M. Oivanen, S. Kuusela, H. LÖnnberg, Kinetics and mechanism for the cleavage and isomerization of the phosphodiester of RNA by Brønsted acids and bases, Chem. Rev. 98 (1998) 961-990.

55. S. Choung, Y.J. Kim, S. Kim, H.O. Park, Y.C. Choi, Chemical modification of siRNAs to improve serum stability without loss of efficacy, Biochem. Biophys. Res. Commun. 342 (2006) 919–927.

56. A.H. Krotz, R.C. Mehta, G.E. Hardee, Peroxide-mediated desulfurization of phosphorothioate oligonucleotides and its prevention, J. Pharm. Sci. 94(2)(2004) 341-352.

57. N.A. Porter, S.E. Caldwell, K.A. Mills, Mechanisms of free radical qxidation of unsaurated lipids, Lipids. 30(4) (1995) 277-290.

58. S. Agrawal, J.Y. Tang, D.M. Brown, Analytical study of phosphorothioate analogues of oligodeoxynucleotides using high-performance liquid chromatography, J. Chromatogr. A 509 (1990) 396-399.

59. Y. Kato, T. Ktamura, A. Mitsui, Y. Yamasaki, T. Hashimoto, Separation of oligonuclaotides by high-performance ion-exchange chromatography on a non-porous ion exchanger, J. Chromatogr. 441 (1988) 212-220.

60. K. Cook, J. Thayer, Advantages of ion-exchange chromatography for oligonucleotide analysis, Bioanalysis, 3(10) (2011) 1109–1120.

61. D. Sýkora, F. Svec, J.M.J. Fréchet, Separation of oligonucleotides on novel monolithic columns with ion-exchange functional surfaces, J. Chromatogr. A 852 (1999) 297–304.

62. C.G. Huber, P.J. Oefner, G.K. Bonn, High-resolution liquid chromatography of oligonucleotides on nonporous alkylated styrene-divinylbenzene copolymers, Anal. Biochem. 212 (1993) 351-358.

63. M. Gilar, K.J. Fountain, Y. Budman, U.D. Neue, K.R. Yardley, P.D. Rainville, R.J. Russell II, J.C. Gebler, Ion-pair reversed-phase high-performance liquid chromatography analysis of oligonucleotides: retention prediction, J. Chromatogr. A 958 (2002) 167–182.

64. M. Gilar, K.J. Fountain, Y. Budman, J.L. Holyoke, H. Davoudi, J.C. Gebler, Characterization of therapeutic oligonucleotides using liquid chromatography with on-line mass spectrometry detection. Oligonucleotides. 13(4) (2003) 229-43.

65. G.J.M. Bruin, K.O. Bornsen, D. Husken, D.E. Gassmann, H.M. Widmer, A. Paulus, Stability measurements of antisense oligonucleotides by capillary gel electrophoresis J. Chromatogr. A 709 (1995) 181-195.

66. Z.J. Lin, W.K. Li, G.W. Dai, Application of LC–MS for quantitative analysis and metabolite identification of therapeutic oligonucleotides, J. Pharm. Biomed. Anal. 44 (2007) 330–341.

67. K.M.R. Kallury, G. Scott, M. McGinley, IP-RP-HPLC of oligonucleotides: Role of stacking and dipolar interactions in modulating selectivity and application to N/N-1-mer and single-nucleotide polymorph separations, Am. Biotech. Lab. 24(10) (2006) 20-23.

68. S.M. McCarthy, M. Gilar, J. Gebler, Reversed-phase ion-pair liquid chromatography analysis and purification of small interfering RNA, Anal. Biochem. 390 (2009) 181–188.

69. G.S. Srivatsa, P. Klopchin, M. Batt, M. Feldman, R.H. Carlson, D.L. Cole, Selectivity of anion exchange chromatography and capillary gel electrophoresis for the analysis of phosphorothioate oligonucleotides, J. Pharm. Biomed. Anal. 16(1997) 619–630.

70. X.B. Yang, R.P. Hodge, B.A. Luxon, R. Shope, D.G. Gorenstein, Separation of synthetic oligonucleotide dithioates from monothiophosphate impurities by anion-exchange chromatography on a mono-Q column. Anal. Biochem. 306 (2002) 92–99.

71. W. Wieder, C.P. Bisjak, C.W. Huck, R. Bakry, G.K. Bonn, Monolithic poly(glycidyl methacrylate-codivinylbenzene) capillary columns functionalized to strong anion exchangers for nucleotide and oligonucleotide separation. J. Sep. Sci. 29 (2006) 2478 – 2484.

72. J. Skeidsvoll, P.M. Ueland, Analysis of RNA by capillary electrophoresis, Electrophoresis. 17 (1996)1512-1517.

73. L.A. DeDionisio, D.H. Lloyd, Capillary gel electrophoresis and antisense therapeutics analysis of DNA analogs, J. Chromatogr. A 735 (1996)191-208.

74. L. Szekely, S. Kiessig, M.A. Schwarz, F. Kalman, Capillary gel electrophoresis of therapeutic oligonucleotides – Analysis of single- and double-stranded forms, Electrophoresis. 30 (2009) 1579–1586.

75. J.E. Vance, D.E. Vance, editors. Biochemistry of lipids, lipoproteins and membranes, Amsterdam: Elsevier; 2002.

76. M.R. Wenk, The emerging field of lipidomics. Nat Rev Drug Disc 2005;4:594e610.

77. J.B. German, L.A. Gillies, J.T. Smilowitz, A.M. Zivkovic, S.M. Watkins, Lipidomics and lipid profiling in metabolomics, Curr. Opin. Lipidol. 18 (2007) 66–71.

78. G. van Meer, Cellecular Lipodomics, The EMBO Journal 24 (2005) 3159–3165.

79. A. Carrasco-Pancorbo, N. Navas-Iglesias, L. Cuadros-Rodríguez, From lipid analysis towards lipidomics, a new challenge for the analytical chemistry of the 21st century. Part I: Modern lipid analysis, Trends Anal. Chem. 28(3) (2009) 263-278.

80. M. Li, L. Yang, Y. Bai, H.W. Liu, Analytical methods in lipidomics and their applications, Anal. Chem. 86 (2014) 161−175.

81. S. Sethi, E. Brietzke, Recent advances in lipidomics: Analytical and clinical perspectives, Prostag. Oth. Lipid M. 128-129 (2017) 8-16.

82. W.W. Christie, Gas chromatography–mass spectrometry methods for structural analysis of fatty acids, Lipids, 33(4) (1998) 343-353.

83. F. Gao, J. Dong, W. Li, T. Wang, J. Liao, Y. P. Liao, H. W. Liu, Separation of phospholipids by capillary zone electrophoresis with indirect ultraviolet detection, J. Chromatogr. A 1130 (2006) 259-264.

84. T. Cajka, O. Fiehn, Comprehensive analysis of lipids in biological systems by liquid chromatography-mass spectrometry, Trends Anal. Chem. 61 (2014) 192-206.

85. J.T. Lin, HPLC separation of Acyl lipid classes, J. Liq. Chromatogr. Relat. Technol. 30 (2007) 2005-2020.

86. A. Schaefer, T. Küchler, T.J. Simat, H. Steinhart, Migration of lubricants from food packagings: Screening for lipid classes and quantitative estimation using normal-phase liquid chromatographic separation with evaporative light scattering detection, J. Chromatogr. A 1017 (2003) 107–116.

87. R. Singh, M. Ajagbe, S. Bhamidipati, Z. Ahmad, I. Ahmad, A rapid isocratic high-performance liquid chromatography method for determination of cholesterol and 1,2-dioleoyl-*sn*-glycero- 3-phosphocholine in liposome-based drug formulations, J. Chromatogr. A 1073 (2005) 347–353.

88. Z.M. Zhong, Q. Ji, J.A. Zhang, Analysis of cationic liposomes by reversed-phase HPLC with evaporative light-scattering detection, J. Pharm. and Biomed. Anal. 51(2010) 947–951.

89. N.C. Megoulas, M.A. Koupparis, Twenty Years of Evaporative Light Scattering Detection, Crit. Rev. Anal. Chem. 35 (2005) 301–316.

90. T. Vehoveca, A. Obrezab, Review of operating principle and applications of the charged aerosol detector, J. Chromatogr. A 1217 (2010) 1549–1556.

Chapter 3: Separation of siRNA stereoisomers using ion-pair reversed phase liquid chromatography

The contents of this chapter were previously published in the following peer-reviewed article, with the first author contributing substantially (≈ 80-90%): Li Li, Tony Leone, Joe P. Foley, and Christopher J. Welch, *J. Chromatogr. A* 2017, *1500*. 84-88, DOI: 10.1016/j.chroma.2017.04.008.

3.1 Introduction

Small interfering RNAs (siRNAs) are complex molecular assemblies consisting of a duplex of RNA strands with a chain length of about 21 nucleotides.[1, 2] The sugar-phosphate backbone of native RNA is subject to enzymatic degradation by nucleases and also by non-enzymatic hydrolytic degradation, which can be accelerated by acidic or basic conditions.[3] Synthetic siRNAs often incorporate chemically modified nucleotides to improve *in vivo* serum stability, with replacement of the phosphodiester linkage by a phosphorothioate moiety being a common motif.[4] The modification of the hydroxyl group at the 2' ribose position with methoxy (–OMe) or fluorine (F) is also routinely used to stabilize the siRNA against hydrolysis. The phosphorothioate group in synthetic siRNAs can undergo oxidation in a desulfurization process that replaces the sulfur atom with oxygen. Studies showed that an antisense RNA drug, ISIS-2302, underwent spontaneous phosphorothioate desulfurization in a PEG-based formulation, with the oxidation being mediated by residual peroxides present in the excipients. [5] Desulfurization of phosphorothioate linkages has also been reported to take place during ESI-MS analysis, where abundant peroxy radicals formed in the gas phase promote the replacement of sulfur with oxygen.[6] Desulfurization of phosphorothioate-containing siRNAs has implications for the *in vivo* and *in vitro* chemical stability of siRNA therapeutics, and it is therefore important to develop selective and sensitive separation

methodologies to monitor the desulfurization of the phosphorothioate-containing siRNAs to ensure their stability during storage and administration.

Recent advances in RNA-based therapeutics have focused attention on the challenging problem of chromatographic separation of complex mixtures of closely related oligonucleotides. A number of sophisticated separation methods have been reported to improve resolution for the accurate quantitation of oligonucleotides in complex sample matrixes. Separation modes for the chromatographic separation of RNA oligonucleotides include ion-pair reverse phase HPLC,[7,8,9,10,11] ion-exchange chromatography[12], mixed-mode reversed-phase with ion-exchange chromatography[13] and HILIC.[14] Two-dimensional separations combining IP-RPLC or ion exchange LC with CE have been developed to further improve the resolution of oligonucleotides in highly complex sample matrixes.[15] Separation of chemically modified siRNAs containing phosphorothioate groups presents an additional challenge due to the presence of closely-related diastereomers.[16] Diastereomers of small or macromolecules can have unique and different structural and physical properties; hence separation with achiral columns is often feasible, with efforts primarily focusing on separation mode and selection of appropriate stationary and mobile phase combinations. Although the chromatographic separation of some phosphorothioate stereoisomers has been reported for 15 to 30 mer single-stranded RNAs using strong ion exchange or reversed phase HPLC,[17,18] there remains a gap in the literature on systematic investigations of the separation of the diastereomers of complex siRNA duplexes containing multiple phosphorothioate stereocenters. In this study, an ion-pair reversed-phase HPLC (IP-RP HPLC) method was developed to resolve the related diastereomers of an siRNA designed to target the

ApoB gene.[19, 20] We herein report an investigation of the influence of column chemistry, organic modifier, gradient conditions and the type and concentration of ion-pair reagent on the IP-RP UHPLC separation of these stereoisomers.

3.2 Material and methods

3.2.1 Chemicals

The siRNA duplex and the complementary single strands targeting ApoB gene were provided by Merck Sharp & Dohme (MSD) RNA synthesis group. Ion-pair reagents were sourced from two vendors: ethylamine, diethylamine, triethylammonium acetate buffer (pH 7, ~ 1.0 M in water) and tetramethylammonium acetate tetrahydrate, 99%, propylamine, 99% were purchased from Sigma-Aldrich (St. Louis, MO, USA), whereas dipropylammonium acetate (0.5 M in Water) was acquired from Fisher Scientific (Norristown, PA 19403, USA). HPLC grade acetonitrile, methanol, tetrahydrofuran as well as the crystalline Iodine (99%) were obtained from Fisher Scientific.

3.2.2 Instrument

An Agilent 1290 Infinity UHPLC system (Agilent Technologies, Santa Clara, CA, USA) was employed for the separation of siRNA stereoisomers. This UHPLC system consisted of a binary pump, a diode array detector, an autosampler and a column heater, and could be operated at a pressure up to 1200 bars. To measure siRNA melting temperature, a differential scanning microcalorimeter (MicroCal, LLC, Northampton, MA, USA) was used, which can operate over a temperature range of -10° to 130° Celsius.

3.2.3 IP-RP Chromatographic conditions

For the separation of siRNA diastereomers, the samples were subjected to gradient elution using sub-2um UHPLC columns. The columns studied in this work included the Acquity BEH C18, BEH phenyl, and Ascentis Cyano, with nominal particle sizes of 1.7 or 2.0 μm and the same column dimensions (150 x 2.1 mm). Mobile phase A consisted of an ion-pair reagent in water (pH 7) and mobile phase B was a mixture of 20% A and 80% organic modifier (either ACN, MeOH or THF). The initial gradient method was run from 6% to 14% B in 20 minutes, followed by a steeper gradient elution from 14% to 30%B in 7 minutes. The final optimized gradient program is summarized in section 3.4. The siRNA sample was prepared in 20 mM phosphate buffer (pH 7) at a concentration of approximately 0.1 mg/mL.

To achieve an optimum separation, the column should be equilibrated with a minimum of 12 column volumes (e.g., ~ 6 mL) of the mobile phase at initial composition. The column cleaning involved flushing the column with a minimal of 20 column volumes of 50:50 acetonitrile/water at 40^{o}C. The column is stored in 50:50 ACN/water when not in use. The overall of lifetime of the column was not determined at this point.

3.2.4 Differential scanning calorimetry method condition

The melting temperature (T_m, or dissociation temperature) of the siRNA duplex was measured with capillary cell micro-calorimetry. A 2 mg/mL siRNA sample solution was prepared in 0.1 M TEAA or 0.1 TEAA containing 10% of organic modifiers, such as ACN or MeOH. The sample solutions were added to a 96-well plate and automatically applied to the sample capillary controlled by a run sequence. A heating and cooling cycle

from 5^{o}C to 90 ^{o}C was applied to both the reference and sample cells with a scan rate of 1 ˚C/minute. Each sample was run in triplicate.

3.2.5 Desulfurization of siRNA duplex using Iodine

Iodine solution was used as the oxidizing agent to promote the replacement of sulfur by oxygen in phosphorothioate-containing oligonucleotides. The reaction was initiated by adding 500 µL of 0.3 mM iodine solution in ethanol to 4500 µL of the siRNA with molar ratio of about 30 to 1, iodine to siRNA. The siRNA sample solution was analyzed by UHPLC for approximately four hours after the iodine was introduced.

3.3 Results and Discussion

The ApoB gene targeted by duplex siRNA consists of 21-nucleotide sense strand and 23-nucleotide antisense strand (Figure 3.1a). The sense strand contains one phosphorothioate stereocenter, which, together with the stereocenters on the ribose sugar, results in one pair of diastereomers, while the antisense strand contains two phosphorothioate stereocenters, resulting in two pairs of diastereomers. Consequently, as shown in Figure 3.1b and 3.1c, a total of six single strand RNA stereoisomers are present in the denatured siRNA duplex, while eight different stereoisomers (four pairs of diastereomers) of the siRNA duplex are possible.

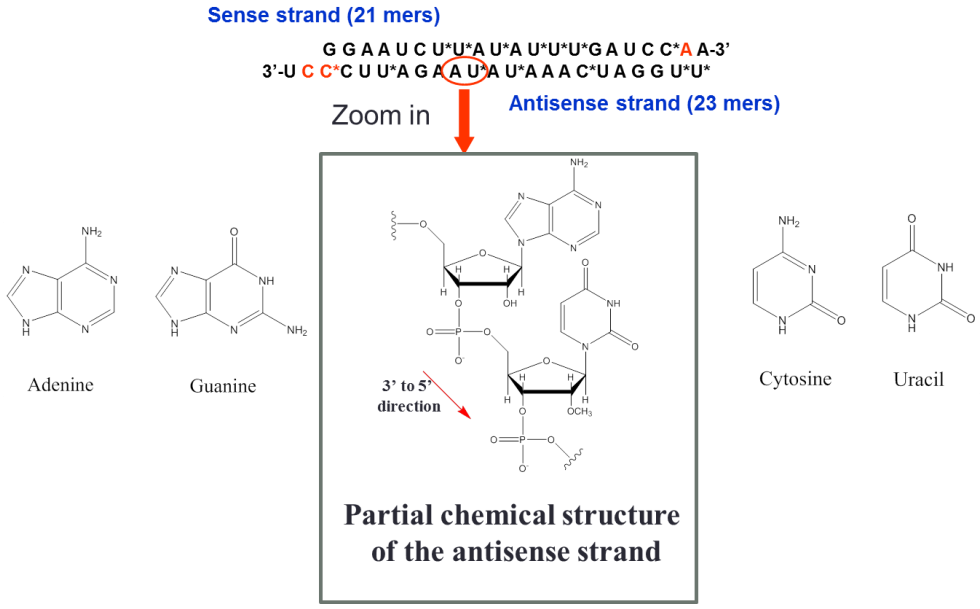

Figure 3.1a Structure of the siRNA duplex that targets the ApoB gene studied in this investigation. Nucleotides marked with asterisks contain chemically modified ribose substituents in which the 2'-OH is replaced with 2'-methoxy. In the nucleotides highlighted in red, naturally occurring phosphodiester linkages have been replaced with phosphorothioate linkages.

2 diastereomeric sense single RNA strands

G G A A U C U*U*A U*A U*U*U*G A U C C*(*S*)A A-5'
G G A A U C U*U*A U*A U*U*U*G A U C C*(*R*)A A-5'

4 diastereomeric antisense single RNA strands

3'- U C C*C U U*A G A A U*A U*A A A C*U A G G U*U*
(*S*)(*S*)
3'- U C C*C U U*A G A A U*A U*A A A C*U A G G U*U*
(*R*)(*R*)
3'- U C C*C U U*A G A A U*A U*A A A C*U A G G U*U*
(*S*)(*R*)
3'- U C C*C U U*A G A A U*A U*A A A C*U A G G U*U*
(*R*)(*S*)

Figure 3.1b: Six single-stranded siRNA species at high temperatures

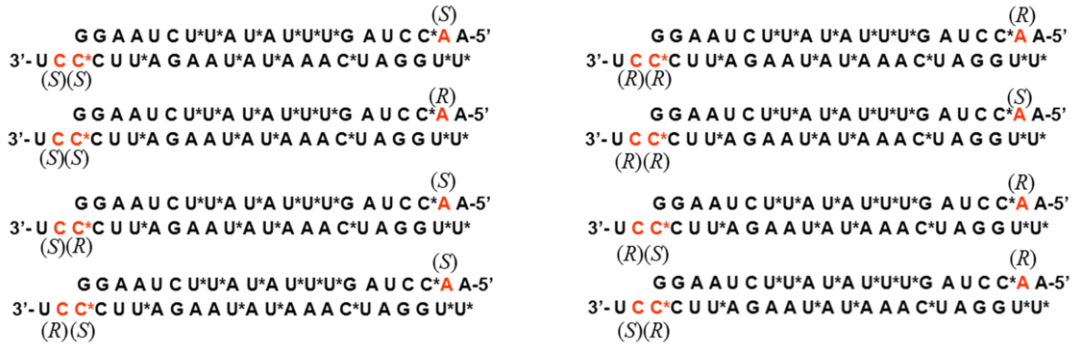

Figure 3.1c: Eight diastereomeric siRNA duplexes at low temperatures

3.3.1 The impact of column stationary phase on the separation of siRNA stereoisomers

Acquity BEH and Ascentis fused-core UHPLC columns of different stationary phase chemistry, including C18, cyano and phenyl, were explored for the separation of the six related stereoisomeric single stranded RNAs shown in Figure 3.1b. The UHPLC separation was performed at two column temperatures, 45^{o}C and 80^{o}C, where the siRNA is partially or completely denatured during gradient elution. The columns studied in this work can tolerate high temperature based on column care and use information provided by the vendor. Figure 3.2a shows the overlaid chromatographic traces for the analysis of the siRNA duplex on various UHPLC columns at 45^{o}C. The results suggest that all three types of columns can resolve up to five species, albeit with relatively poor peak shape. The poor separation at 45^{o}C is not totally unexpected since there are eight diastereomers of the siRNA duplex, making baseline separation very challenging. Figure 3.2b shows the separation of the siRNA mixture at 80^{o}C, where the duplex is presumably completely denatured; the C18 column afforded a near-baseline resolution of all six single-stranded siRNA compounds (two sense diastereomers and four antisense diastereomers) and the

phenyl column resolved four out of the six single-stranded compounds. In contrast, the cyano column provided a much poorer separation, with broad and overlapping peaks. Comparing the results in Figures 3.2a and 3.2b, the cyano column appears to be better suited to resolving siRNA duplex diastereomers, whereas the C18 and phenyl columns were more successful in resolving related single-stranded siRNA stereoisomers under a denaturing condition.

The retention mechanism governing the separation of stereoisomers under an ion-pair reversed phase separation conditions is not fully understood at this point. The C18 column, which is the most non-polar stationary phase in the series, provides the best resolution for siRNA stereoisomers at high column temperature (e.g., under a denaturing condition). This suggests that a separation condition that promotes the hydrophobic interaction between the stereoisomers and the stationary phase is likely important for achieving good selectivity.

a)

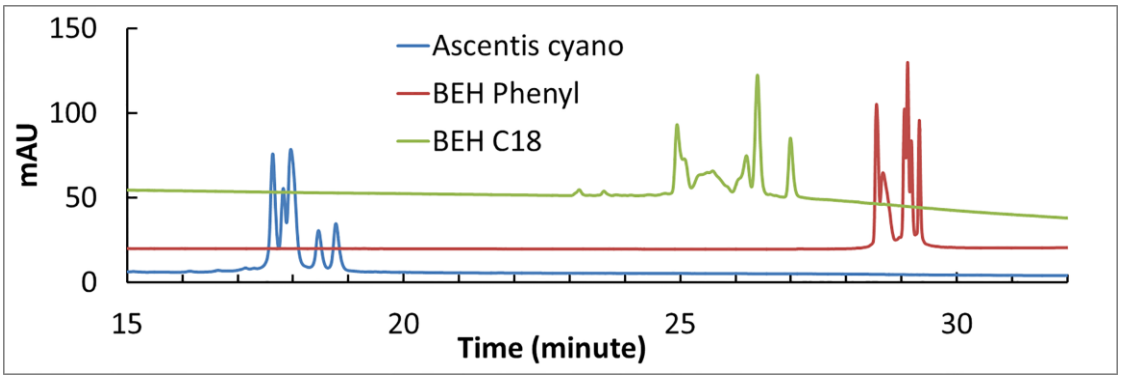

b)

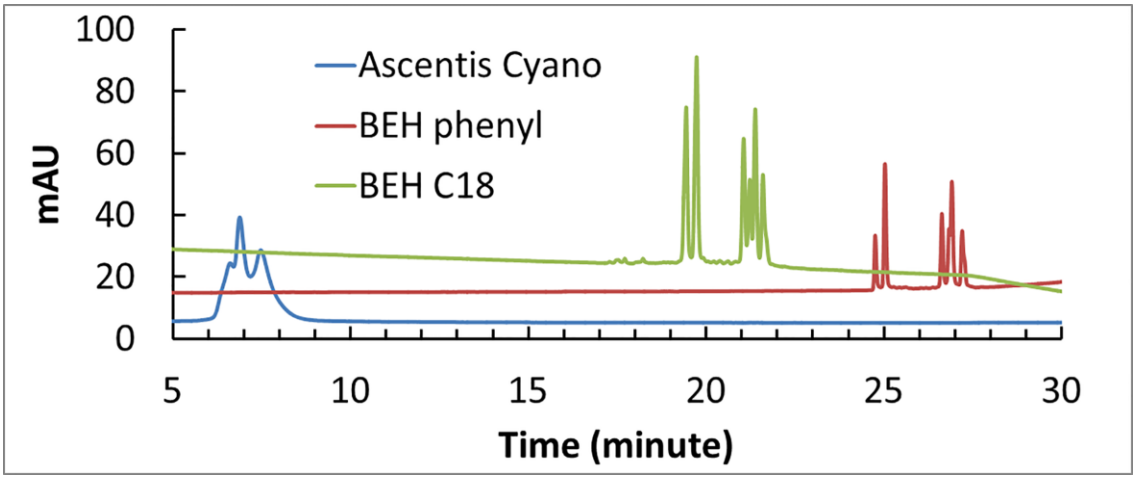

Figure 3.2 Effect of stationary phase chemistry and temperature on the separation of ion-pair reversed phase separation of siRNA stereoisomers.

a) The column temperature @ 45 ^{o}C
b) The column temperature @ 80 ^{o}C

Conditions: Columns (150 x 2.1 mm) and oven temperature as indicated. Mobile phase A consisted of 0.2M triethylammonium acetate (TEAA, pH 7) in water, and mobile phase B was a mixture of 20% A and 80% ACN. The initial gradient method was run from 6% to 14% of mobile phase B in 20 minutes, followed by a steeper gradient elution from 14% to 30% of mobile phase B in 7 minutes. The flow rate was 0.2 mL/minute and the injection volume was 2 µL, with UV absorbance detection at 260 nm. The siRNA sample concentration was approximately 0.1 mg/mL prepared in 20 mM phosphate buffer.

3.3.2 The impact of ion-pair reagents on the separation of siRNA diastereomers

IP-RPLC incorporates a small hydrophobic organic amine in the mobile phase as an ion-pair reagent, which increases the bulk hydrophobicity of the otherwise highly hydrophilic RNAs, allowing retention on the reversed-phase column. In addition, the hydrophobic portion of the ion-pair reagent also adsorbs onto the C18 stationary phase, providing a dynamic ion-exchange phase for retaining analytes with opposite charges. The structure of the ion-pair reagent has a significant influence on the separation of oligonucleotides. [21, 22] The polarity and hydrophobicity of the ion-pair reagent can modulate its dynamic interaction with the oligonucleotides and the stationary phase,

potentially impacting the retention of the analyte. Figure 3.3a shows the overlaid chromatograms for the analysis of the siRNA duplex using ethylammonium acetate, diethylammonium acetate, and triethylammonium acetate, at a concentration of 0.02 M, on a C18 column stationary phase with a column temperature of 80 ^{o}C. Additional ion-pair reagents, such as tetramethylammonium acetate, propylammonium acetate, and dipropylammonium acetate, were also evaluated (results not shown). The screening results suggested that TEAA provided the best separation of the related stereoisomers of the sense and antisense strands of the now-denatured siRNA duplex, while EAA and DEAA provided poor resolution of the same stereoisomers. Additional experiments were performed to explore the impact of ion-pair reagent concentration for ethylammonium acetate (EAA, 0.02M to 0.04M), diethylammonium acetate (DEAA, 0.02M to 0.15M), and triethylammonium acetate (TEAA, 0.05M to 0.2M), respectively. Due to limited miscibility between EAA or DEAA and acetonitrile, the upper limit of concentration was set at 0.04M and 0.15M, respectively. Figure 3.3b, 3.3c and 3.3d showed the overlaid chromatographic traces for siRNA duplex at different concentrations for EAA, DEAA and TEAA. The results show that TEAA achieved a baseline resolution for all six stereoisomers with concentration ranging from 0.05M to 0.2M. In contrast, both EAA and DEAA failed to achieve satisfactory separation at the concentration ranges explored here.

It is worth noting that TEAA, mixed with hexafluoro isopropanol (HFIP), has previously provided an effective separation of single-stranded oligonucleotides differing in sequence structure and length.[22] Our results showed that TEAA is also an efficient ion-pair reagent for the separation of denatured siRNA duplexes. The underlying

mechanism is not clear regarding the role of TEAA in separating siRNA stereoisomers. TEAA is more hydrophobic than the other ion-pair reagents studied here, which would imply that an ion-pair reagent, capable of promoting hydrophobic interaction between the stereoisomers and the stationary phase, favors the separation of the stereoisomers. Future studies should be performed to evaluate additional ion-pair reagents to understand the impact of their structure and hydrophobicity on siRNA stereoisomer separation.

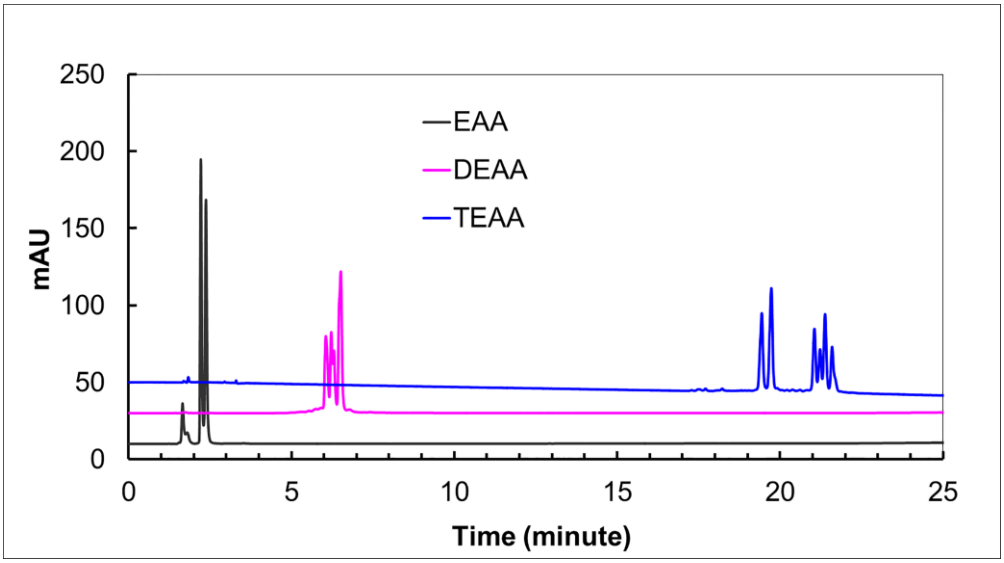

Figure 3.3a: Effect of ion-pair agent on the separation of the siRNA stereoisomers by IP-RPLC**.**
Conditions: UPLC column: BEH C18; column oven temperature: 80 ^{o}C. The concentration of ion-pair reagents is 0.02 M (pH 7). Other conditions as in Figure 3.2.

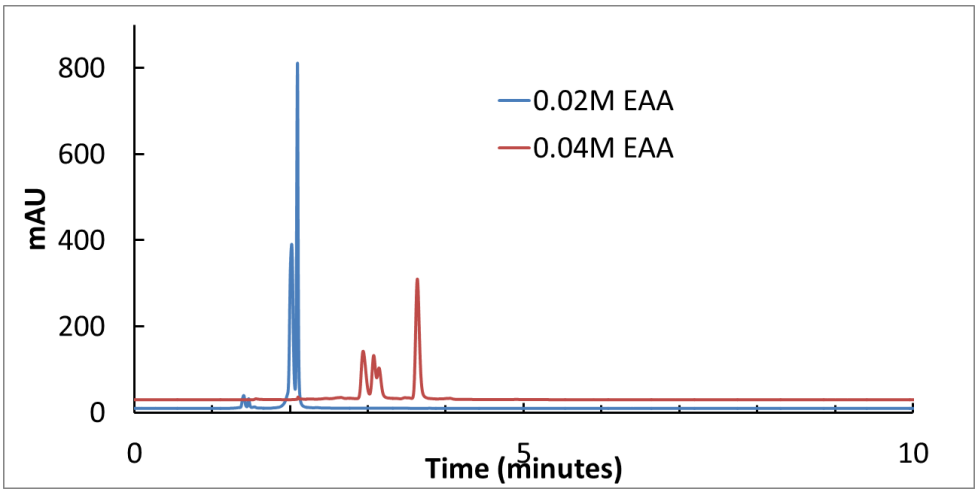

Figure 3.3b: Effect of ethylammonium acetate (pH 7) concentration on the separation of the siRNA stereoisomers by IP-RPLC

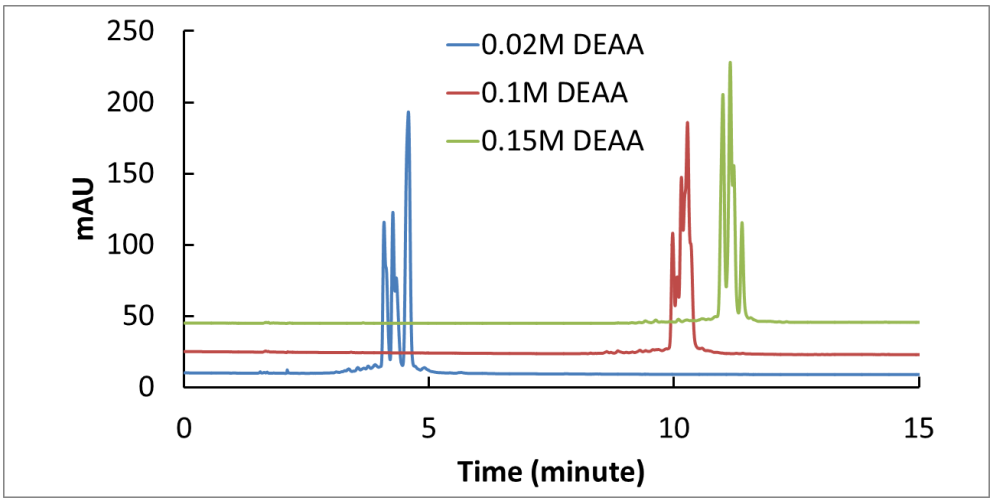

Figure 3.3c: Effect of diethylammonium acetate (pH 7) concentration on the separation of the siRNA stereoisomers by IP-RPLC

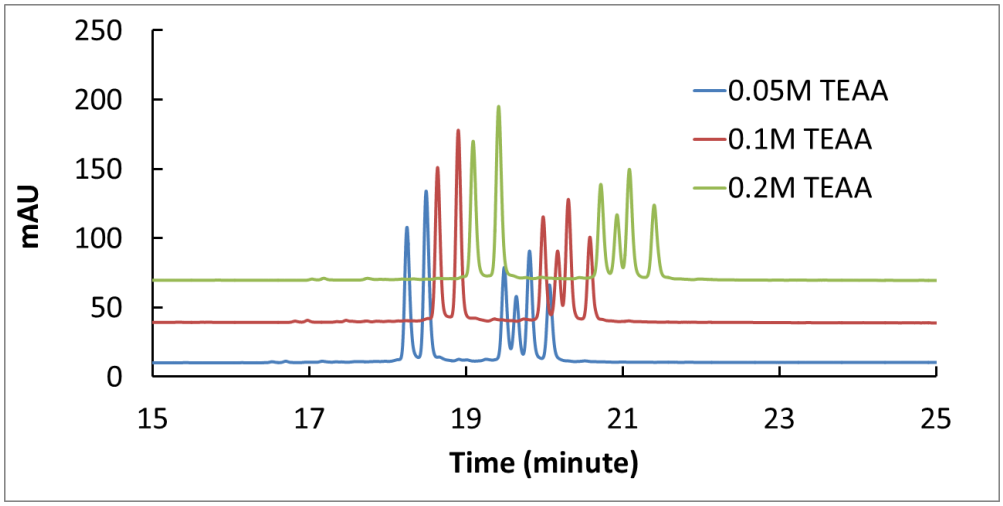

Figure 3.3d Effect of triethylammonium acetate (pH 7) concentration on the separation of the siRNA stereoisomers by IP-RPLC

3.3.3 The impact of organic modifier on the separation of siRNA diastereomers

The siRNA duplex was analyzed using gradient elution, where ACN, MeOH, THF and IPA were evaluated as organic modifiers in the mobile phase. All organic modifiers have some polarity, making them water soluble. The organic solvent imparts hydrophobicity to the mobile phase, which impacts the separation of the oligonucleotide. As shown in Figure 3.4, the use of ACN resulted in a marked improvement in the separation of the sense and antisense diastereomers relative to MeOH. Poor separations were obtained using mobile phases with IPA or THF (data not shown). The overall retention time with ACN as organic modifier is significantly shortened when compared with that of MeOH, reflecting the fact that ACN is a stronger solvent than MeOH for reversed-phase separations.

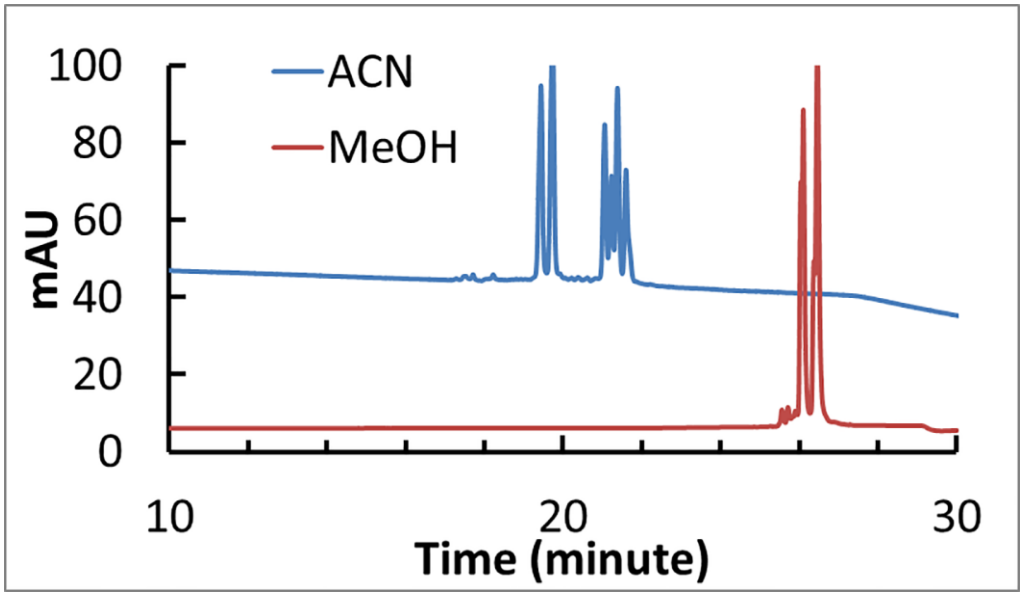

Figure 3.4: Effect of the organic modifier on the separation of siRNA stereoisomers by reversed-phase ion-pair chromatography.
Conditions: Column and oven temperature as in Figure 3.3, other conditions as in in Figure 3.2.

Double-stranded siRNA forms a duplex in an aqueous environment. The binding force between the two strands is largely attributed to hydrogen bonding, hydrophobic and ionic interactions. The separation conditions reported here calls for high column temperature (e.g., 80 ^{o}C) with inclusion of organic modifier in the mobile phase. Under these conditions the siRNA duplex is denatured during the separation, *i.e.*, the sense and antisense strands are dissociated from one another and are migrating down the column independently and with a reduced secondary structure. In addition, it is possible that ACN is more effective in disrupting the siRNA duplex, hence improving the separation of the sense and antisense stereoisomers. Solution calorimetry experiments showed that the siRNA duplex has a melting temperature of 57 ^{o}C in 0.1 M pH 7 TEAA buffer solution (Figure 3.5). The melting temperature dropped to 53 and 48 ^{o}C, respectively, when the TEAA buffer solution contained 10% MeOH or ACN, supporting the

hypothesis that ACN is more effective in disrupting the interstrand interactions of the siRNA duplex.

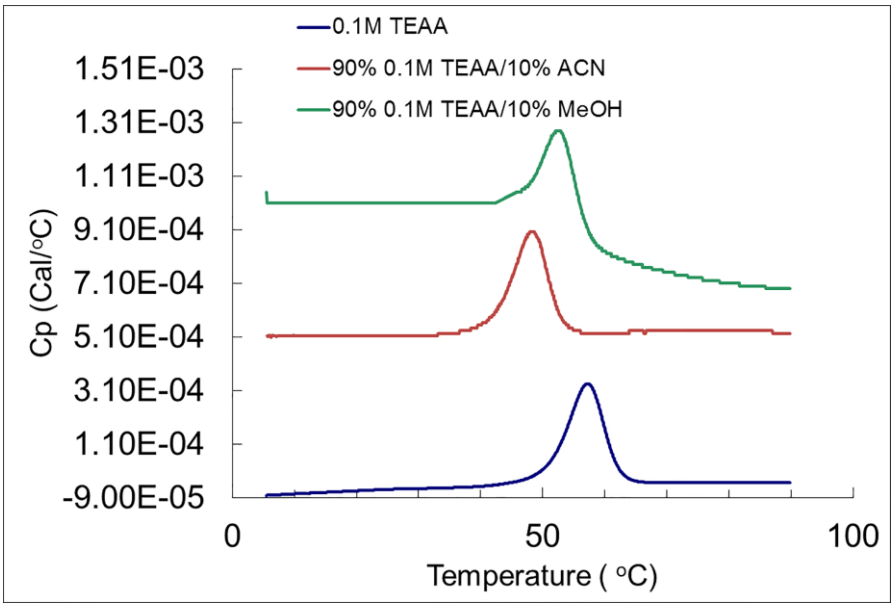

Figure 3.5 Differential Scanning Calorimetry (DSC) showing siRNA duplex mealting temperature in 0.1 M TEAA (pH 7) buffer

3.3.4 Method optimization for the separation of siRNA stereoisomers

The separation conditions were further optimized by evaluating the impact of column temperature (50 to 80 ^{o}C), the concentration of the TEAA ion-pair reagent (0.02 to 0.5 M), the flow rate (0.16 to 0.22 mL/min), and the gradient steepness. Figure 3.6 shows the overlaid chromatograms with column temperatures of 60, 70 and 80 ^{o}C, suggesting that a high temperature above the melting temperature of the siRNA favors stereoisomer separation. Clearly, chromatographic resolution of diastereomeric phosphorothioates within single strands, as opposed to duplex siRNA structures, seems to be preferred. The separation was also evaluated at different concentrations of the ion-pair

agent, and 0.1 M TEAA was selected as the optimal concentration. The flow rate and gradient steepness were then fine-tuned to further optimize the resolution of all species. The optimized conditions enabled a baseline resolution of all components as shown in Figure 3.7. The limit of detection (LOD) for the final method was determined by injecting a series of low level siRNA sample solutions. The LOD was estimated to be 4.2 ng with UV absorbance detection at 260 nm.

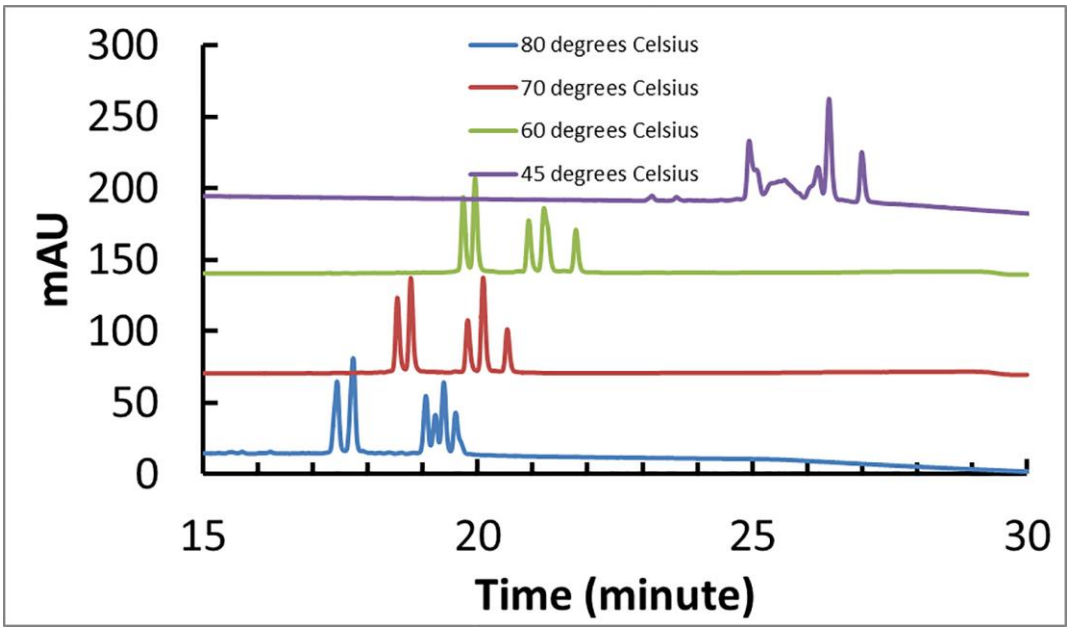

Figure 3.6 Effect of column temperature on the separation of siRNA stereoisomers
Conditions: UHPLC column: BEH C18; Column oven temperature as indicated in the legend, other conditions as in Figure 3.2.

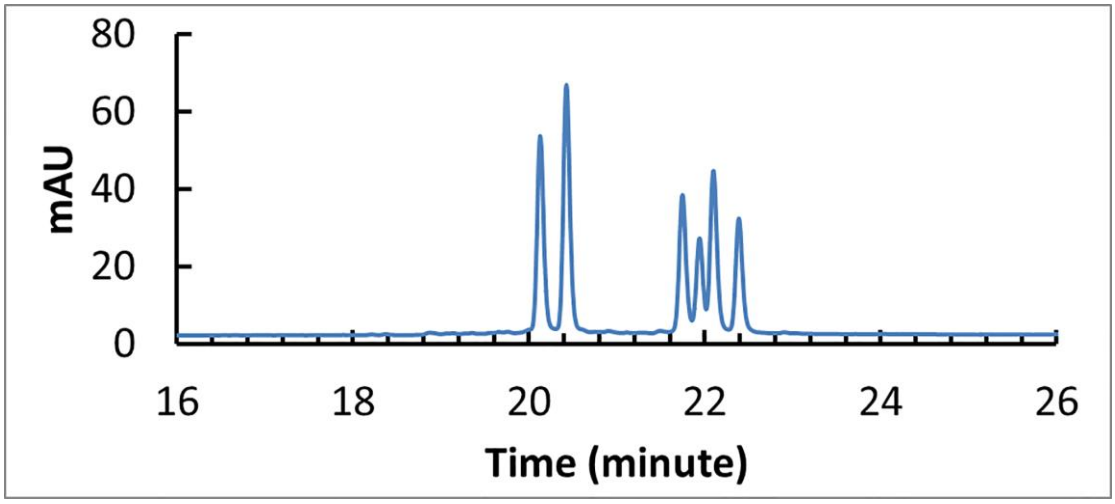

Figure 3.7 Optimized separation of the stereoisomers of the sense and antisense strands of siRNA using ion-pair UHPLC
Final conditions: Column and oven temperature as in Figure 3.3; Mobile phase A is 0.1M TEAA; The gradient elution program was from 6% to 12%B in 19.5 minutes, followed by steeper gradients of 12% to 14%B and 14 to 30%B in 5.5 minutes and 7 minutes, respectively. Other conditions as in Figure 3.2.

3.3.5 Separation of desulfurization products of siRNA stressed with Iodine

Iodine is known to induce a desulfurization reaction in oligonucleotide phosphorothioates without incurring other unwanted reaction products, thereby converting the stereoisomerically complex phosphorothioates into a single phosphodiester linked species. [23] Desulfurization of the siRNA duplex was performed by stressing the aqueous sample solution in a dilute (e.g., 0.03mM) iodine solution for one hour at an ambient condition. The sample was then analyzed by IP-RP UHPLC to monitor the potential desulfurization of the phosphorothioate group in the siRNA. Figure 3.8 shows the overlaid chromatograms of siRNA control and the stressed sample. A total of six degradation products were resolved from the parent siRNA stereoisomers, presumably due to a partial desulfurization reaction.

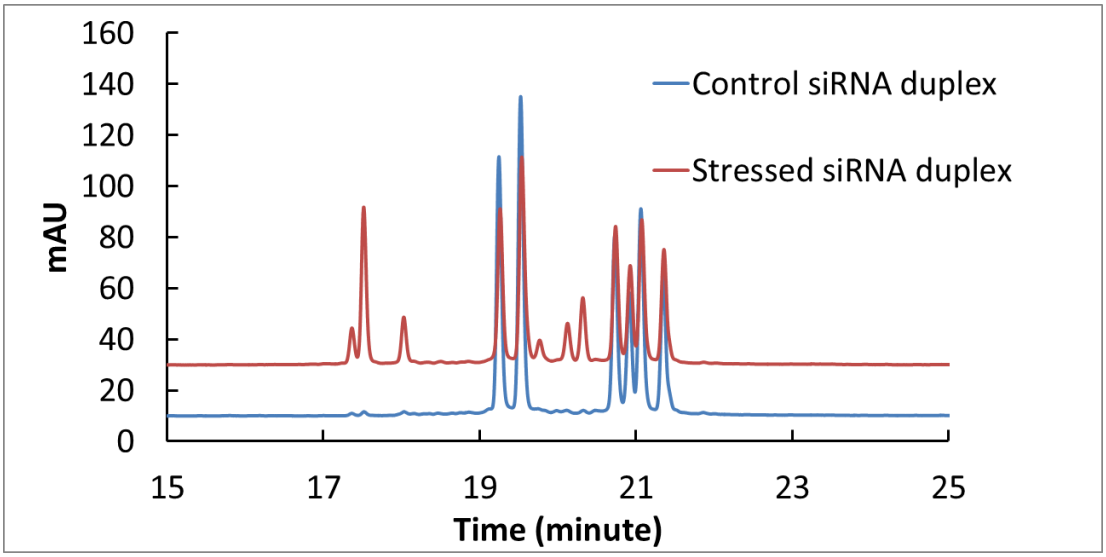

Figure 3.8 Oxidation of siRNA duplex by iodine
Conditions: Column and oven temperature as in Figure 3.3, other conditions as in in Figure 3.2.

3.4 Conclusions

A reversed-phase ion-pair chromatography method was developed for the baseline separation of multiple stereoisomers of a double-stranded siRNA containing three phosphorothioate modification sites. Key chromatographic parameters relevant to diastereomer separation included the structure of the ion-pair reagent, the organic modifier, and the chemistry of the stationary phase. Separation conditions that promote a hydrophobic interaction between the analyte and the stationary phase appear to be critical to separating closely related siRNA stereoisomers. Together with BEH C18 as the stationary phase and acetonitrile as the organic modifier, TEAA provided a superior separation efficiency and selectivity than its structural analogs, such as EAA, DEAA or TMAA. ACN is a key component that facilitates diastereomer separation, while other organic modifiers, including MeOH, THF or IPA, failed in this aspect. Solution-state

differential scanning calorimetry analysis of siRNA suggested that ACN can effectively disrupt the self-association of siRNA double strands, which appeared to be important to stereoisomer separation. The optimized separation method was applied to a siRNA sample deliberately stressed with an iodine solution to induce desulfurization, where up to six degradation products were resolved from the parent siRNA stereoisomers.

List of References

1. A. Fire, S. Xu, M.K. Montgomery, S.A. Kostas, S.E. Driver, C.C. Mello, Potent and specific genetic interference by double-stranded RNA in Caenorhabditis elegans, Nature. 391 (1998) 806-811.

2. S.M. Elbashir, J. Harborth, W. Lendeckel, A. Yalcon, K. Weber, T. Tuschl, Duplexes of 21-nucleotide RNAs mediated RNA interference in cultured mammalian cells, Nature. 411 (2001) 494-498.

3. D. Pogochi, C. Shoneich, Chemical stability of nucleic acid–derived drugs, J. Pharm. Sci. 89(4) (2000) 443-455.

4. S. Choung, Y.J. Kim, S. Kim, H.O. Park, Y.C. Choi, Chemical modification of siRNAs to improve serum stability without loss of efficacy, Biochem. Biophys. Res. Commun. 342 (2006) 919–927.

5. A.H. Krotz, R.C. Mehta, G.E. Hardee, Peroxide-mediated desulfurization of phosphorothioate oligonucleotides and its prevention, J. Pharm. Sci. 94(2) (2004) 341-352.

6. L.M. Wu, D.E. White, C. Ye, F.G. Vogt, G.J. Terloth, H. Matsuhashi, Desulfurization of phosphorothioate oligonucleotides via the sulfur-by-oxygen replacement induced by the hydroxyl radical during negative electrospray ionization mass spectrometry, J. Mass. Spec. 47 (2012) 836-844.

7. V. Murugaiah, W. Zedalis, G. Lavine, K. Charisse, M. Manoharan, Reverse-phase high-performance liquid chromatography method for simultaneous analysis of two liposome-formulated short interfering RNA duplexes, Anal. Biochem. 401 (2010) 61-67.

8. M. Biba, E. Jiang, B. Mao, D. Zewge, J.P. Foley, C.J. Welch, Factors influencing the separation of oligonucleotides using reversed-phase/ion-exchange mixed-mode high performance liquid chromatography columns, J. Chromatogr. A 1304 (2013) 69-77.

9. C. Anacleto, R. Ouye, N. Schoenbrunner, Orthogonal ion pairing reversed phase liquid chromatography purification of oligonucleotides with bulky fluorophores, J. Chromatogr. A 1329 (2014) 78-82.

10. S. Studzinska, L. Pietrzak, B. Buszewski, The effects of stationary phases on retention and selectivity of oligonucleotides in IP-RP-HPLC, J. Chromatogr. A 77 (2014) 1589-1596.

11. M. Biba, C.J. Welch, J.P. Foley, Investigation of a new core–shell particle column for ion-pair reversed-phase liquid chromatography analysis of oligonucleotides, J. Pharm. Biomed. Anal. 96 (2014) 54–57.

12. M. Bunbek, V. Babkovská, K. Holasová, H. Radilová, M. Kafálová, F. Kunc, F. Haluza, Unusual chromatographic behavior of oligonucleotide sequence isomers on two different anion exchange HPLC columns, Anal. Biochem. 348 (2006) 300–306.

13. A. Zimmermann, R. Greco, I. Walker, J. Horak, A. Cavazzini, M. Lämmerhofer, Synthetic oligonucleotide separations by mixed-mode reversed-phase/weak anion-exchange liquid chromatography, J. Chromatogr. A 1354 (2014) 43-55.

14. M. Mateos-Vivas, E. Rodríguez-Gonzalo, D. García-Gómez, R. Carabias-Martínez, Hydrophilic interaction chromatography coupled to tandem mass spectrometry in the presence of hydrophilic ion-pairing reagents for the separation of nucleosides and nucleotide mono-, di- and triphosphates, J. Chromatogr. A 1414 (2015) 129–137.

15. P.A. Porebski, F. Frederic Lynen, Combining liquid chromatography with multiplexed capillary gel electrophoresis for offline comprehensive analysis of complex oligonucleotide samples, J. Chromatogr. A 1336 (2014) 87–93.

16. H.J. Jahns, M. Roos, J. Imig, F. Baumann, Y. Wang, R. Gilmour, J. Hall, Stereochemical bias introduced during RNA synthesis modulates the activity of phosphorothioate siRNAs, Nat. Commun. 6:6317 doi: 10.1038/ncomms7317 (2015).

17. J.K. Frederiksen, J.A. Piccirilli, Separation of RNA phosphorothioate oligonucleotides by HPLC, Methods in Enzymology. 468 (2009) 289-309.

18. J.R. Thayer, Y. Wu, E. Hansen, M.D. Angelino, S. Rao, Separation of oligonucleotide phosphorothioate diastereoisomers by pellicular anion-exchange chromatography, J. Chromatogr. A 1218 (2011) 802-808.

19. J. Soutschek, A. Akinc, B. Bramlage, K. Charisse, R. Constien, M. Donoghue, S. Elbashir, A. Geick, P. Hadwiger, J. Harborth, M. John, V. Kesavan, G. Lavine, P.K. Pandey, T. Racie, K.G. Rajeev, I. Röhl, I. Toudjarska, G. Wang, S. Wuschko, D. Bumcrot, V. Koteliansky, S. Limmer, M. Manoharan, H.P. Vornlocher, Therapeutic silencing of an endogenous gene by systemic administration of modified siRNAs, Nature. 432(11) (2004)173-178.

20. T.S. Zimmermann, A.C.H. Lee, A. Akinc, B. Bramlage, D. Bumcrot, M.N. Fedoruk, J. Harborth, J.A. Heyes, L.B. Jeffs, M. John, A.D. Judge, K. Lam, K. McClintock, L.V. Nechev, L.R. Palmer, T. Racie, I. Röhl, S. Seiffert, S. Shanmugam,V. Sood, J. Soutschek, I. Toudjarska, A.J. Wheat, E. Yaworski, W. Zedalis, V. Koteliansky, M. Manoharan, H.P. Vornlocher, I. MacLachlan, RNAi-mediated gene silencing in non-human primates, Nature. 441(4) (2006) 111-114.

21. D.S. Levin, B.T. Shepperd, C.J. Gruenloh, Combining ion pairing agents for enhanced analysis of oligonucleotide therapeutics by reversed phase-ion pairing ultra performance liquid chromatography (UPLC), J. Chromatogr. B 879 (2011) 1587–1595.

22. M. Gilar, K.J. Fountain, Y. Budman, J.L. Holyoke, H. Davoudi, J.C. Gebler, Characterization of therapeutic oligonucleotides using liquid chromatography with on-line mass spectrometry detection, Oligonucleotides13(4) (2003) 229-43.

23. T.K. Wyrzykiewicz, D.L. Cole, Sequencing of oligonucleotide phosphorothioates based on solid-supported desulfurization, Nucleic Acids Res. 22(13) (1994)2667-69.

Chapter 4 Simultaneous separation of small interfering RNA and phospholipids in lipid nanoparticle formulations

4.1 Introduction

Small interfering RNA (siRNA)-based therapeutics have several advantages compared to gene therapy, protein, and small molecule-based drugs owing to the direct interference with protein translation. The key advantage of siRNA-based drugs is that siRNA catalytically degrades mRNA, hence suppressing harmful proteins implicated in disease before they are made. Furthermore, siRNA is easy to design and has the potential of engaging a broader range of targets than traditional therapeutics. [1,2,3] Many delivery systems have been explored in the past, including lipid nanoparticles (LNP), polymer conjugates, and siRNA single chemical entities. [4,5,6,7] Among the various delivery systems, the lipid nanoparticle formulation has been the most extensively studied platform. It represents an important formulation strategy for siRNA therapeutics with the potential to overcome the delivery barriers. With particle size less than 100 nm, a fully assembled LNP typically contains siRNA, cationic lipids, phospholipids, PEG-containing short-chain lipids, and cholesterol. The cationic lipids are the most critical components in the LNP for modulating the cell uptake of siRNA. They directly influence siRNA encapsulation efficiency, the particle size, and surface charge of LNPs, which are critical parameters for siRNA delivery to cell cytoplasm. [8] The lipid bilayers contain a minor component of a PEGylated short-chain lipid decorated on the bilayer surface. The PEGylated short-chain lipid improves the physical stability of LNPs in systemic circulation upon intravenous (IV) injection, preventing particle aggregation in plasma. [9]

Chemical analysis of LNPs is routinely performed during formulation development. Quantification of each component in an LNP is important for ensuring a target potency of siRNA. The desired lipid composition must be determined for the achievement of optimum physical properties, such as particle size, surface charge, etc. The analysis and control of low-level breakdown products from siRNA and lipids ensures that patients are not exposed to potentially harmful species. [10,11,12]

Due to inherent differences in their chemical structure, polarity, and hydrophobicity, the separation and analysis of oligonucleotides or phospholipids in LNP formulations are typically performed with multiple HPLC methods. Oligonucleotides are polyanionic at a pH range compatible with most stationary phases. The separation modes for oligonucleotides analysis include ion-pair reverse phase HPLC, ion exchange chromatography, mixed-mode chromatography combining reversed-phase with ion exchange, and hydrophilic interaction chromatography. [13,14,15,16]

Lipids have drawn renewed interest in recent years owing to its biological functions vital for energy storage, regulation of metabolic processes, cellular signaling, morphogenesis, secretion, and protein trafficking. A comprehensive study of lipid species and their related networks has evolved into a significant scientific discipline – coined lipidomics. This discipline is dedicated to understanding the role of lipids in regulating metabolic pathways in cells or other biologic systems. [17,18] The separation and characterization of lipids in biological samples present an unprecedented challenge to the analytical community due to their enormous molecular diversity. Historically, the separation of lipids was achieved mainly by two separation modes - normal phase HPLC (NP-HPLC) and reverse phase HPLC (RP-HPLC). [19,20,21,22,23,24] The retention mechanism

on NP-HPLC is attributed to hydrophilic interactions between the polar groups of the lipids and the polar stationary phase, such as silica gel or polar bonded-phase derivatives thereof. The lipids are separated according to the chemical structure of the polar functional groups, such as the headgroups, making NP-HPLC an effective method for separating lipids of different classes. In contrast, RP-HPLC differentiates lipids based on their hydrophobicity defined by the alkyl chain length and degree of unsaturation of their tails as well as the charge state of the head groups. The chromatographic analysis of lipids has an added technical challenge, relative to oligonucleotides, due to the lack of chromophores for UV detection. Universal detectors, including the evaporative light scattering detector (ELSD) and the corona charged aerosol detector (corona CAD), are commonly used for lipid analysis. [25,26] UHPLC-mass spectrometry is another emerging technical field with significant advances in recent years for total lipid analysis and structure elucidation, with applications ranging from food analysis, quality control for cosmetics and pharmaceutical, as well as metabolic profiling. [27]

While there is a significant literature presence concerning the separation and analysis of oligonucleotides or lipids in their respective sample matrix, to the best of our knowledge there is no prior work on the simultaneous separation of siRNA and phospholipids in the context of an LNP delivery system. A literature survey of separation techniques developed for oligonucleotides or phospholipids identified two separation modes with the potential for the simultaneous separation of siRNA, phospholipids, and their related species: ion-pair reversed-phase chromatography and mixed-mode chromatography. Ion-pair reversed-phase HPLC has been extensively applied to oligonucleotide analysis. The selectivity and retention characteristics of siRNA can be

modulated through careful selection of the ion-pair reagent, stationary phase, and organic modifier. In contrast to the numerous reports for oligonucleotides, ion-pair reversed-phase HPLC has fewer applications for lipid analysis largely due to their significant hydrophobicity. One application involved the separation of phosphatidylinositol (PI) and its related molecular species using ion-pair reversed-phase HPLC, where tetrabutylammonium acetate was used as the ion-pair reagent. The method was selective to anionic PI lipids with different degrees of unsaturation in the lipid chains. Other studies showed that ion-pair RP-HPLC, coupled with ESI mass spectrometry, significantly improve method sensitivity for a range of trace level phospholipids. [27]

Mixed-mode chromatography is another separation technique with increasing popularity in biopharmaceutical applications owing to its unique selectivity and retention, often defined by a combination of hydrophobic, hydrophilic or ionic interactions. Mixed-mode chromatography with reversed-phase and ion-exchange retention characteristics, in theory, could accommodate the separation of analytes with orthogonal physical and chemical properties. Key separation parameters relevant to the mixed-mode separation technique, incorporating both the reversed-phase and ion-exchange retention mechanisms into one integrated stationary phase chemistry, are fundamentally different from ion-pair reversed-phase HPLC. For mixed-mode chromatography, the important factors influencing oligonucleotide separations include the type of counterion in buffers, the pH, and the ionic strength.

In this chapter, an ion-pair reverse phase HPLC method, coupled with UV and corona charged aerosol detectors, was developed to separate a group of siRNA duplexes and phospholipids with significant diversity in physical and chemical properties. We

elected to employ ion-pair reversed phase HPLC as our separation mode, owing to the tunable retention time for oligonucleotides, whose retention is primarily dominated by hydrophobic and electrostatic interactions. The latter interaction between an oligonucleotide's polyanionic phosphate moieties and the positively charged alkylammonium ions in the mobile phase reduced the polarity of the analyte, promoting hydrophobic interaction between the nitrogenous nucleobases and the stationary phase. Variation of the alkyl functional group of the ion-pair agent can further modulate the hydrophobic interaction. Five different siRNA duplexes were used in the study. The purpose of studying a small library of siRNAs was to create sufficient variation in the sample set so that the target separation method can be potentially used for the analysis of the LNP systems that contain multiple siRNAs for silencing various genes in the body. [28]

An LNP system is a multi-functional delivery vehicle, consisting of a range of lipids with different structural features. To ensure the target method is suitable for separating lipids of various structures that can exist in an LNP, we selected six different lipids, of which five are zwitterionic phospholipids that vary in the alkyl chain length and the degree of unsaturation of the tail. A cationic lipid was also included in the study. The selected lipids not only present a suitable matrix to developing a separation method, but it also allows us to study the retention behavior of the lipids under an ion-pair reverse phase separation conditions, which has not been systematically studied before in the literature. We herein report an investigation of the influence of stationary phase chemistry, column temperature and the type and concentration of ion-pair reagent on the IP-RP UHPLC separation of both siRNA and phospholipids.

4.2 Material and methods

4.2.1 Chemicals

The siRNA duplex targeting ApoB gene (Zimmerman sequence) and four additional proprietary siRNA duplexes were provided by Merck Sharp & Dohme (MSD) RNA synthesis group. Phospholipids of different chain length or headgroups were sourced from Avanti Polar Lipids (Alabaster, AL, USA). The lipids are 1,2-dipalmitoyl-*sn*-glycero-3-phosphocholine (DPPC), 1,2-dilauroyl-*sn*-glycero-3-phosphocholine (DLPC), 1,2-dioleoyl-*sn*-glycero-3-phosphocholine (DOPC), 1,2-didecanoyl-*sn*-glycero-3-phosphocholine (DDPC), 1,2-dioleoyl-3-trimethylammonium-propane chloride salt (DOTAP), and dimyristoleoyl phosphocholine (DMPC). **Figure 4.1** shows the chemical structure of the phospholipids. Ion-pair reagents were purchased from the following vendors: triethylammonium acetate buffer (pH 7, ~ 1.0 M in water) was obtained from Sigma-Aldrich (St. Louis, MO, USA), whereas dipropylammonium acetate (DPAA, 0.5 M in water), dibutylammonium acetate (DBAA, 1M in water), and diamylammonium acetate (DAAA, 0.5M in water) were acquired from Fisher Scientific (Norristown, PA 19403, USA). HPLC grade acetonitrile (ACN) was obtained from Fisher Scientific. Experimental lipid nanoparticle (LNP) suspensions were provided by Merck Sharp & Dohme (MSD) Sterile formulation group. The LNP formulation consisted of a proprietary siRNA duplex, two types of phospholipids, cholesterol and PEGylated short chain lipid.

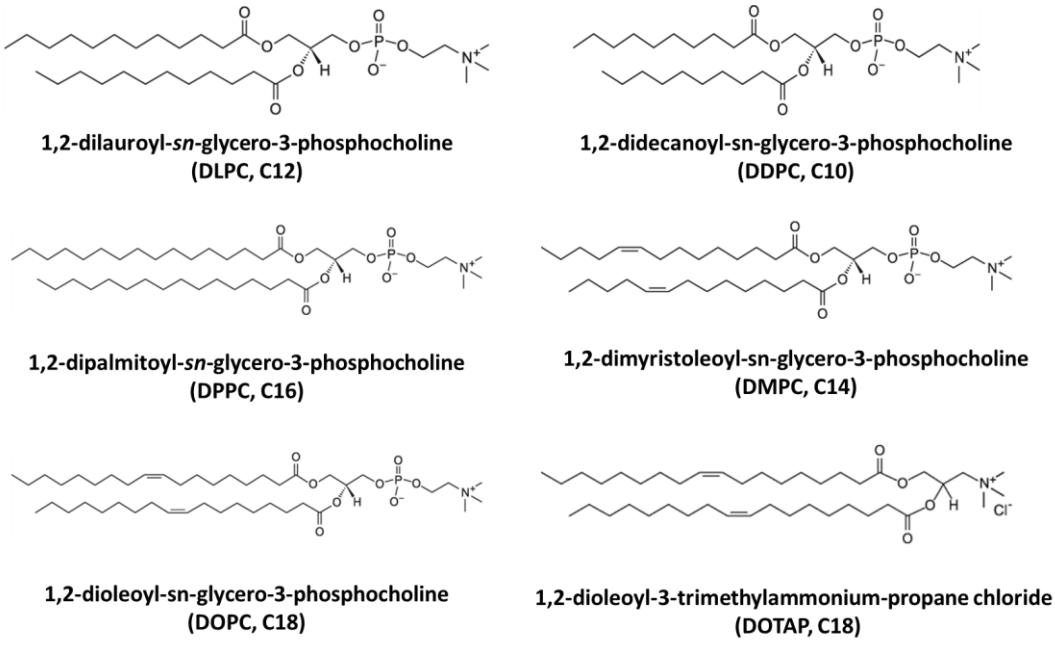

Figure 4.1 Chemical structures of the lipids

4.2.2 Instrument

An Agilent 1290 Infinity UHPLC system (Agilent Technologies, Santa Clara, CA, USA) was employed for the separation of siRNA and phospholipids. This UHPLC system consisted of a binary pump, a diode array detector (DAD), a corona charged aerosol detector (CAD), an autosampler and a column heater. This system could be operated at a pressure up to 1200 bar. Because the CAD is a destructive detector, it was connected in series and after the DAD. Data collection rate was 5 Hz for the CAD. The corona nebulizer was controlled at 35^{o}C while the evaporator tube was kept at ambient temperature.

A differential scanning microcalorimeter (MicroCal, LLC, Northampton, MA, USA) was used to measure the melting temperature of the various siRNA duplexes. The system can operate at a temperature range of -10° to 130° Celsius.

4.2.3 Ion-pair reversed phase chromatographic conditions

For the separation of siRNA and phospholipids, the samples were subjected to gradient elution using sub-2um UHPLC columns. The columns studied in this work had the same dimensions (150 x 2.1 mm) and included the Acquity BEH phenyl, BEH C8, BEH C18, CSH fluoro-Phenyl, and HSS cyano. The nominal particle size of the stationary phase packings was 1.7 μm, except for the HSS cyano, which had a particle size of 1.8 μm. Mobile phase A consisted of aqueous solutions of ion-pair reagents, and mobile phase B was pure ACN. The initial gradient method was run from 10% to 35% B in 15 minutes, followed by a steeper gradient elution from 35% to 100 %B in 15 minutes and an isocratic hold at 100% B for 10 minutes. The siRNA samples were prepared in 20 mM phosphate buffer (pH 7) at a concentration of approximately 0.1 mg/mL. The phospholipids were dissolved in ethanol at a concentration of approximately 0.3 mg/mL.

For siRNA analysis in the LNP formulation, an aliquot the LNP suspension (100 uL) was transferred to a 1.5-mL centrifuge tube. 600 μL of ethanol was then added to the centrifuge tube with a calibrated micropipette. The mixture of the LNP suspension and ethanol was mixed by inverting the test tube for at least three times, followed by 30-second vortex mixing. An additional 600 μL of ethanol was added to the tube, and the sample was mixed by inversion and vortex mixing. The sample tube was centrifuged at 14,000 RPM for 10 minutes. The supernatant was discarded from the tube using a glass Pasteur pipette. Care was taken to ensure the RNA pellet was not disturbed during the

supernatant removal process. The residual ethanol from the pellet was evaporated by purging with nitrogen gas for about five minutes. One microliter of 20 mM phosphate buffer solution was added to the dry pellet. The dry pellet in the buffer solution was mixed with vortexing for 30 seconds to dissolve the dried pellet. For lipid analysis in LNP formulation, about 100 uL of LNP suspension was transferred into a clean HPLC vial. An aliquot of ethanol (1 mL) was added to the HPLC vial with a calibrated micropipette, and the sample solution was mixed by vortexing for 30 seconds.

4.2.4 Differential scanning calorimetry method condition

The melting temperature (T_m, or dissociation temperature) of the siRNA duplexes were measured using capillary cell micro-calorimetry. A 0.1 - mg/mL siRNA sample solution was prepared in phosphate buffer solution at pH 7. The sample solutions were added to a 96-well plate and automatically applied to the sample capillary of which the run sequence was controlled. The heating and cooling cycle from 5^{o}C to 110 ^{o}C was applied to both the reference and sample cells with a scan rate of 1 ˚C/minute. Each sample was run in two replicates. The difference between the melting temperatures from the two replicates is typically within 1 ^{o}C.

4.3 Results and Discussion

4.3.1 Initial assessment of ion-pair reversed phase method for simultaneous analysis of siRNA duplexes and phospholipids

Ion-pair reversed-phase HPLC has the potential to reduce the retention time gap between siRNA and phospholipids owing to the versatility of the ion-pair reagent. **Figure 4.2a and 4.2b** show the results of our initial attempt to simultaneously separate

five siRNA duplexes and six lipids using ion-pair reverse phase chromatography with dual detectors – a diode array absorbance detector for the siRNAs and a charged aerosol detector (CAD) for the lipids. With 100mM TEAA in the aqueous component of the mobile phase, the retention time of siRNA duplexes ranged from 2.8 to 7 minutes, which represents 15 to 22% ACN in mobile phase as the siRNAs exited the column. Most of the phospholipids (DDPC, DLPC, DMPC, and DPPC) eluted between 26 and 32 minutes, corresponding to 83% and 100% ACN in the mobile phase. The percentage of strong solvent needed to elute the lipids is about 4- to 5-fold higher than that for the siRNAs due to their significant difference in hydrophobicity. DOPC and DOTAP are structurally different lipids with zwitterionic and cationic head groups, respectively. Neither was eluted on the C18 column under these separation conditions. The large retention gap between the siRNAs and lipids on the BEH C18 column with 0.1 M TEAA was not unexpected as the polarity of the two classes of molecules is very different from each other. The initial separation results highlighted the challenges of developing a unified separation method capable of simultaneously separating both siRNAs and lipids with a minimal retention gap. The remaining portion of this study will focus on the investigation of the influence of stationary phase chemistry, column temperature, and the type of the ion-pair reagent on the IP-RPLC separation of both siRNA and lipids.

a)

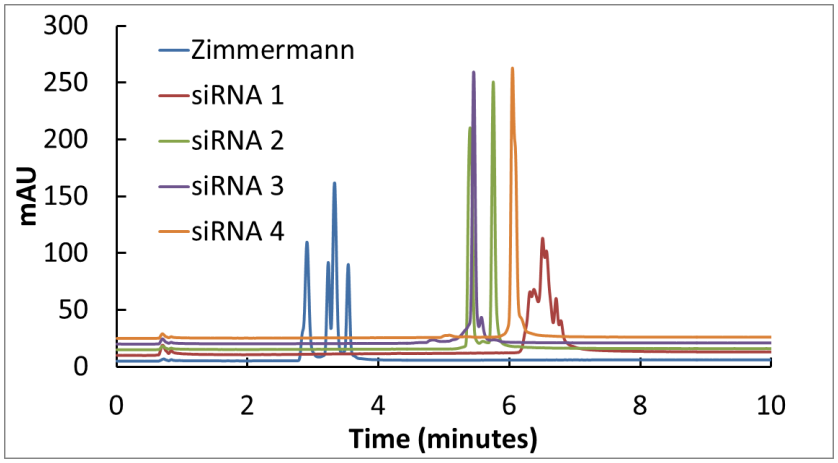

b)

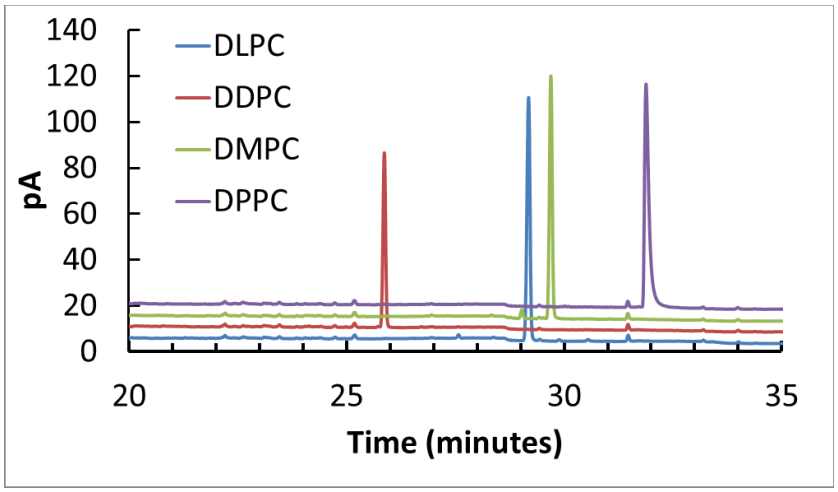

Figure 4.2 UHPLC-UV-CAD separation and detection of siRNA duplexes and phospholipids using TEAA as the ion-pair reagent on a BEH C18 column.
a) Overlaid chromatographic traces for the siRNA duplexes with UV detection at 260 nm.
b) Overlaid chromatographic traces for the phospholipids with corona CAD detection
Conditions: UPLC column: BEH C18 (150 x 2.1 mm). Column oven temperature: 50 ^{o}C. Mobile phase A consisted of 0.1M triethylammonium acetate (TEAA, pH 7) in water, and mobile phase B was ACN. The gradient method was run from 10% to 35% B in 15 minutes, followed by a steeper gradient elution from 35% to 100 %B in 15 minutes and an isocratic hold at 100% B for 10 minutes. The flow rate was 0.4 mL/minute and the injection volume was 5 µL. A diode array detector, with UV absorbance detection at 260 nm, was used to monitor siRNA and a corona CAD was used for phospholipids. The siRNA sample concentration was approximately 0.1 mg/mL prepared in 20 mM phosphate buffer. The lipid concentration was about 0.3 mg/mL.

4.3.2 The impact of stationary phase chemistry on the separation of siRNA duplexes and phospholipids

Acquity BEH, CSH and HSS UHPLC columns of different stationary phase chemistry, including C18, C8, cyano, phenyl, and fluoro-phenyl, were investigated for the separation of siRNA duplexes and phospholipids. The UHPLC separation was performed at 50 ^{o}C, which is below the dissociation temperature of the siRNA duplexes measured in an aqueous medium (Refer to Section 4.3.4 for the DSC data). **Figures 4.3 to 4.6** show the overlaid chromatographic traces for the analysis of the siRNA duplex and phospholipids on various UHPLC columns. The retention time for siRNA duplex ranged from 0.8 to 4.5 minutes, 1.5 to 6 minutes, 3 to 6.5 minutes, 3 to 8 minutes and 4 to 8 minutes using the cyano, C8, C18, fluoro-phenyl and phenyl columns, respectively. The results are to a certain degree unexpected. We anticipated that the siRNAs should have a longer retention time on a C18 column than the other stationary phases due to a stronger hydrophobic interaction between the analytes and the non-polar, C18 stationary phase. Instead, our data showed that the siRNAs are more retentive on the fluoro-phenyl or phenyl columns than the other ones, presumably due to a specific π- π interaction between the phenyl groups on stationary phase and the nucleobases of the siRNAs, in addition to hydrophobic interactions. The peak shape for the siRNA duplexes is complex both in terms of the number of peaks observed and their asymmetric feature. The siRNA duplexes studied here contained phosphorothioate stereocenters, which together with the stereocenters on the ribose sugar, results in siRNA stereoisomers that are partially resolved at temperatures below their dissociation temperature. The presence of

stereoisomers may explain the complex peak shape observed. Efforts to improve siRNA peak shape will be discussed later in this chapter.

The retention behavior of the phospholipids under ion-pair reversed-phase HPLC is relatively predictable and appears to be consistent with the retention mechanism of a traditional reversed-phase HPLC, with hydrophobic interactions as the dominant feature. As expected, the retention time of each lipid slightly increased as the alkyl chain length on the stationary phase increased from propyl for the fluoro-phenyl column to octadecyl for the C18 column. In addition, the elution order of the phospholipids remained the same regardless of the stationary phase chemistry, which is also consistent with our expectation for a retention process that is dominated by a hydrophobic interaction between the analytes and the stationary phase. We anticipate that the alkyl chain length of the lipid tail will determine the retention time. Indeed, the retention time of the lipids increased in the following order: DDPC (saturated C10) < DLPC (saturated C12) < DMPC (C14 with 2 double bonds) < DPPC (saturated C16) < DOPC (C18 with two double bonds) < DOTAP (C18 with two double bonds). Although the alkyl chain length for both DOTAP and DOPC is the same, DOTAP is more hydrophobic than DOPC because a large portion of the molecule is hydrophobic and the phosphate group is missing.

The strategy for simultaneous and efficient separation of siRNAs and lipids depends in part on identifying a stationary phase chemistry that minimizes the retention gap between the siRNAs and phospholipids, i.e., one that maximizes siRNA – stationary phase interactions while reducing hydrophobic lipid – stationary phase interactions. The column screening showed that the fluoro-phenyl and phenyl phases, both having short

alkyl chain lengths, are the potential leads. The BEH phenyl column was selected for further evaluation since the column can operate at high temperature (80 ^{o}C), while the temperature limit for the fluoro-phenyl column is only 60 ^{o}C. As shown in section 3.4, the separation of siRNA duplexes at higher column temperature is often preferred to maintain a good peak shape.

a)

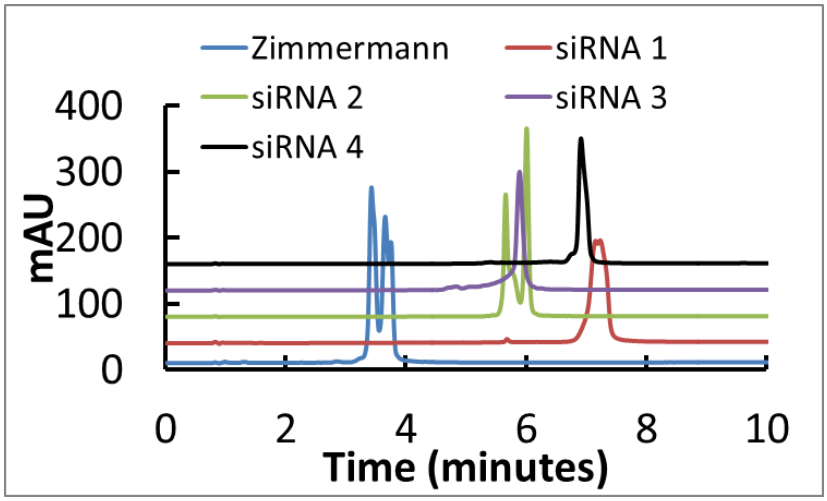

b)

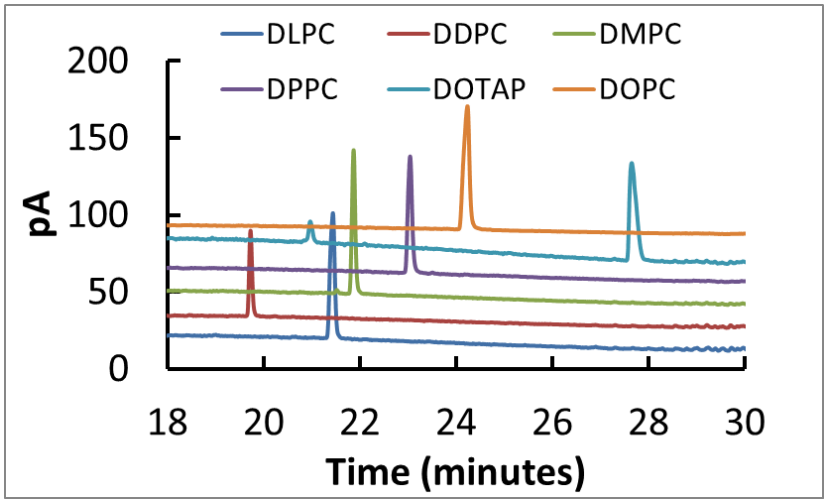

Figure 4.3 UHPLC-UV-CAD separation and detection of siRNA duplexes and phospholipids using TEAA as the ion-pair reagent on a CSH fluoro-phenyl column.
a) Overlaid chromatographic traces for siRNA with UV detection at 260 nm.
b) Overlaid chromatographic traces for phospholipids with corona CAD detection
Conditions: UPLC column: CSH fluoro-phenyl C18 (150 x 2.1 mm). Other conditions are as in Figure 4.2.

a)

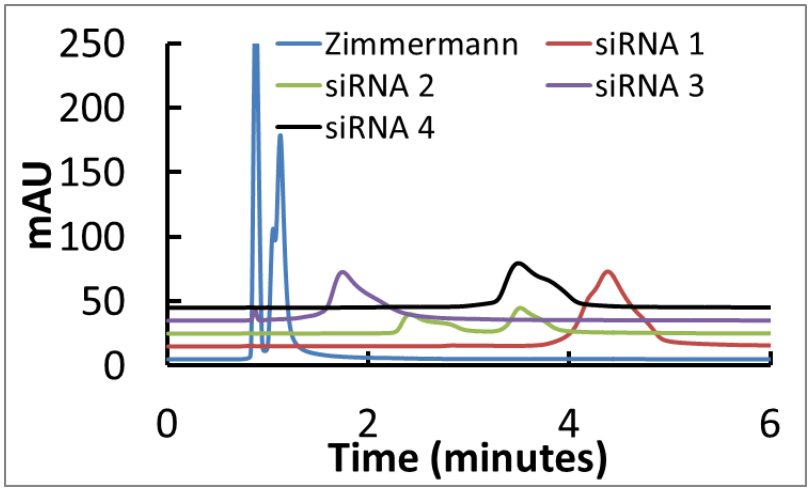

b)

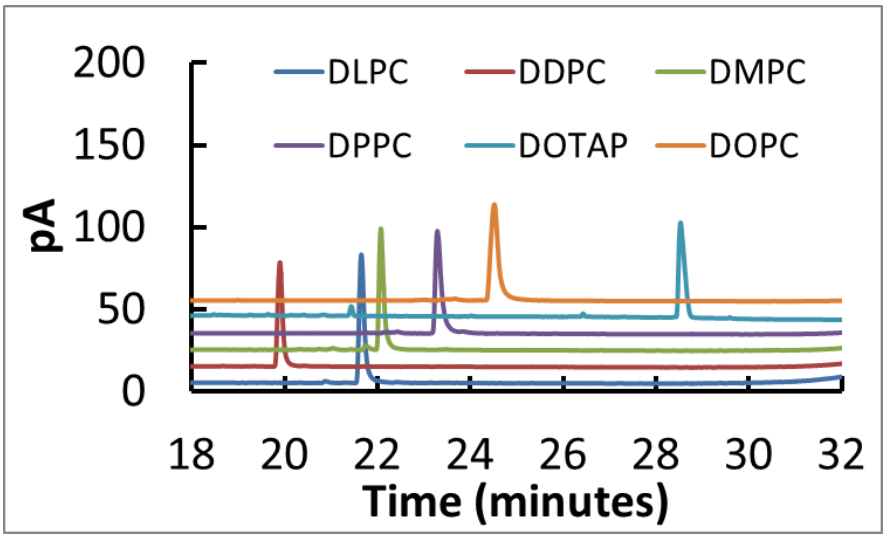

Figure 4.4 UHPLC-UV-CAD separation and detection of siRNA duplexes and phospholipids using TEAA as the ion-pair reagent on a HSS cyano column.
a) Overlaid chromatographic traces for siRNA with UV detection at 260 nm.
b) Overlaid chromatographic traces for phospholipids with corona CAD detection
Conditions: UPLC column: HSS cyano (150 x 2.1 mm). Other conditions are as in Figure 4.2.

a)

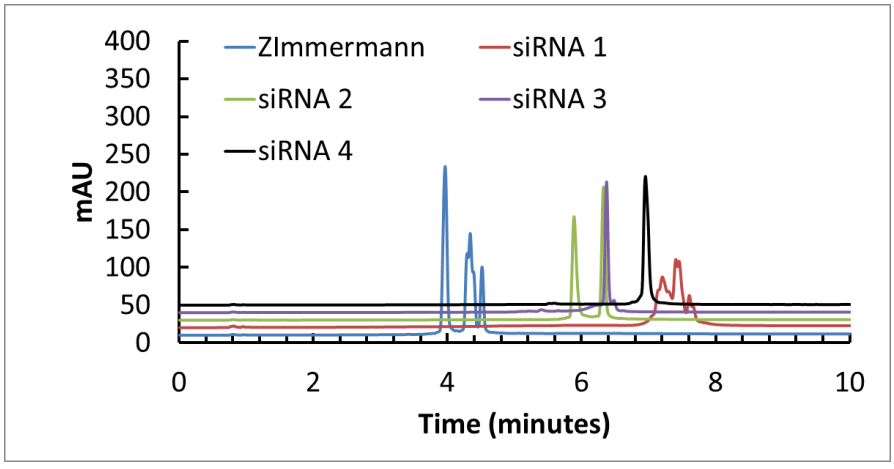

b)

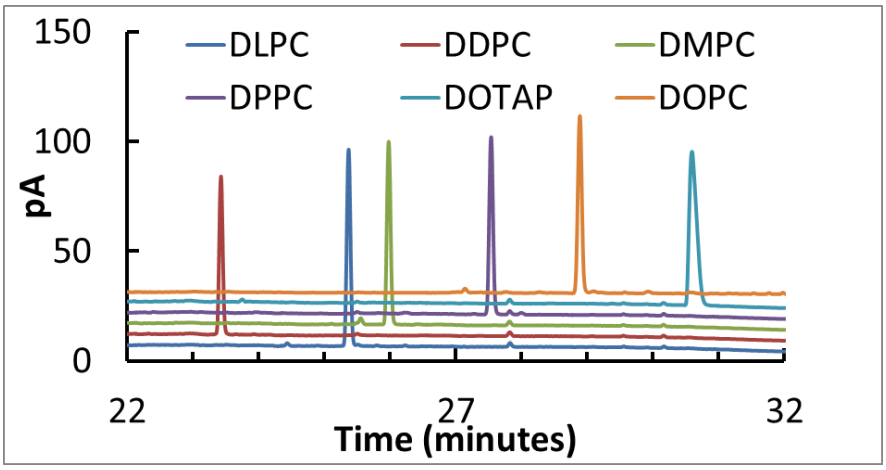

Figure 4.5 UHPLC-UV-CAD separation and detection of siRNA duplexes and phospholipids using TEAA as the ion-pair reagent on a BEH phenyl column.
a) Overlaid chromatographic traces for siRNA with UV detection at 260 nm.
b) Overlaid chromatographic traces for phospholipids with corona CAD detection
Conditions: UPLC column: BEH phenyl (150 x 2.1 mm). Other conditions are as in Figure 4.2.

a)

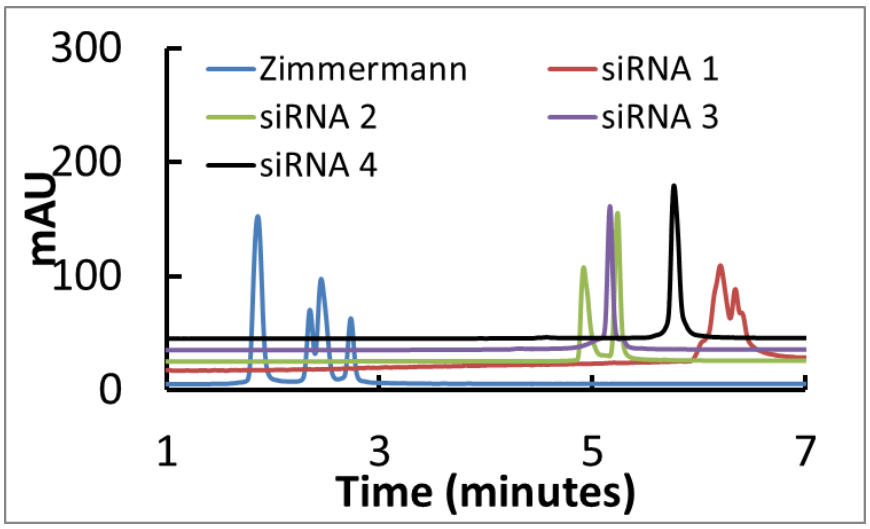

b)

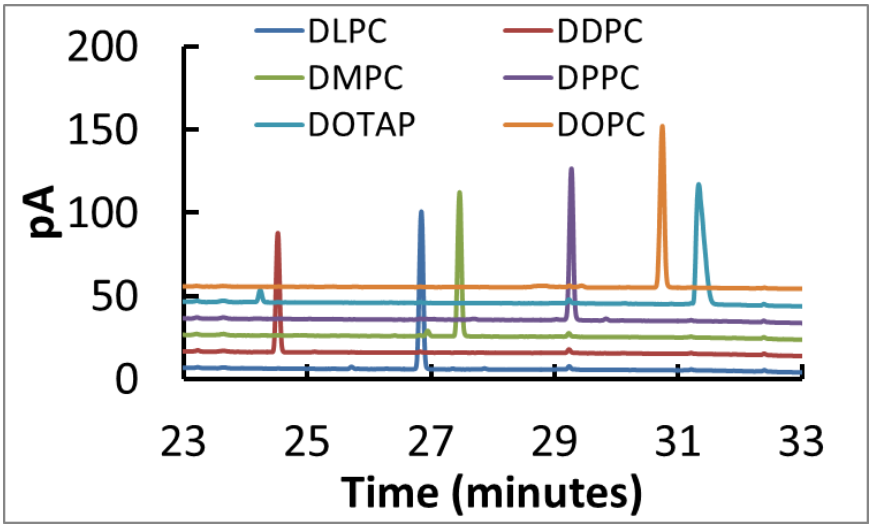

Figure 4.6 UHPLC-UV-CAD separation and detection of siRNA duplexes and phospholipids using TEAA as the ion-pair reagent on a BEH C8 column.
a) Overlaid chromatographic traces for siRNA with UV detection at 260 nm.
b) Overlaid chromatographic traces for phospholipids with corona CAD detection
Conditions: UPLC column: BEH C8 (150 x 2.1 mm). Other conditions are as in Figure 4.2.

4.3.3 The impact of ion-pair reagents on the separation of siRNA duplexes and phospholipids

In IP-RPLC, oligonucleotides are retained and separated through ion-pair formation between the protonated hydrophobic organic amine (i.e., the ion-pair reagent) in the mobile phase and the negatively charged analyte, followed by partitioning of the complex into reversed-phase stationary phase. In addition, the hydrophobic ion-pair reagent can adsorb onto the stationary phase, exhibiting a dynamic ion-exchange retention mechanism for analytes of opposite charges. Aside from stationary phase chemistry, the chemical nature of the ion-pair reagents, specifically their hydrophobicity and the degree of substitution at the amine group by short alkyl chains, can influence the

separation of oligonucleotides. [29, 30] **Figures 4.7 to 4.9** show the overlaid chromatograms for the analysis of the siRNA duplexes and phospholipids with a BEH phenyl column and DPAA, DBAA and DAAA as the ion-pair reagents, respectively. The overall separation results showed that the retention time of the siRNA duplexes is in the range of 7 to 12 minutes, 16 to 20 minutes and 22 to 25 minutes for DPAA, DBAA, and DAAA. The increase in siRNA retention time as a function of hydrophobicity of the ion-pair reagent is as expected and consistent with the retention mechanism described earlier in this section. Furthermore, we plotted the natural logarithm of the retention factor (k) for each siRNA sample as a function of the number of carbons in the ion-pair reagent. **Figure 4.10** shows a typical plot for Zimmerman siRNA; **Table 4.1** summarizes the retention factor for the entire sample set as well as the correlation coefficient for linear regression of the individual plot. TEAA was not included in the group since it is a structural isomer of DPAA and does belong to the homologous series. The data analysis suggested that Ln k (retention factor) of the siRNA has a linear relationship with the number of the carbons in the alkyl chains. The same trend was observed for the ion-pair reagents when they were injected as samples and separated using a mobile phase that is free of any ion-paring species. This observation suggested that the retention of siRNA duplex is largely dominated by the partitioning of the alkyl chains in the ion-pair reagents between the mobile phase and stationary phase. The partitioning process in reversed phase separation obeys the law of thermodynamics (refer to eqn. (1.14) in Chapter 1) where the Ln K (K - partition coefficient) has a linear relationship with the free energy associated with transferring the molecules from the mobile phase to the stationary phase.

In contrast to siRNA duplexes, the retention time of each lipid varied slightly as the ion-pair reagent was changed. The lack of impact of the ion-pair reagent on the lipid separation is an interesting observation, and this could be rationalized by proposing a partitioning process as the primary mode of separation mechanism for the lipids, where hydrophobic interactions between the stationary phase and the lipid's alkyl chain are dominant. Ion-pair reagents are not expected to promote additional interaction between zwitterionic or cationic lipids and a reversed-phase stationary phase. Furthermore, we observed that the retention time of the lipid increased as the alkyl chain length increased regardless the type of ion-pair reagent. This again is consistent with the retention mechanism of the hydrophobic lipids under s reversed-phase separation conditions. Comparing the overall separation outcome for siRNA duplexes and phospholipids, DBAA and DAAA are the lead candidates that significantly reduce the retention gap, making simultaneous separation possible for these two classes of biomolecules with orthogonal physical and chemical properties. We further selected DBAA over DAAA based on (i) a reduced impurity level in the reagent and (ii) the quality of the baseline during separation of siRNA duplex with UV as detection.

a)

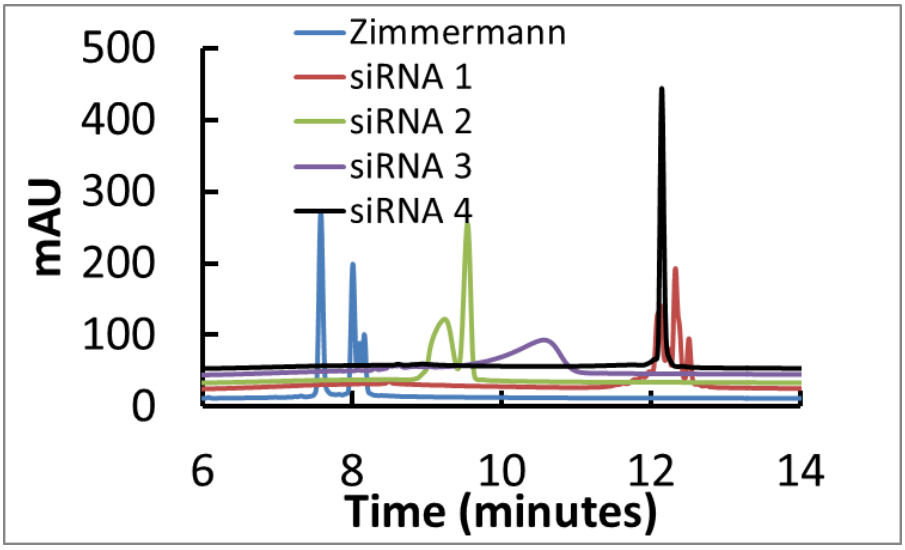

b)

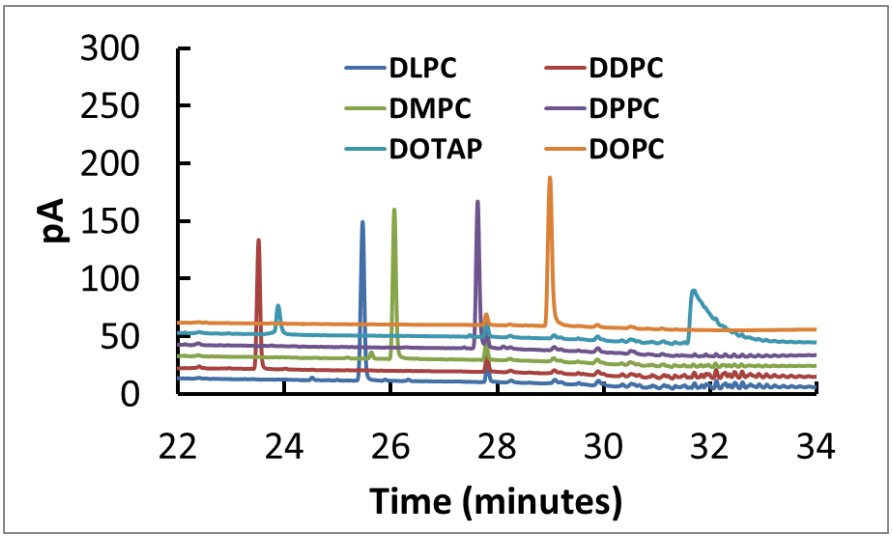

Figure 4.7 UHPLC-UV-CAD separation and detection of siRNA duplexes and phospholipids with DPAA as the ion-pair reagent on a BEH phenyl column.
a) Overlaid chromatographic traces for siRNA with UV detection at 260 nm.
b) Overlaid chromatographic traces for phospholipids with corona CAD detection
Conditions: Mobile phase A consisted of 0.1 M DPAA. UPLC column: BEH Phenyl (150 x 2.1 mm). Other conditions are as in Figure 4.2.

a)

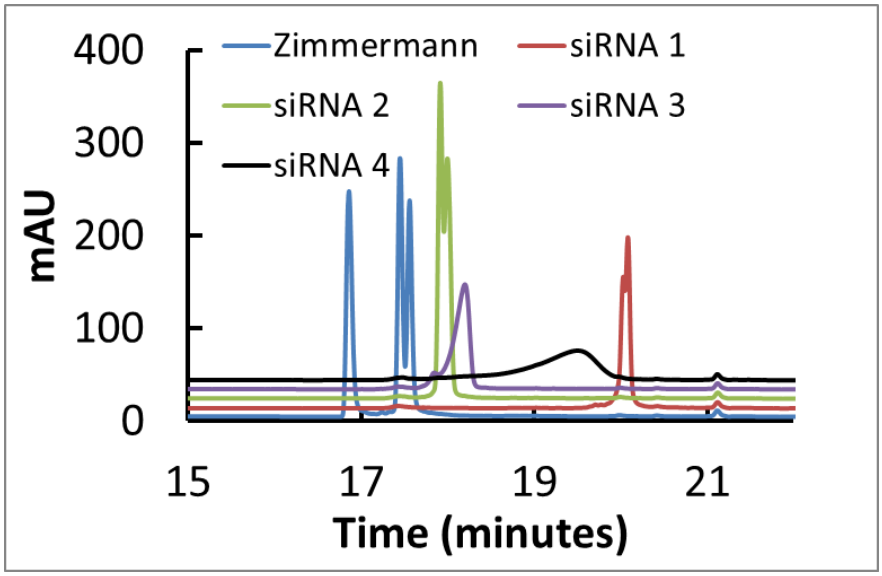

b)

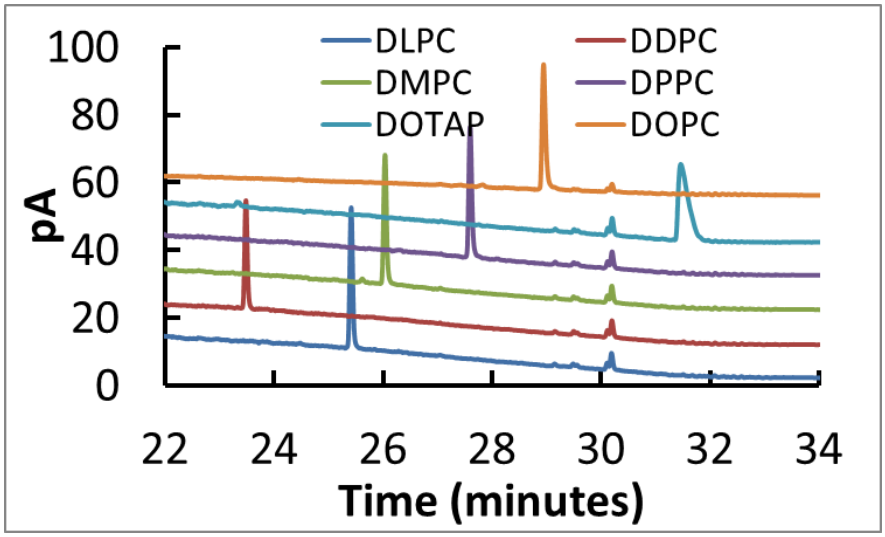

Figure 4.8 UHPLC-UV-CAD separation and detection of siRNA duplexes and phospholipids with DBAA as the ion-pair reagent on a BEH phenyl column
a) Overlaid chromatographic traces for siRNA with UV detection at 260 nm.
b) Overlaid chromatographic traces for phospholipids with corona CAD detection
Conditions: Mobile phase A consisted of 0.1 M DBAA. UPLC column: BEH phenyl (150 x 2.1 mm); other conditions are as in Figure 4.2.

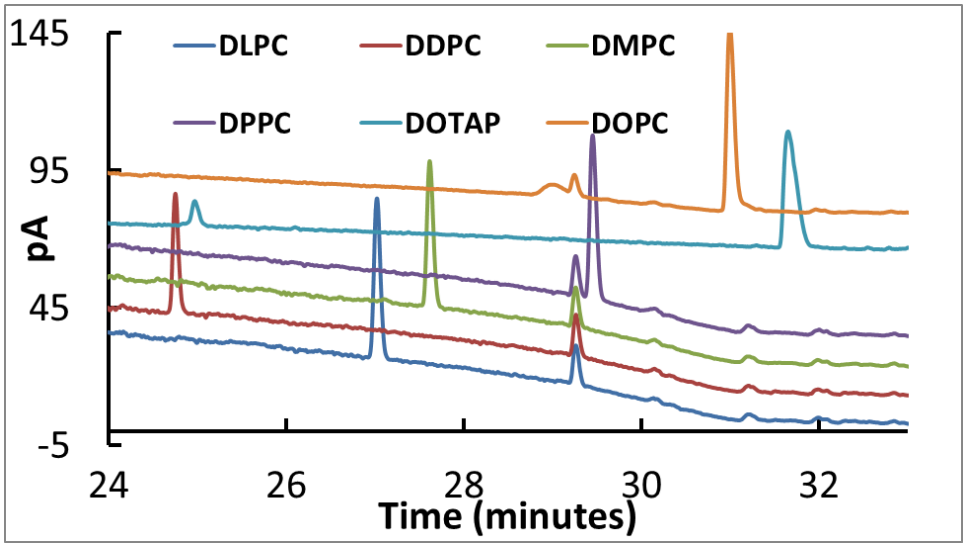

Figure 4.9 UHPLC-CAD separation and detection of phospholipids with DAAA as the ion-pair reagent on a BEH phenyl column
Conditions: Mobile phase A consisted of 0.1 M DAAA. UPLC column: BEH phenyl (150 x 2.1 mm); other conditions are as in Figure 4.2.

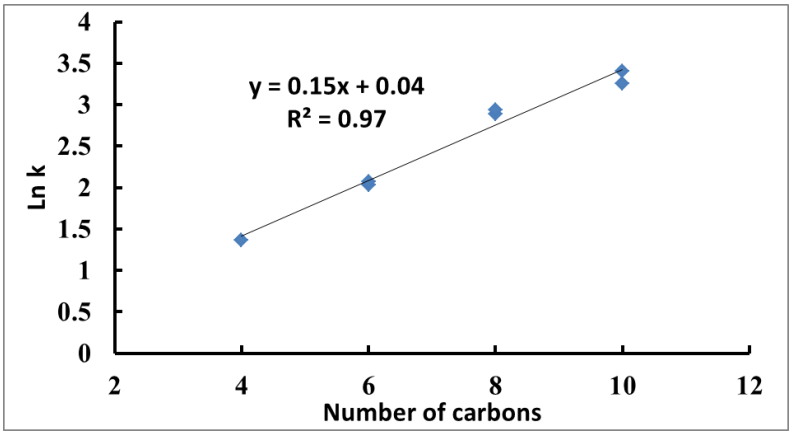

Figure 4.10 A representative plot showing the Ln k of Zimmermann siRNA as a function of the number of carbons in ion-pair reagents

Table 4.1 Summary of the retention factor for various siRNA samples and the correlation coefficient for Ln k vs the number of carbons plots

		Retention factor				
Ion pair reagent	**The number of carbons**	**Zimmermann siRNA**	**siRNA 1**	**siRNA 2**	**siRNA 3**	**siRNA 4**
DEAA	4	3.9	7.2	5.7	5.0	5.8
DPAA	6	7.8	12.8	9.7	10.9	12.6
DBAA	8	18.4	22.0	19.6	19.9	21.5
DAAA	10	27.8	29.1	26.9	27.8	29.3
Correleration coefficient		0.97	0.97	0.97	0.96	0.96

Note: The retention factor was reported as an average of two replicate injections except for DEAA where the measurement was based on a single injection.

4.3.4 The impact of column temperature on the peak shape of siRNA sample

With DBAA identified as the lead ion-pair reagent, we next explored column temperature to improve the peak shape for siRNA duplexes. As shown in Figure 4.8a (with a column temperature of 50 ^{o}C), the Zimmermann duplex is the only sample for which baseline resolution between the two single strands could be achieved, one eluting as a single peak and the other as a partially resolved doublet. Samples siRNA 1 and siRNA 2 exhibited a single peak with a poor resolution between the two strands, while siRNA 3 and siRNA4 showed a broad peak shape with no resolution between the two complementary strands.

The column temperature is expected to impact the peak shape of the siRNA duplex. The peak shape of a duplex can undergo two transitions as the column temperature increases within a range that covers the melting temperature of a double-stranded siRNA. In its native conformation, the duplex adopts a double-helix structure with the two strands strongly associated primarily through hydrogen bond interaction. If the column temperature is below the melting temperature, the siRNA duplex will elute as

a single peak. As the column temperature increases and approaches the onset melting temperature of the duplex, the siRNA could be a mixture of several closely related species in equilibrium with each other, including the denatured single strands, the intact duplex, and their respective stereoisomers. The complex sample mixture can result in poor peak shapes due to insufficient resolution of the components and where the equilibrium kinetics are slow, the latter of which is often the case for biological macromolecules. [31] When the column temperature exceeds the melting temperature, siRNA duplexes can undergo rapid melting upon injection onto the column and then elute as sharp single-stranded peaks.[32]

To improve the peak shape of a siRNA duplex, we need to set the column temperature either below the onset melting temperature of or above the peak melting temperature of the sample. First, we utilized solution differential scanning calorimetry (DSC) to assess the melting temperature of the siRNA duplexes. **Figure 4.11** shows the overlaid DSC thermograms for five different siRNA duplexes. The respective onset melting temperatures were 53 ˚C, 56 ˚C, 70 ˚C, 75 ˚C and 85 ˚C for the Zimmerman siRNA and siRNAs 1 through 4. The measured melting temperatures in phosphate buffer solution were 60 ˚C, 95 ˚C, 64 ˚C, 76 ˚C and 82 ˚C for the Zimmerman siRNA and siRNAs 1 through 4, respectively. Next, we attempted to separate the siRNA duplexes at temperatures ranging from 40 to 70˚C to verify how the column temperature impact the peak shape; the results are shown in **Figure 4.12 (a-e)**.

The impact of column temperature on the peak shape of siRNA duplex is complex and intriguing. For the siRNA duplex with the Zimmermann sequence (**Figure 4.12a**), the two complementary strands were well separated over the entire temperature range.

This implies that the Zimmermann duplex underwent on-column melting at a temperature (e.g., 40 ˚C or lower) significantly below the measured on-set melting temperature of 53 ˚C (in phosphate buffer). The on-column melting temperature depression is likely due to the presence of an organic solvent (e.g., ACN) in the mobile phase and/or the pressure-induced shear stress. The later eluting strand shows a doublet peak shape, which is attributed to the partial resolution of diastereomers. [33] Since the partial resolution of diastereomers negatively impacts siRNA peak shape, it is desirable to eliminate the separation of diastereomers during the analysis of siRNA duplexes and the potential low-level impurities by UHPLC. Hexafluoroisopropanol (HFIP) has been reported in the literature as an effective organic additive to inhibit the separation of diastereomers of phosphorothioate oligonucleotides on achiral columns by reducing the hydrophobic interaction between oligonucleotide and the stationary phase. [30] Indeed, the addition of 0.1M HFIP in mobile phase A (i.e., 0.1M DBAA, pH 7) improved the peak shape for Zimmermann siRNA under denaturing conditions, where the duplex eluted as two symmetrical single-stranded peaks. (**Figure 4.13**)

For siRNA 1 (**Figure 4.12b**), the duplex remained a single peak with a slight partial resolution of the two strands at a temperature from 40 to 60 ˚C. The peak shape showed a sharp transition as temperature increased from 60 to 70 ˚C. Significant peak broadening at 70 ˚C suggested the column temperature is approaching the on-column melting temperature for siRNA 1, which once again is lower than in PBS buffer (e.g., an onset temperature of 85 ^{o}C) as acetonitrile in the mobile phase and/or pressure-induced shear stress during elution could lower the melting temperature. The column temperature for siRNA 1 should thus be kept below 70 ˚C to avoid this peak broadening effect. The

asymmetric peak shape at temperatures below 70 ˚C can be improved by adding 0.2M HFIP into the mobile phase A, where the duplex eluted as a single, symmetric peak (data not shown).

The change of peak shape as a function of column temperature is similar for siRNA 2 and 3 (**Figure 4.12c and d**). In both cases, the siRNA duplex showed a broad and asymmetric peak shape at 40 ^{o}C. The peak width narrowed as the temperature increased, and the siRNA sample exhibited a single, symmetric peak at 70 ˚C. Significant peak broadening at 40 ^{o}C for both siRNA 2 and 3 suggested that the column temperature at this point started to approach the onset melting temperature for both RNA duplexes on the column. This was confirmed by conducting additional separations at lower column temperatures, such as 20 or 30 ^{o}C, which revealed a sharp transition in peak width as the temperature increased from 20 to 30 ^{o}C for siRNA 2 and 30 to 40 ^{o}C for siRNA 3, respectively. In contrast to siRNA 1, the ideal column temperature for siRNA 2 and 3 is around 70 ˚C. Higher temperatures (> 70 ^{o}C) were not evaluated due to concerns over column instability.

The temperature dependent peak shape for siRNA 4 (**Figure 4.12e**) showed two distinct transition temperatures. The peak width significantly narrowed as the column temperature was increased from 60 to 70 ˚C (which is consistent with those for siRNA 2 and 3) and broadened as it was increased from 40 to 50 ˚C, respectively. The transition at the low-temperature end corresponded to the onset of on-column melting of siRNA 4 duplex and the transition at high temperature was related to complete on-column melting. Similar to siRNA 2 and 3, a column temperature of 70 ^{o}C is preferred for duplex quantitation as the siRNA eluted as a single, slightly asymmetric peak. **Table 4.2**

summarizes the general recommendations on mobile phase A composition and column temperature for direct analysis of siRNA duplex. It is worth noting that while the column temperature has a significant impact on the retention time and peak shape for siRNA, it has little influence over the separation of phospholipids using ion-pair reverse phase method (data not shown).

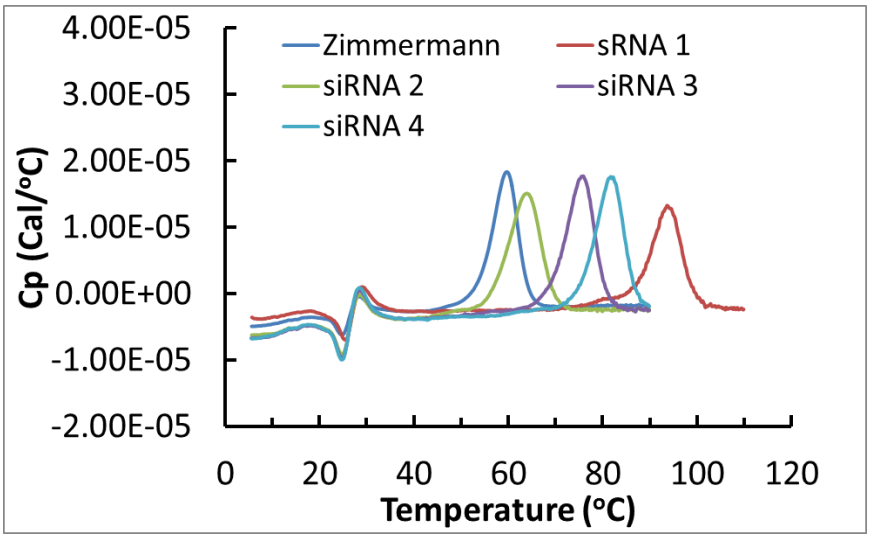

Figure 4.11 Overlaid DSC thermograms for a series of siRNA duplexes

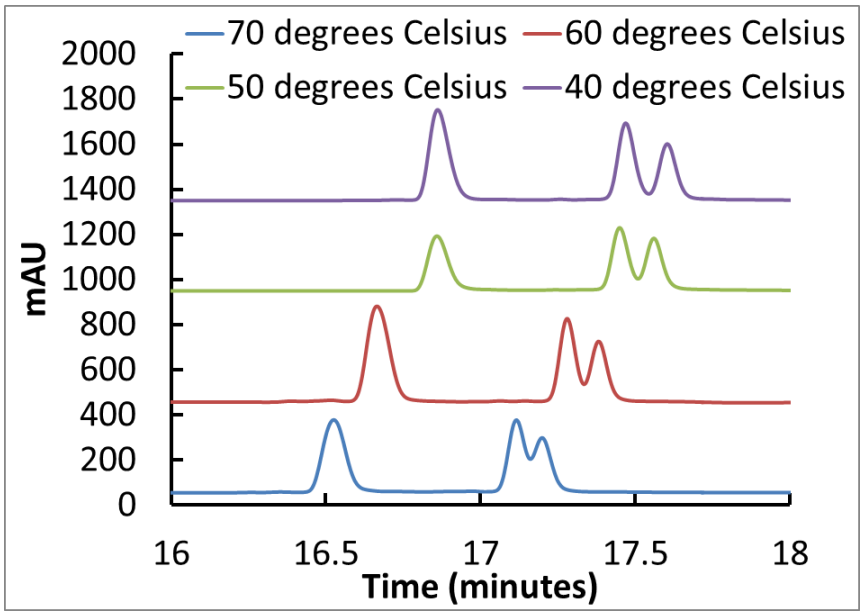

Figure 4.12a Effect of column temperature on the separation of Zimmermann siRNA duplex.
Conditions: Mobile phase A consisted of 0.1 M DBAA. UPLC column: BEH phenyl (150 x 2.1 mm); other conditions are as in Figure 4.2.

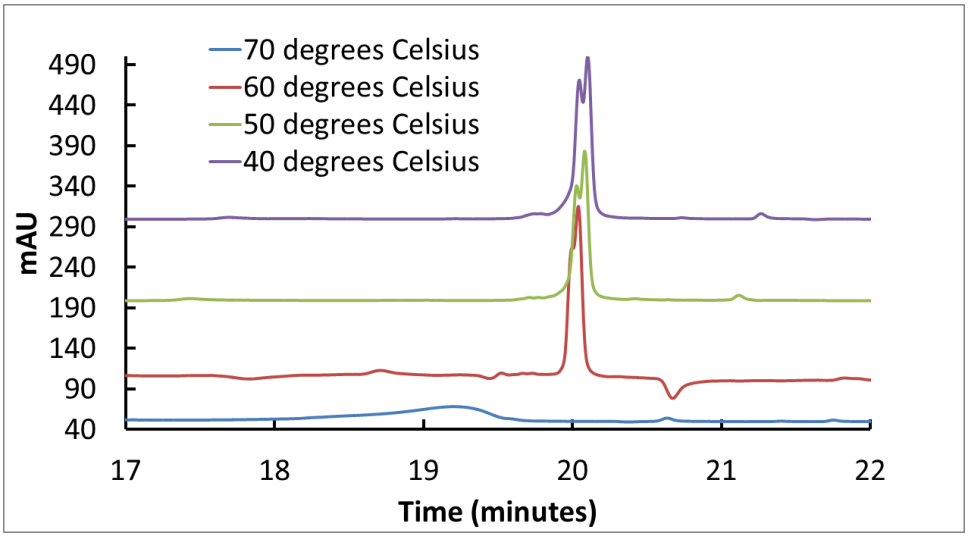

Figure 4.12b Effect of column temperature on the separation of sRNA 1 duplex
Conditions: Mobile phase A consisted of 0.1 M DBAA. UPLC column: BEH phenyl (150 x 2.1 mm); other conditions are as in Figure 4.2.

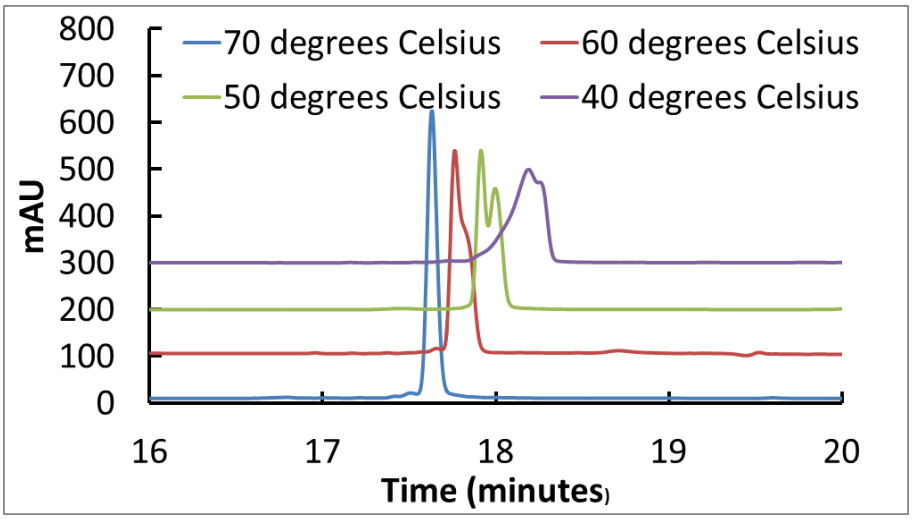

Figure 4.12c: Effect of column temperature on the separation of siRNA 2 duplex. **Conditions:** Mobile phase A consisted of 0.1 M DBAA. UPLC column: BEH phenyl (150 x 2.1 mm); other conditions are as in Figure 4.2.

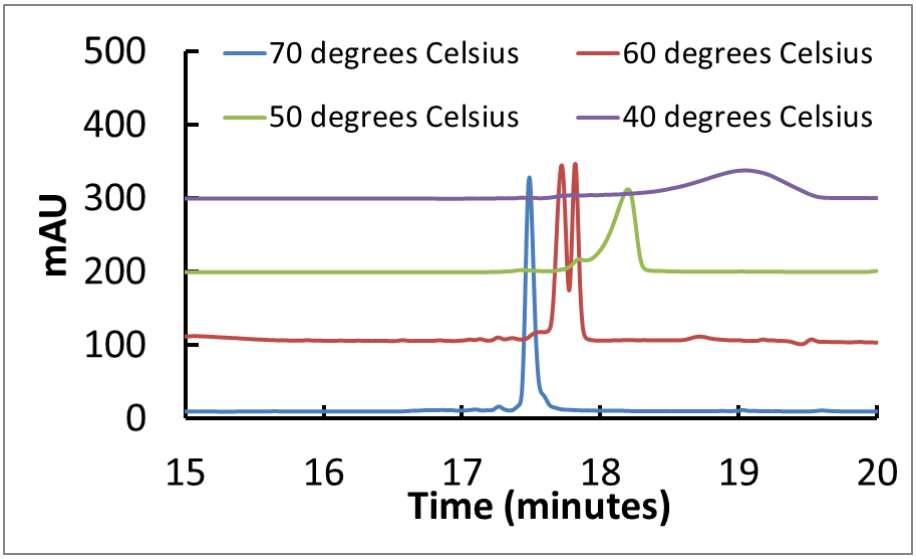

Figure 4.12d Effect of column temperature on the separation of siRNA 3 duplex **Conditions:** Mobile phase A consisted of 0.1 M DBAA. UPLC column: BEH phenyl (150 x 2.1 mm); other conditions are as in Figure 4.2.

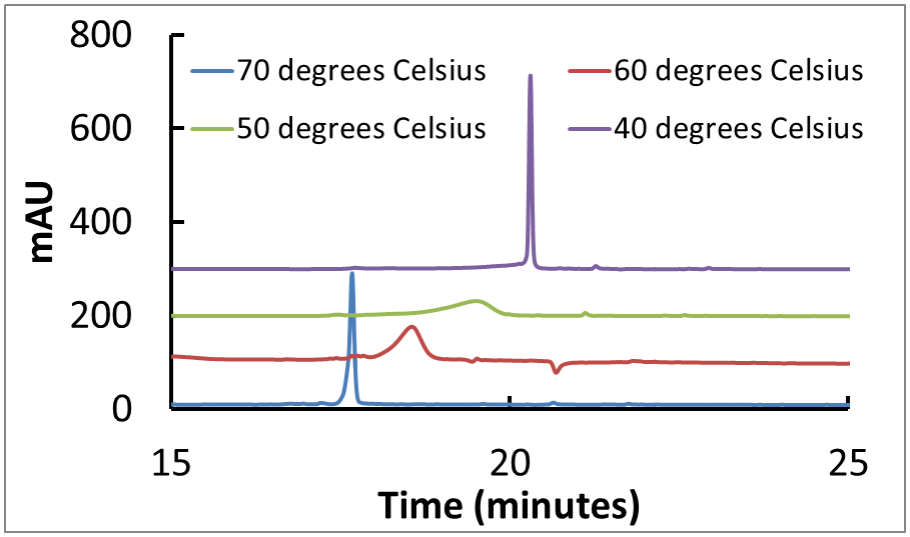

Figure 4.12e Effect of column temperature on the separation of siRNA 4 duplex
Conditions: Mobile phase A consisted of 0.1 M DBAA. UPLC column: BEH phenyl (150 x 2.1 mm); other conditions are as in Figure 4.2.

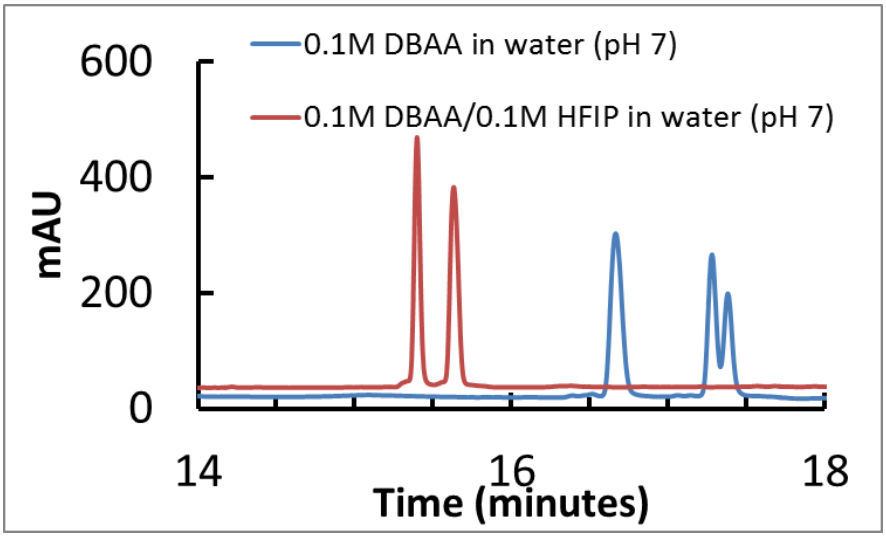

Figure 4.13 The impact of HFIP in mobile phase A on the peak shape of Zimmermann siRNA
Conditions: Mobile phase A consisted of 0.1 M DBAA and 0.1 M HFIP. UPLC column: BEH phenyl (150 x 2.1 mm); other conditions are as in Figure 4.2.

Table 4.2 Summary of recommended mobile phase A compositions and column temperatures for various siRNA duplexes

Sample ID	Mobile phase A	Column Temperature
Zimmermann siRNA	0.1 M DBAA/0.1 M HFIP	40 to 60 ^{o}C
siRNA 1	0.1 M DBAA/0.2 M HFIP	60 ^{o}C
siRNA 2	0.1 M DBAA	70 ^{o}C
siRNA 3	0.1 M DBAA	70 ^{o}C
siRNA 4	0.1 M DBAA	70 ^{o}C

4.3.5 Separation of siRNA and lipids in LNP formulation with ion-pair reverse phase UHPLC

The UHPLC method discussed in the previous sections can be further optimized concerning the gradient condition to reduce the runtime. Figure 4.14 shows a representative chromatogram of siRNA samples and phospholipids in a 25-minute gradient method, demonstrating an adequate separation of the entire sample set with good selectivity. The peak shapes for DOTAP and siRNA 4 are broad, and their root causes are likely different. The broad peak shape for DOTAP, a cationic lipid bearing a positive charge at neutral pH (or the pH of the mobile phase), is likely due to a secondary interaction (e.g., electrostatic interaction) between the stationary phase and the analyte. The peak broadening for siRNA 4 can be attributed to the column temperature that is close to the onset melting of the duplex. Additional studies are needed to optimize the separation conditions in order to improve the peak shape for DOTAP and siRNA 4 while maintaining the separation of the rest of siRNAs and lipids.

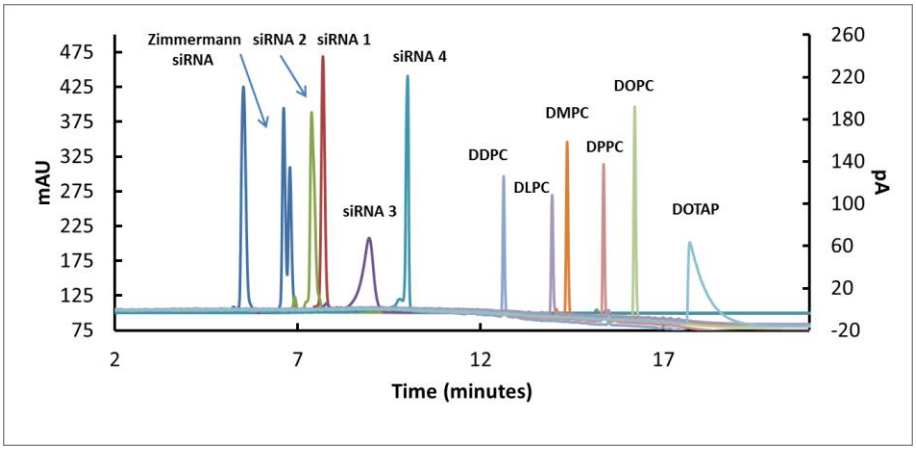

Figure 4.14 UHPLC-UV-CAD separation and detection of siRNA duplexes and phospholipids with DBAA as the ion-pair reagent on a BEH phenyl column
c) Overlaid chromatographic traces for siRNA with UV detection at 260 nm.
d) Overlaid chromatographic traces for phospholipids with corona CAD detection
Conditions: Mobile phase A consisted of 0.1 M DBAA. UPLC column: BEH phenyl (150 x 2.1 mm); column temperature: 70 ^{o}C. The gradient method was run from 30% to 35% B in 5 minutes, followed by a steeper gradient from 35% to 100% B in 10 minutes and isocratic hold at 100% B for 5 minutes. Other conditions are as in Figure 4.2.

The ion-pair reversed phase methods (both the short and long gradient) were applied to the analysis of an experimental LNP formulation that consisted of a double-stranded siRNA, two types of phospholipids, cholesterol and PEGylated short-chain lipid. Figure 4.15 shows the chromatographic traces of all key components in the formulation using UV and corona-CAD dual detectors. Forced stressed testing with base (e.g., 0.01 M NaOH) and 0.3% hydrogen peroxide suggested that siRNA is more stable than the lipid components. The fact that the siRNA is more stable than the lipids is not surprising as the siRNA has been chemically modified to prevent hydrolysis in an aqueous environment. Whereas the siRNA was stable with respect to base stress, one minor degradation product (~18 minutes) was detected when stressed with hydrogen peroxide, presumably due to the desulfurization of the siRNA that contains phosphorothioate

linkage. The lipid components are susceptible to hydrolysis and oxidation. Under ambient conditions, lipid 1 and PEGylated lipid underwent complete hydrolysis within 60 minutes in the presence of 0.01M NaOH. Lipid 2 and cholesterol are stable with respect to base hydrolysis, but lipid 2, when stressed with hydrogen peroxide, can form an oxidative product with a retention time close to 30.6 minutes. Figure 4.16 shows the stacked chromatograms for both siRNA and lipids components with gradient elution, achieving an analysis time of less than 20 minutes and demonstrating good selectivity for all key ingredients in LNP.

a)

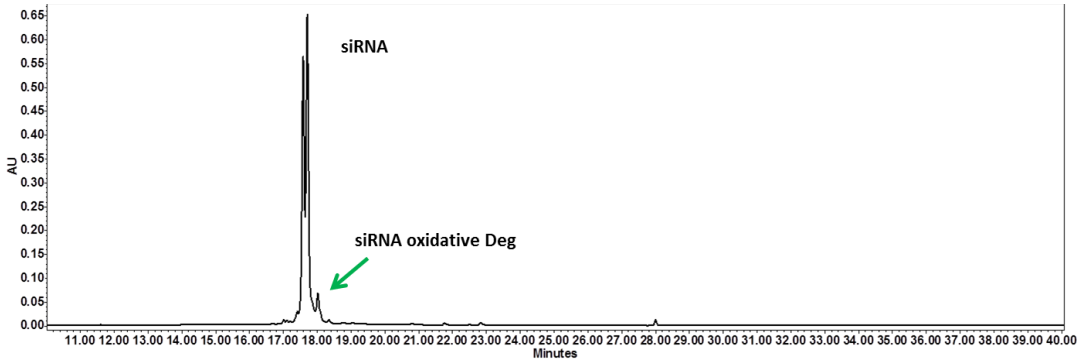

b).

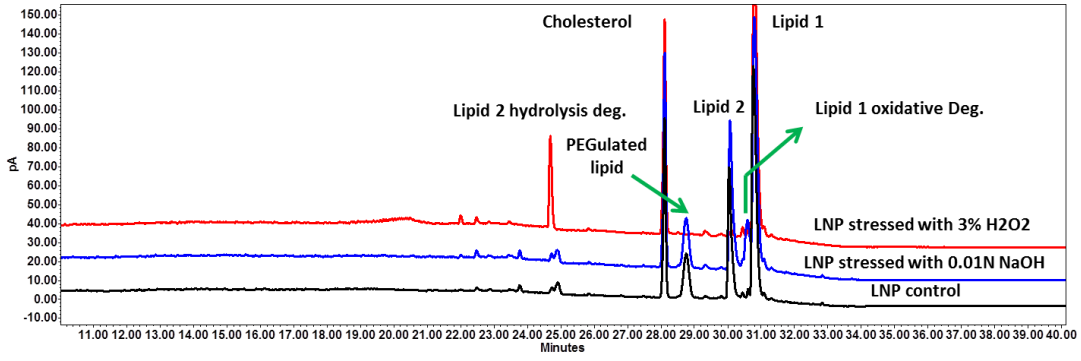

Figure 4.15 UHPLC-UV-CAD separation and detection of siRNA duplex and lipid vehicles in the LNP formulation

Figure 4.15 (cont'd)
a).Chromatogram of siRNA in LNP with UV absorbance detection at 260 nm.
b).Chromatogram of lipids in LNP with corona CAD detection
Conditions: Mobile phase A consisted of 0.1 M DBAA and 0.1 M HFIP. UPLC column: BEH phenyl (150 x 2.1 mm); other conditions are as in Figure 4.2.

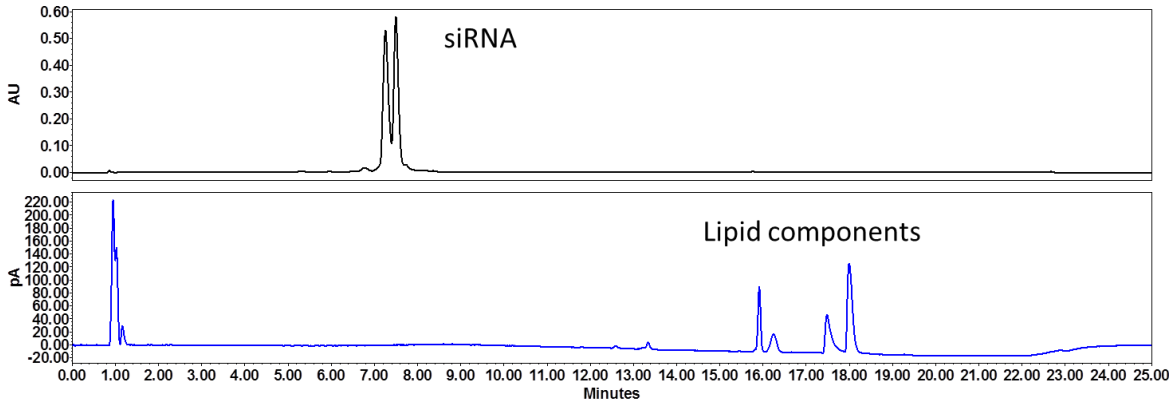

Figure 4.16 UPLC analysis of the LNP formulation with UV and CAD as dual detectors
Conditions: Mobile phase A consisted of 0.1 M DBAA. UPLC column: BEH phenyl (150 x 2.1 mm). The gradient method was run from 35% to 100% B in 10 minutes, followed by an isocratic hold at 100% B for 5 minutes. Other conditions are as in Figure 4.2.

4.4 Conclusions

A reversed-phase ion-pair chromatography method was developed for the simultaneous separation of multiple siRNA duplexes and phospholipids, the main components of the lipid nanoparticle formulation. Key chromatographic parameters critical to reducing the retention gap between hydrophilic siRNA and hydrophobic phospholipids included the chemistry of the stationary phase and the structure of the ion-pair reagent. With BEH phenyl as the stationary phase and ACN as the organic modifier in the mobile phase, ion-pair reagent dibutylammonium acetate (DBAA) provided a superior separation efficiency and selectivity compared to other structural analogs, such as TEAA, DPAA, and DAAA. The column temperature has a significant impact on the

peak shape of double-stranded siRNA; the selection of column temperature depends on the on-column melting temperature of the siRNA duplex. A temperature range covering both the onset and peak melting temperature of the siRNA should be avoided in order to maintain a good peak shape.

List of References

1. Y.K. Oh, T.G. Park, siRNA delivery systems for cancer treatment, Adv. Drug Delivery Rev. 61 (2009) 850-862.

2. H.Yin, R.L. Kanasty, A.A. Eltoukhy, A.J. Vegas, J.R. Dorkin, D.G. Anderson, Non-viral vectors for gene-based therapy, Nat. Rev. 15 (2014) 541-555.

3. A.Wittrup, J. Lieberman, Knocking down disease: a progress report on siRNA therapeutics, Nat Rev Genet. 16(9) (2015) 543–552.

4. L. Li, Y. Shen, Overcoming obstacles to develop effective and safe siRNA therapeutics, Expert Opin. Biol. Ther. 9(5) (2009) 609-619.

5. S.Y. Wu, N.A.J. McMillan, Lipidic Systems for *in vivo* siRNA Delivery, The AAPS J. 11(4 (2009) 639-652.

6. K.A. Whitehead, R. Langer, D.G. Anderson, Knocking down barriers: advances in siRNA delivery, Nat. Rev. 8 (2009) 129-138.

7. J.A Wolff, D.B. Rozema, Breaking the bonds: non-viral vectors become chemically dynamic, 16 (1) (2008) 8–15.

8. Semple, S.C. et. al. Rational design of cationic lipids for siRNA delivery. *Nat. Biotechnol.* **2010**, 28 (2), 172-176.

9. V. Kumar, et al., Shielding of lipid nanoparticles for siRNA delivery: impact on physicochemical properties, cytokine induction, and efficacy. Molecular Therapy: Nucleic Acids. 3 (2014) e210.

10. V. Murugaiah, W. Zedalis, G. Lavine, K. Charisse, M. Manoharan, Reverse-phase high-performance liquid chromatography method for simultaneous analysis of two liposome-formulated short interfering RNA duplexes, Anal. Biochem. 401 (2010) 61-67.

11. R.L. Ball, P. Bajaj, K.A. Whitehead, Achieving long-term stability of lipid nanoparticles: examining the effect of pH, temperature, and lyophilization, Inter. J. Nanomed. 12 (2017) 305-315.

12. Y. Suzuki, K. Hyodo, Y. Tanaka, H. Ishihara, siRNA-lipid nanoparticles with long-term storage stability facilitate potent gene-silencing in vivo, J. Control. Release. 220 (2015) 44–50.

13. M. Biba, E. Jiang, B. Mao, D. Zewge, J.P. Foley, C.J. Welch, Factors influencing the separation of oligonucleotides using reversed-phase/ion-exchange mixed-mode high performance liquid chromatography columns, J. Chromatogr. A 1304 (2013) 69-77.

14. M. Biba, C.J. Welch, J.P. Foley, Investigation of a new core–shell particle column for ion-pair reversed-phase liquid chromatography analysis of oligonucleotides, J. Pharm. Biomed. Anal. 96 (2014) 54–57.

15. A. Zimmermann, R. Greco, I. Walker, J. Horak, A. Cavazzini, M. Lämmerhofer, Synthetic oligonucleotide separations by mixed-mode reversed-phase/weak anion-exchange liquid chromatography, J. Chromatogr. A 1354 (2014) 43-55.

16. M. Mateos-Vivas, E. Rodríguez-Gonzalo, D. García-Gómez, R. Carabias-Martínez, Hydrophilic interaction chromatography coupled to tandem mass spectrometry in the presence of hydrophilic ion-pairing reagents for the separation of nucleosides and nucleotide mono-, di- and triphosphates, J. Chromatogr. A 1414 (2015) 129–137.

17. S. Sethi, E. Brietzke, Recent advances in lipidomics: Analytical and clinical perspectives, Prostag. Oth. Lipid M. 128–129 (2017) 8–16.

18. P. Donato, V. Inferrera, D. Sciarrone, L. Mondello, Supercritical fluid chromatography for lipid analysis in foodstuffs, J. Sep. Sci. 40 (2017) 361–382.

19. K.C. Arnoldsson, P. Kaufmann, Lipid class analysis by normal phase high performance liquid chromatography, development and optimization using multivariate methods, Chromatographia, 38 (1994) 317-324.

20. P.M. Hutchins, R.M. Barkley, R.C. Murphy, Separation of cellular nonpolar neutral lipids by normal-phase chromatography and analysis by electrospray ionization mass spectrometry, J. Lip. Res. 49 (2008) 804-813.

21. D.G. McLaren, P.L. Miller, M.E. Lassman, J.M. Castro-Perez, B.K. Hubbard,T.P. Roddy, An ultraperformance liquid chromatography method for the normal-phase separation of lipids, Anal. Biochem. 414 (2011) 266–272.

22. M.I. Aveldano, M.VanRollins, L.A. Horrocks, Separation and quantitation of free fatty acids and fatty acid methyl esters by reverse phase high pressure liquid chromatography, J Lip. Res., 24 (1983) 83-93.

23. S.S. Bird, V.R. Marur, I.G. Stavrovskaya, B.S. Kristal, Separation of Cis-*Trans* phospholipid isomers using reversed phase LC with high resolution MS detection, Anal Chem. 84(13) (2012) 5509–5517.

24. T. Cajka, O. Fiehn, Comprehensive analysis of lipids in biological systems by liquid chromatography-mass spectrometry, Trends Anal. Chem. 61 (2014) 192–206.

25. A. Avalli, G. Contarini, Determination of phospholipids in dairy products by SPE/ HPLC/ ELSD, J Chromatogr. A 1071 (2005) 185–190.

26. R.A. Moreau, The analysis of lipids *via* HPLC with a charged aerosol detector, Lipids, 41(7) (2006), 727-734.

27. E. Dodbiba, C. Xu, T. Payagala, E. Wanigasekara, M.H. Moon, D. W. Armstrong, Use of ion pairing reagents for sensitive detection and separation of phospholipids in the positive ion mode LC-ESI-MS. Analyst, 136 (2011) 1586–1593.

28. K.T. Love, K.P. Mahon, C.G. Levins, K.A. Whitehead, W. Querbes, J. R. Dorkind, et al., Lipid-like materials for low-dose in vivo gene silencing, Proc. Natl. Acad. Sci. U.S.A, 107(21) (2010) 1864-1869.

29. D.S. Levin, B.T. Shepperd, C.J. Gruenloh, Combining ion pairing agents for enhanced analysis of oligonucleotide therapeutics by reversed phase-ion pairing ultra performance liquid chromatography (UPLC), J. Chromatogr. B 879 (2011) 1587–1595.

30. M. Gilar, K.J. Fountain, Y. Budman, J.L. Holyoke, H. Davoudi, J.C. Gebler, Characterization of therapeutic oligonucleotides using liquid chromatography with on-line mass spectrometry detection, 13(4) (2003) 229-43.

31. M. Gilar, K.J. Fountain, Y. Budman, U.D. Neue, K.R. Yardley, P.D. Rainville, R.J. Russell, J.C. Gebler, Ion-pair reversed-phase high-performance liquid chromatography Analysis of oligonucleotides: Retention prediction, J. Chromatogr. A 958 (2002) 167–182.

32. S.M. McCarthy, M. Gilar, J. Gebler, Reversed-phase ion-pair liquid chromatography analysis and purification of small interfering RNA, Anal. Biochem. 390 (2009) 181–188.

33. L. Li, T. Leone, J.P. Foley, C.J. Welch, Separation of siRNA stereoisomers using reversed phase ion-pairing chromatography, J Chromatogr. A 1500 (2017) 84-88.

Chapter 5 Separation and stability evaluation of siRNA duplex under forced stress conditions

5.1 Introduction

Native RNA is highly susceptible to enzymatic degradation by ribonucleases and non-enzymatic hydrolysis by acid or base. [1,2] Synthetic siRNAs often incorporate chemically modified nucleotides to improve *in vivo* serum stability. Chemical modification of siRNA includes the replacement of 2'-hydroxyl group of the ribose with fluorine or methoxy. In addition, the 3'-5' phosphodiester is often replaced by phosphorothioate at specific locations of the siRNA sequence to prevent hydrolytic degradation. [3,4] Various stability studies are routinely conducted during drug product development. The goal of the stability studies is to predict stability performance of the product and to inform quality control strategy if chemical degradation is flagged as a potential risk. Forced stress testing is one of the many tools that can be used to predict stability problems, develop analytical methods, and help elucidate degradation pathways for a new drug candidate. [5,6] Stress testing is a systematic study where the molecule of interest is deliberately exposed to a series of aggressive conditions to invoke a controlled chemical degradation. The stress study can be performed to probe the intrinsic stability of the molecule concerning hydrolysis, oxidation, and photolysis, the three primary modes of drug degradation, including RNA. [7] The stress testing conditions typically include acid, base, hydrogen peroxide, radical initiator (e.g., AIBN or ACVA), light, and heat. The primary degradation products observed under these conditions are known as signaling degradation products, as they may form in drug product during long-term storage. Since the signaling degradants present a suitable sample matrix, it can be used to

assess HPLC method selectivity towards degradation products in a formulation. The outcome of the stress testing can inform intrinsic stability issues of the molecule and provide a scientific framework for a rational selection of excipients for formulation development. While forced stress testing is routinely conducted during formulation development for the small molecule-based drug product, few studies have been reported in the literature on the use of this predictive tool to evaluate the stability of a chemically modified siRNA. Here we conducted a systematic forced degradation study for a synthetic double-stranded siRNA, aiming to probe the intrinsic stability of the molecule with respect to hydrolysis and oxidation.

5.2 Material and methods

5.2.1 Chemicals

The siRNA duplex and the complementary single strands targeting ApoB gene were provided by Merck Sharp & Dohme (MSD) RNA synthesis group. This is the same siRNA duplex investigated in Chapter 3. Triethylammonium acetate, hydrogen peroxide (30%), 4, 4′-Azobis (4-cyanovaleric acid) (ACVA), and copper (II) sulfate were sourced from Sigma-Aldrich (St. Louis, MO, USA). HPLC grade acetonitrile as well as crystalline Iodine (99%) were obtained from Fisher Scientific.

5.2.2 Instrument

An Agilent 1290 Infinity UHPLC system (Agilent Technologies, Santa Clara, CA, USA) was employed for the separation of siRNA stereoisomers. This UHPLC system

consisted of a binary pump, a diode array detector, an autosampler, and a column heater. The system could be operated up to pressure to 1200 bar.

5.2.3 Ion-pair reversed phase chromatographic conditions

The siRNA control and stressed samples were analyzed with an ion-pair reversed phase UHPLC. The column was an Acquity BEH C18 (150 x 2.1 mm) with a nominal particle size of 1.7 µm. Mobile phase A consisted of 0.1 M TEAA in water (pH 7), and mobile phase B was a mixture of 20% A and 80% organic modifier (ACN). The gradient method was run from 6% to 12% B in 19.5 minutes, followed by steeper gradients of 12% to 14%B and 14 to 30%B in 5.5 minutes and 7 minutes, respectively.

5.2.4 Procedure for forced stress testing

siRNA was dissolved in 20 mM phosphate buffer solution (pH 7) to approximately 0.2 mg/mL; aliquots were then subjected to the various stress tests below. The forced degradation study is intended for a qualitative assessment of the chemical stability property of the siRNA; hence, it is only performed in a single replicate.

5.2.4.1 Acid and base stress

Hydrochloric acid (HCl) or sodium hydroxide (NaOH) was added to separate aliquots of the siRNA sample solution to achieve 0.1 M acid or base concentration. The aliquots were stored for 24 hours at room temperature. The 0.1 M HCl and NaOH were chosen as the reactants based on the recommended acid and base degradation conditions for small molecule drug products. [8]

5.2.4.2 Oxidative stress with hydrogen peroxide

A sufficient amount of hydrogen peroxide solution was added to the siRNA solution aliquots to achieve a concentration of 0.3 % (v/v). To evaluate the impact of a

transition metal on oxidative degradation by hydrogen peroxide, 1 ppm Cu (II) was added to a siRNA solution that contained 0.3% hydrogen peroxide. The samples were stored at room temperature for two and four hours before UPLC analysis. The 0.3% hydrogen peroxide was used for the stress testing of siRNA based on the recommended conditions for the oxidative degradation of small molecule drug products. [8]

5.2.4.3 Oxidative stress with radical initiator

4,4′-Azobis(4-cyanovaleric acid) (ACVA) was added to the siRNA solution to obtain a final concentration of 5 mM. This level was used for the stress testing of the siRNA based on prior experience from the oxidative degradation study of small molecule drug products. [9] The siRNA sample containing ACVA was stored at 40 ^{o}C for 24 hours before UPLC analysis.

5.2.4.4 Desulfurization of siRNA duplex using Iodine

Iodine solution was used as the oxidizing agent to promote the replacement of sulfur by oxygen in phosphorothioate-containing oligonucleotides. [10] The reaction was initiated by adding 500 µL of 0.03mM iodine solution in ethanol to 4500 µL of the siRNA with a molar ratio of about three to one between iodine and siRNA. The siRNA sample solution was analyzed by UHPLC approximately one hour after the iodine was introduced.

5.3 Results and Discussion

The siRNA duplex targeting ApoB gene is composed of a 21-nucleotide sense strand and 23-nucleotide antisense strand (Figure 5.1). Both sense and antisense strands were chemically modified to prevent siRNA degradation due to nuclease-induced

hydrolysis. Specifically, the 2'-hydroxyl groups in seven nucleotides for both strands were functionalized with methoxy groups. In addition, three phosphodiester linkages, one from the sense strand and two from the antisense strand, were replaced by a phosphorothioate moiety. A detailed structure was also presented in Figure 3.1a. Figure 5.2 shows a typical separation with ion-pair reversed-phase chromatography for double-stranded siRNA that was denatured on-column. The sense and antisense strands are well resolved from each other, with the sense strand eluting earlier than the antisense strand. The sense strand contains one phosphorothioate stereocenter that, together with the stereocenters on the ribose sugar, results in one pair of diastereomers as well-resolved doublet peaks. The antisense strand contains two phosphorothioate stereocenters, resulting in two pairs of diastereomers, forming four peaks in the chromatogram.

The siRNA sample solution was subjected to various stress conditions prior to UHPLC analysis. The chromatograms were compared to the control sample to assess the extent of degradation.

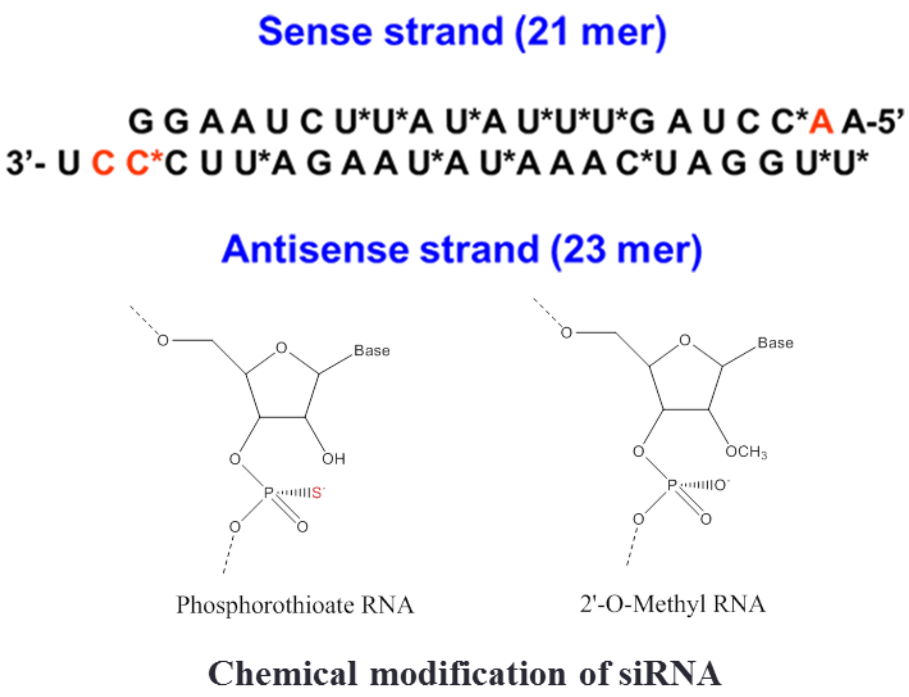

Figure 5.1 Structure of the ApoB gene-targeting siRNA duplex. Nucleotides marked with asterisks contain chemically modified ribose substituents in which the 2'-OH is replaced with 2'-methoxy. In the nucleotides highlighted in red, naturally occurring phosphodiester linkages have been replaced with phosphorothioate linkages.

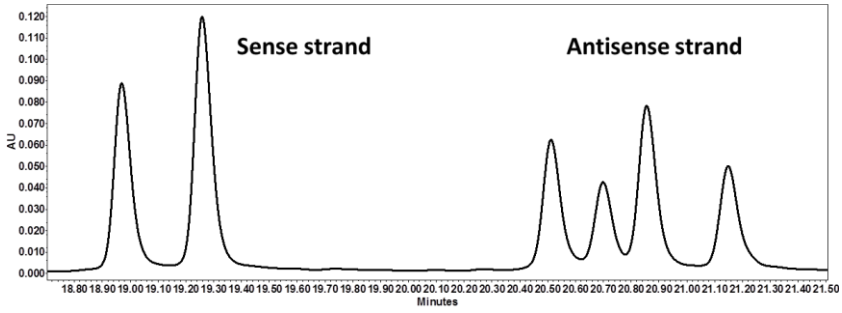

Figure 5.2 A representative chromatogram of siRNA duplex using ion-pair reversed phase UHPLC.
Conditions: UPLC column: BEH C18 (150 x 2.1 mm); Oven temperature: 80 ^{o}C; Mobile phase A consisted of 0.1M triethylammonium acetate (TEAA, pH 7) in water, and mobile phase B was a mixture of 20% A and 80% ACN. The gradient method was run from 6% to 12% B in 19.5 minutes, followed by steeper gradients of 12% to 14% B and 14 to 30% B in 5.5 minutes and 7 minutes. The flow rate was 0.2 mL/minute and the injection volume was 2 µL, with UV absorbance detection at 260 nm. The siRNA sample concentration was approximately 0.2 mg/mL prepared in 20 mM phosphate buffer.

5.3.1 Chemical stability of siRNA under acid and base stress conditions

siRNA sample was stressed with 0.1 M HCl or 0.1 M NaOH under ambient conditions. UPLC analysis of the stressed samples showed that siRNA underwent significant degradation after 24 hours. This was to some degree unexpected since we predicted that the chemically-modified siRNA should have some resistance to hydrolysis. Figure 5.3 shows the overlaid chromatograms of the stressed samples and the control. The stressed siRNA in 0.1 M NaOH showed complete drug loss after 24 hours, forming a myriad of degradation products with retention times ranging from 2 to 12 minutes. The siRNA sample became slightly hazy upon addition of 0.1 M HCl, and this is likely due to the protonation of phosphodiester groups with pK_as close to 1. (Scheme 5.1) The neutral siRNA has low solubility in an aqueous medium, which leads to precipitation. Twenty percent methanol was added to the acid-stressed sample to solubilize the precipitates. Analysis of the stressed sample showed about 38% (area percentage) of drug loss after 24 hours in 0.1 M HCl.

The acid-mediated degradation pathway of the siRNA is different from that by the base; therefore, we anticipated that the acid- and base-stressed samples would exhibit distinct chromatographic traces. Indeed, the degradation product profiles, characterized by the retention time distribution, are different between the acid and base stressed samples. While both stressed samples formed degradation products with retention times between 2 to 12 minutes, the acid-stressed samples showed another cluster of degradation peaks with longer elution times, ranging from 14 to 20 minutes. The degradation product distribution is related to the underlying mechanisms governing the hydrolysis of siRNA. A base-catalyzed hydrolysis proceeds with deprotonation of 2'-hydroxyl group by

hydroxide to form the nucleophilic 2'-oxyanion. The attack of 2'-oxyanion nucleophile on the tetrahedral phosphate leads to the cleavage of a P-5'O bond of the phosphodiester linkage. [11] A similar mechanism can be described for the acid hydrolysis, where the 2'-hydroxy group is the nucleophile attacking the phosphorus, resulting in the cleavage of the phosphodiester. In addition, the RNA can undergo isomerization reaction in the presence of an acid with reaction pathway shown in Scheme 5.2. [12] Since acid can promote both phosphodiester breakage and isomerization, this may explain why the acid-stressed siRNA has a more complex degradation profile than the base stressed one.

siRNA is typically formulated as nanoparticles at pH 7 with lipid or polymer as the delivery vehicle; therefore, chemical stability under neutral conditions is more relevant for predicting siRNA chemical stability performance during long-term storage. Stress testing at pH 7 showed that siRNA is chemically stable after 48 hours at 40 ^{o}C, and the solution is also stable for at least one year when stored at room temperature.

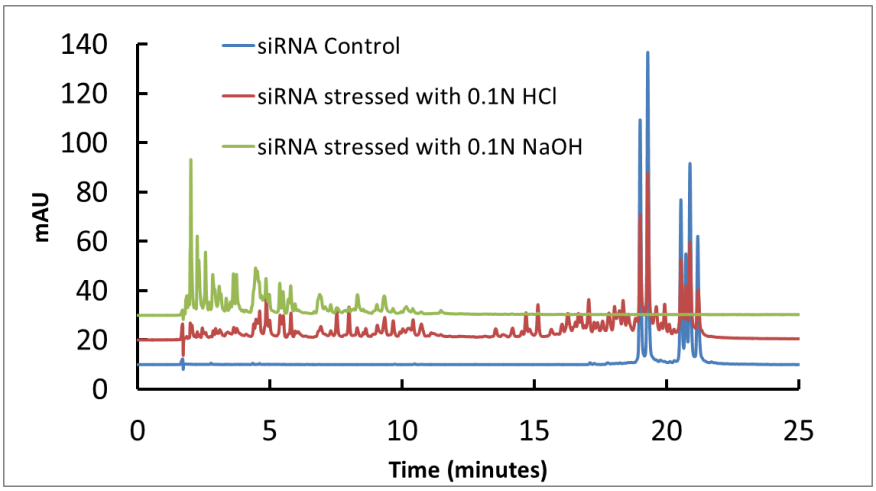

Figure 5.3 Overlaid chromatograms of the acid or base stressed siRNA and the control UHPLC conditions: Same as in Figure 5.2.

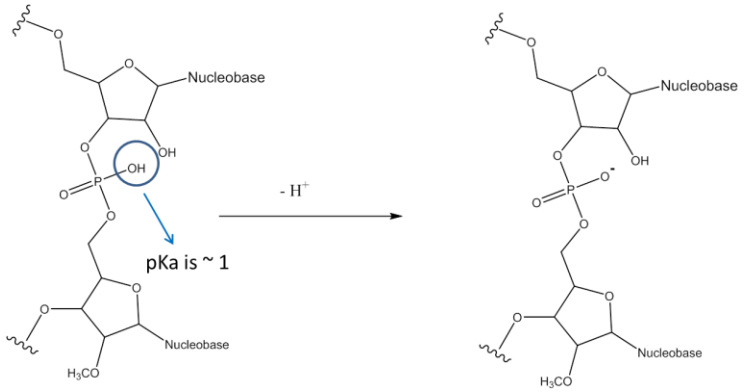

Scheme 5.1 Deprotonation of a neutral phosphodiester group (pK_a approximately 1)

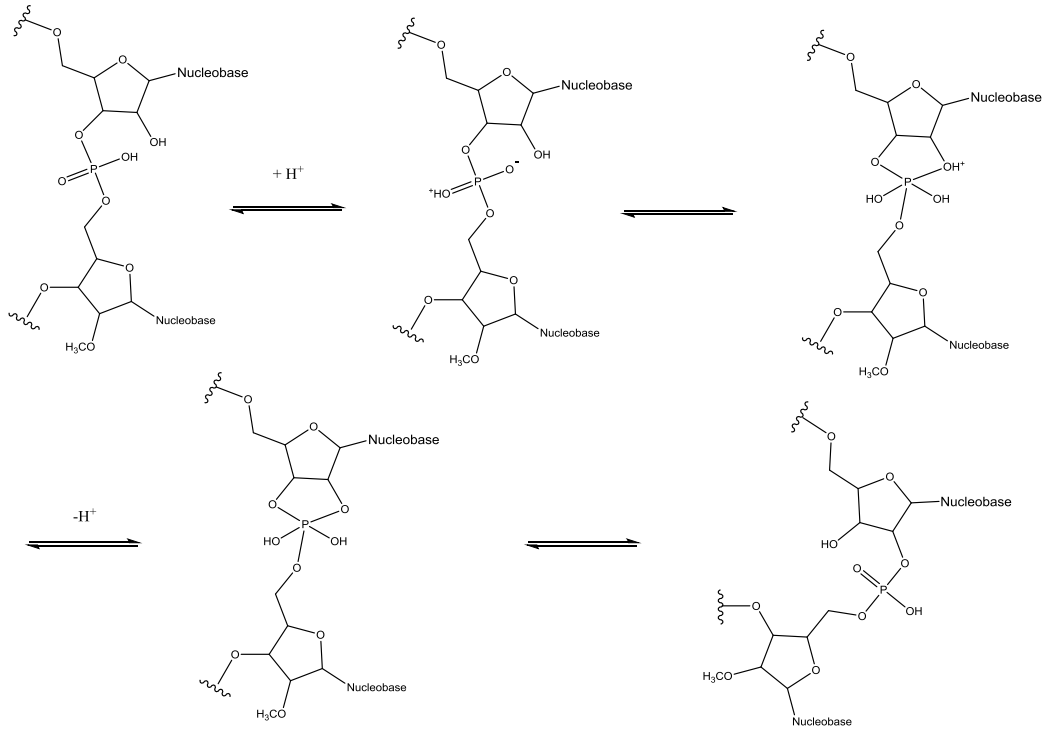

Scheme 5.2 Isomerization of RNA in the presence of acid.[12]

5.3.2 Chemical stability under oxidative stress with hydrogen peroxide

The oxidation of pharmaceuticals is often attributed to exposure to peroxides. RNA oxidative degradation caused by reactive peroxides is well known in the literature. [13,14] Residual peroxides can be found in many common excipients for use in oral and parenteral formulations. [15] Stress testing of the chemically-modified siRNA with hydrogen peroxide can be used to probe the oxidative potential of the parent drug and to inform excipient selection in support of formulation development. Here we stressed the siRNA sample with 0.3% hydrogen peroxide at room temperature for two and four hours. Figure 5.4 shows the overlaid chromatograms of the stressed samples and the control. siRNA showed significant reactivity with hydrogen peroxide with approximately 90% and 82% parent siRNA loss after 2 and 4 hours, respectively. Most of the degradation products were clustered around the active peak. Peaks at 17.0, 17.2, 17.6 minutes were likely the desulfurization products with oxygen replacing sulfur in the phosphorothioate linkage. Iodine is known to induce a desulfurization reaction in oligonucleotide phosphorothioates without incurring other unwanted reaction products. [16] Figure 5.5 shows the overlaid chromatograms of the siRNA samples stressed with hydrogen peroxide and molecular iodine. The oxidation products in the peroxide-stressed siRNA, with retention times of 17.0, 17.2, 17.6 minutes, matched with those in the iodine-stressed sample. Although hydrogen peroxide induced the desulfurization reaction, its underlying mechanism is different from that of iodine. For hydrogen peroxide, the reactive species is likely the hydroxyl radical with the proposed mechanism shown in Scheme 5.3. [17]

In the hydrogen peroxide stressed siRNA sample, three early eluting degradants were also formed with retention time at 1.7, 2.0 and 2.3 minutes. The formation of the early eluting peaks suggested that siRNA underwent significant strand scission (e.g., phosphodiester bond breakage) in the presence of hydrogen peroxide.

Transition metals, such as Fe (II) or Cu (II), can generate a significant amount of hydroxyl radical ($OH^{\cdot}$) with hydrogen peroxide. The hydroxyl radicals can cause efficient degradation of RNA. [18] Figure 5.6 showed the overlaid chromatogram of a stressed siRNA samples with Cu (II)/H_2O_2 and the control. Indeed, siRNA sample treated with 1 ppm of Cu (II) and 0.3% hydrogen peroxide led to complete degradation of siRNA after 2 hours. The main degradation products are the three early eluting degradants, observed previously in the hydrogen peroxide-stressed siRNA sample.

The significant degradation observed for a chemically-modified siRNA, when treated with hydrogen peroxide with or without transition metal, is not entirely unexpected because the chemical modification is mainly intended for preventing hydrolytic degradation. Given the reactive nature of the chemically-modified siRNA towards peroxides, a siRNA-based drug product should not be formulated with polyethylene glycol 400 (PEG 400), polyvinylpyrrolidone (PVP), and tween 80 as they are known to carry a high concentration of organic peroxides. The degradation risk imposed by the transition metals can be mitigated by incorporating chelating agents, such as EDTA, in the formulation.

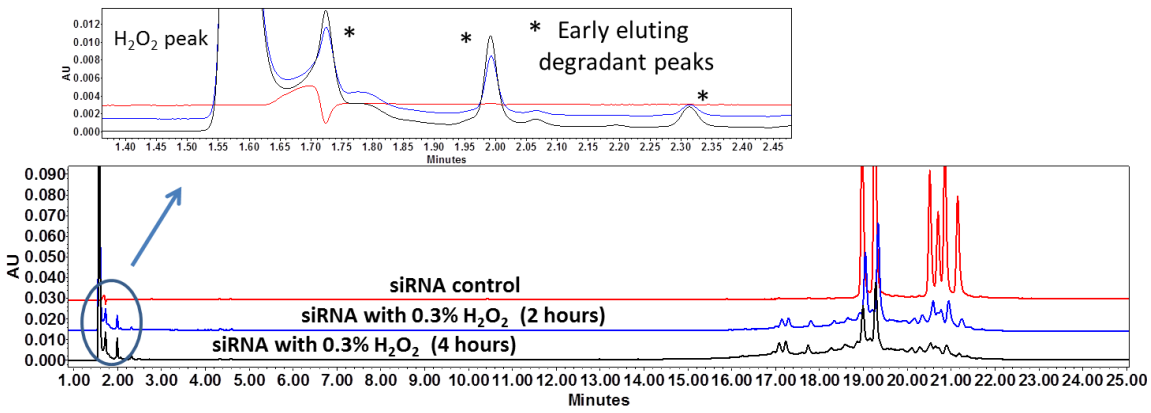

Figure 5.4 Overlaid chromatograms of the stressed siRNA with H_2O_2 and the control UHPLC Conditions: Same as in Figure 5.2.

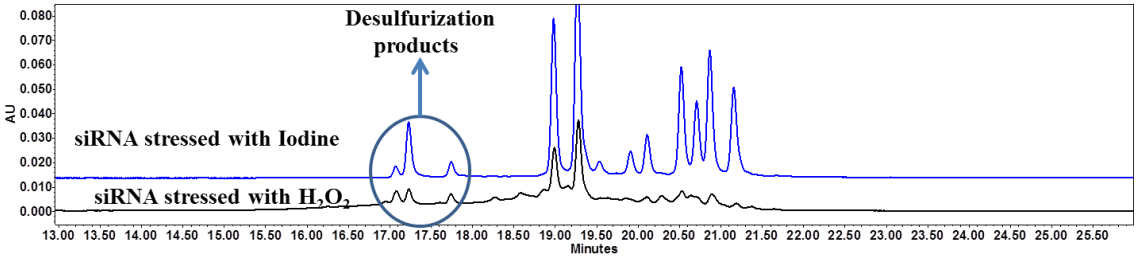

Figure 5.5 Overlaid chromatograms of the stressed siRNA with H_2O_2 or molecular iodine. UHPLC Conditions: Same as in Figure 5.2.

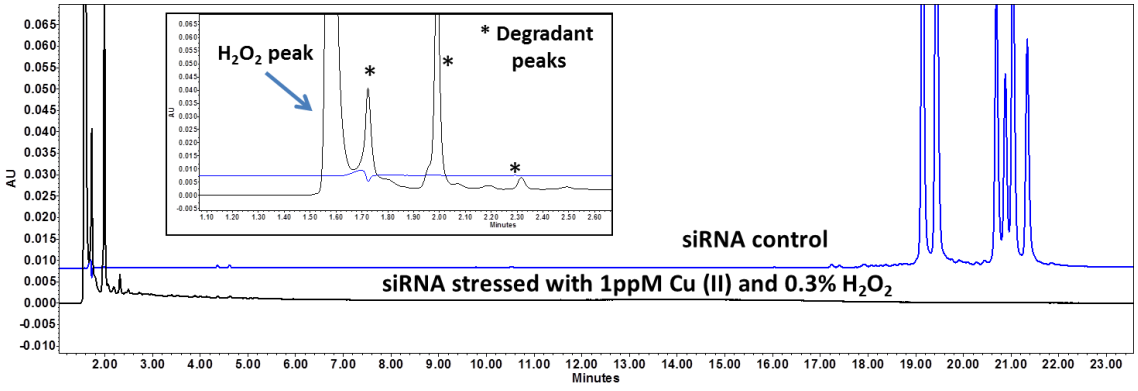

Figure 5.6 Overlaid chromatograms of the stressed siRNA with Cu(II)/H_2O_2 and the control. UHPLC Conditions: Same as in Figure 5.2.

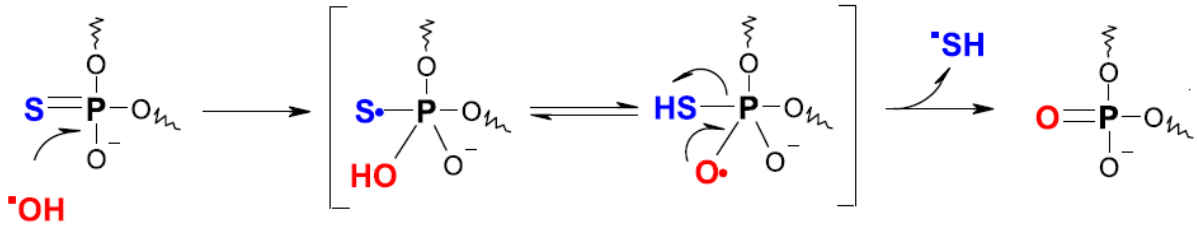

Scheme 5.3 Proposed mechanism for desulfurization of phosphorothioate linkage induced by hydroxyl radical. [17]

5.3.3 Chemical stability under oxidative stress with radical initiator

In addition to peroxide stress, forced stress testing with a radical initiator was also performed for siRNA. 4, 4′-Azobis (4-cyanovaleric acid) (ACVA) is an azonitrile radical initiator that can thermally decompose to release nitrogen, leaving two cyanoalkyl radicals that can rapidly react with oxygen to form peroxy radical. (Scheme 5.4) [19] Peroxy radical promotes oxidation via abstraction of a hydrogen atom from C-H bonds with low bond dissociation energy, creating a drug molecule radical that can facilely react with molecular oxygen. Figure 5.7 shows overlaid chromatograms of siRNA stressed with ACVA versus molecular iodine. The oxidation products induced by ACVA are exclusively desulfurization products, as the chromatogram (e.g., the retention time of the peaks) is identical with that with molecular iodine. ACVA appears to be more selective in forming desulfurization product than hydrogen peroxide. The oxidative degradation pathways mediated by ACVA is different from that by hydrogen peroxide. While the hydrogen peroxide promotes both desulfurization reaction and strand scission, the ACVA system exclusively invokes the desulfurization reaction.

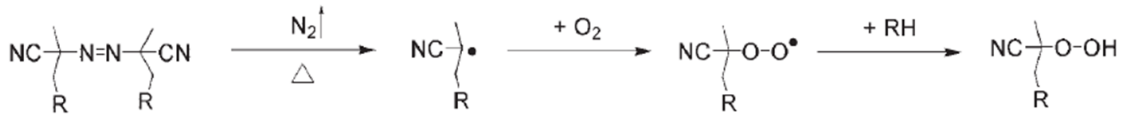

R= CH_2COOH

Scheme 5.4 Thermal decomposition of ACVA to form peroxy radical[19]

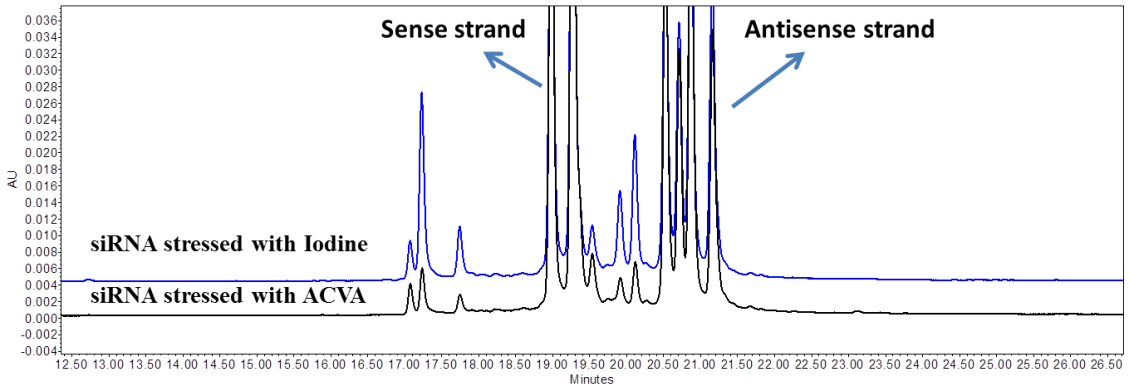

Figure 5.7 Overlaid chromatograms of siRNA samples stressed with ACVA and molecular Iodine. UHPLC conditions: Same as in Figure 5.2.

5.4 Conclusions

Forced stress testing can be used to probe the main degradation pathway of the molecule and provide a rational design for drug product through proper selection of excipients. The stress testing of a chemically modified siRNA showed that the molecule is stable at neutral pH. In contrast, significant hydrolytic degradation was observed under extreme acidic or basic conditions. HPLC analysis showed that the base-stressed sample formed more early eluting peaks than the acid-stressed one. The studies also showed that

siRNA is oxidatively labile with respect to hydrogen peroxide. Desulfurization products were detected in the peroxide-stressed sample. In addition, the hydrogen peroxide incurred siRNA strand scission, as evidenced by the formation of early eluting peaks. Transition metals, such as copper (II), promote the formation of hydroxyl radical, significantly increasing the oxidative degradation of siRNA. A radical initiator, such as ACVA, is a highly selective oxidant and preferentially forms desulfurization products with siRNA. Given the intrinsic stability attributes of siRNA under various stress conditions, excipient selection should avoid the use of certain polymers (e.g., Polyvinylpyrrolidone (PVP) and PEG) and surfactants (Tween 80) that contain a high level of peroxides. An elevated level of peroxide in PEG and Tween 80 is attributed to oxidative degradation of the excipients during storage. In the case of PVP, residual peroxide is the product of a radical-mediated polymerization process used for making the polymer. Control of residual transition metal is also important in the raw material. The degradation risk posed by transition metals can be mitigated by incorporating chelating agents, such as EDTA, in the formulation.

List of References

1. R. Markham, J. D. Smith, The structure of ribonucleic acids, 1. Cyclic nucleotides produced by ribonuclease and by alkaline hydrolysis, Biochem. J 52(4) (1952) 552-557.

2. D.M. Zhou, K. Taira, the Hydrolysis of RNA: From Theoretical Calculations to the Hammerhead Ribozyme-Mediated Cleavage of RNA, Chem. Rev. 98(1998) 991-1026.

3. Y.L. Chiu, T.M. Rana, siRNA function in RNAi: A chemical modification analysis, RNA (2003), 9:1034–1048.

4. S. Gao, F. Dagnaes-Hansen, E.J.B. Nielsen, J. Wengel, F. Besenbacher, K.A. Howard, J. Kjems, The Effect of Chemical Modification and Nanoparticle Formulation on Stability and Biodistribution of siRNA in Mice, Mol. Ther. 17(7) (2009) 1225–1233.

5. K.C. Waterman, R.C. Adami, Accelerated aging: prediction of chemical stability of pharmaceuticals, Int. J. Pharm. 293 (2005) 101-25.

6. K.C. Waterman, A.J. Carella, M.J. Gumkowski, Improved protocol and data analysis for accelerated shelf-life estimation of solid dosage forms, Pharm. Res. 24 (2007)780-790.

7. C. J. Calvitt, D.S. Levin, B.T. Shepperd, C.J. Gruenloh, Chemistry at the 20 Position of Constituent Nucleotides Controls Degradation Pathways of Highly Modified Oligonucleotide Molecules, Oligonucleotides, 20(5) (2010) 239-251.

8. S.W. Baertschi, P.J. Jansen, K.M. Alsante, "Stress testing: a predictive tool" *Pharmaceutical Stress Testing: Predicting Drug Degradation*, edited by S.W. Baertschi, K.M. Alsante, R.A. Reed, Informa Healthcare, London (UK), 2011, pp10-48.

9.P. Harmon, G. Boccardi, "Oxidative susceptibility testing" *Pharmaceutical Stress Testing: Predicting Drug Degradation*, edited by S.W. Baertschi, K.M. Alsante, R.A. Reed, Informa Healthcare, London (UK), 2011, pp168-191.

10. L. Li, T. Leone, J.P. Foley, C.J. Welch, Separation of siRNA stereoisomers using reversed phase ion-pairing chromatography, J Chromatogr. A 1500 (2017) 84-88.

11. Y.F. Li, R. Breaker, Kinetic of RNA degradation by specific base catalysis of transesterification involving the 2'-hydroxyl group, J. Am. Chem. Soc. 121 (1999) 5364-5372.

12. M. Oivanen, S. Kuusela, H. Lonnberg, Kinetics and mechanisms for the cleavage and isomerization of the phosphodiester bonds of RNA by BrØnsted acids and bases. Chem. Rev. 98 (1998) 961-990.

13. Q.M. Kong, C.L.G. Lin, Oxidative damage to RNA: mechanisms, consequences, and diseases. Cell Mol. Life Sci. 67(11) (2010) 1817–1829.

14. T. Hofer, C. Badouard, E. Bajak, J.L. Ravanat, A. Mattsson, L.A. Cotgreave, Hydrogen peroxide causes greater oxidation in cellular RNA than in DNA, Biol. Chem., 386 (2005) 333–337.

15. Y.M. Wu, J. Levons, A.S. Narang, K. Raghavan, V.M. Rao, Reactive Impurities in excipients: profiling, identification and mitigation of drug–excipient Incompatibility, AAPS Pharm. Sci. Tech. 12(4) 2011 1248-1263.

16. T.K. Wyrzykiewicz, D.L. Cole, Sequencing of oligonucleotide phosphorothioates based on solid-supported desulfurization, Nucleic Acids Research. 22(13) (1994)2667-69.

17. L.M. Wu, D.E. White, C. Ye, F.G. Vogt, G.J. Terloth, H. Matsuhashi, Desulfurization of phosphorothioate oligonucleotides via the sulfur-by-oxygen replacement induced by the hydroxyl radical during negative electrospray ionization mass spectrometry, J. Mass. Spec. 47 (2012) 836-844.

18. C.J. Burrows, J.G. Muller, Oxidative Nucleobase Modifications Leading to Strand Scission, Chem. Rev. 98 (1998) 1109-1151.

19. E.D. Nelson, P.A. Harmon, R.C. Szymanik, M. G. Teresk, L. Li, R. A. Seburg, R. A. Reed, Evaluation of Solution Oxygenation Requirements for Azonitrile-Based Oxidative Forced Degradation Studies of Pharmaceutical Compounds, J Pharm. Sci. 95(7) (2006) 1527-1539.

Chapter 6 Conclusions and future research on the analytical characterization of LNPs

6.1 Conclusions

siRNA-based therapy has harnessed powerful molecular machinery and significantly expanded the target space for drug discovery and development, potentially offering new treatments for diseases that cannot be addressed with existing classes of drugs. The systemic delivery of siRNA to target organs or tissues remains a key challenge due to various physical and chemical barriers, which can deactivate siRNA before it reaches the site of action in a cell's cytoplasm. Lipid nanoparticle (LNP) delivery technology represents the most advanced platform, with many development candidates being tested in human clinical trials. An LNP system is a complex nanoscale assembly, consisting of siRNA, cationic and neutral lipids, including PEGylated lipid to maintain physical stability of the nanocarriers. Developing a stable and high-quality LNP formulation not only requires a fundamental understanding of engineering controls during the manufacturing process, but it also relies on advanced analytical separation tools to ensure that the key constituents in LNPs maintain their potency and purity during an intended shelf-life. Motivated by the significant interest in advancing siRNA therapeutics into the marketplace, this research project set out to develop novel chromatographic methods capable of separating and quantitating siRNA, lipids, and their potential breakdown products due to oxidation or hydrolysis.

Synthetic siRNAs often incorporate chemically modified nucleotides to improve *in vivo* serum stability, with the replacement of the phosphodiester linkage by a phosphorothioate moiety being a common strategy. Desulfurization of phosphorothioate-containing siRNAs compromises the chemical stability of siRNA therapeutics, and it is

therefore important to develop a selective separation method to monitor the desulfurization of the phosphorothioate-containing siRNAs. Here a reversed-phase ion-pairing chromatography method was developed for a baseline separation of multiple stereoisomers of a double-stranded siRNA. With acetonitrile (ACN) as the organic modifier, triethylammonium acetate (TEAA) provided a superior separation efficiency and selectivity than its structural ion-pair reagent analogs, including ethylammonium acetate (EAA), diethylammonium acetate (DEAA) and tetramethylammonium acetate (TMAA). Solution state DSC analysis of siRNA suggested that ACN can effectively disrupt the self-association of siRNA double strands, which appeared to be important to stereoisomer separation. This explains why ACN is more effective in stereoisomer separation than other organic modifiers, such as methanol. Other chromatographic parameters relevant to diastereomer separation included the chemistry of the stationary phase and the column temperature. The upper temperature limit of the BEH C18 column (80 ^{o}C) was higher than that of the BEH phenyl- and cyano-derivatized silica columns, and was an essential condition for the baseline resolution of stereoisomers of the denatured siRNA. The optimized separation method was applied to a siRNA sample deliberately stressed with an iodine solution to induce desulfurization, where up to six degradation products were resolved from the parent siRNA stereoisomers.

In addition to the analytical separation of siRNA stereoisomers and their potential oxidation products, we also explored ion-pair reversed phase UHPLC for the simultaneous separation of siRNA and phospholipids in the context of an LNP delivery system, an overlooked need that was previously unaddressed due to the challenge of the significant differences in the physical and chemical properties of siRNA and

phospholipids. To reduce the retention gap between these two classes of biomolecules, we focused our research efforts on identifying ion-pair reagents that can enhance the retention of siRNA, as well as a separation column capable of promoting both hydrophobic interactions and π- π interactions between siRNA and the stationary phase. With BEH phenyl as the stationary phase and ACN as the organic modifier in the mobile phase, dibutylammonium acetate (DBAA) provided a superior separation efficiency and selectivity than its structural analogs, such as TEAA, DPAA, and DAAA. Column temperature had a significant impact on the peak shape of double-stranded siRNA, and its selection depended on the on-column melting temperature of the siRNA duplex. The method was successfully applied to the separation and analysis of an experimental LNP formulation, demonstrating satisfactory selectivity for both siRNA, key constituents in lipid vehicles and their respective degradation products.

Lastly, a systematic forced stress test was conducted to probe the intrinsic chemical stability of siRNA model system using the ion-pair reverse phase UHPLC separation developed in Chapter 3. Forced stress testing is a powerful tool that can predict a stability problem during formulation development, assist analytical methods, and, by providing a relevant sample matrix, elucidate degradation pathways for a new chemical candidate, thus providing a scientific framework for the rational selection of key functional excipients. The stress testing of a model siRNA system showed that the molecule is stable with respect to hydrolysis at neutral pH. In contrast, siRNA is very oxidatively labile with respect to hydrogen peroxide, where low-level hydroxyl radical is likely the cause for drug degradation. Desulfurization and phosphodiester strand scission are likely the main degradation pathways based on retention behavior of the degradants,

as well as by comparison with the iodine-induced desulfurization products. Transition metals, such as copper (II), promote the formation of hydroxyl radical, significantly increasing the oxidative degradation of siRNA. Finally, our studies showed that radical initiator, capable of creating peroxy radicals, is a highly selective oxidant that can preferentially form desulfurization products. The instabilities identified in the stress testing suggested that the excipients selected should not be comprised of certain polymers and surfactants that contain a high level of peroxides. Furthermore, the degradation risk posed by transition metals can be mitigated by incorporating chelating agents, such as EDTA, in the formulation.

6.2 Future research

Stereoisomer separation remains a key challenge as the number of sulfur modifications is increased to promote greater stability. Preliminary work on the separation of additional siRNAs containing greater than two chiral centers per strand showed limited resolution for the stereoisomers using the denaturing ion-pairing UHPLC method developed in Chapter 3. Future work should explore alternative separation modes, including ion-exchange chromatography or mixed-mode chromatography that incorporates both ion-exchange and ion-pair separation modes.

Another potential research area is the direct analysis of free siRNA and the intact lipid nanoparticle using columns where the nanoparticles can interact reversibly with the stationary phase, i.e., without irreversible adsorption. Preliminary work using ProSwift weak cationic exchange (WAX) monolithic column showed some promising results. Figure 6.1 shows the chromatographic traces of the intact lipid nanoparticles and free siRNA. The HPLC analysis requires no sample preparation, and the LNP suspension

formulation can be directly injected into the column. The method could be extremely useful in supporting LNP formulation developmental efforts, where the determination of encapsulation efficiency of siRNA in LNP is a critical quality attribute for quality control.

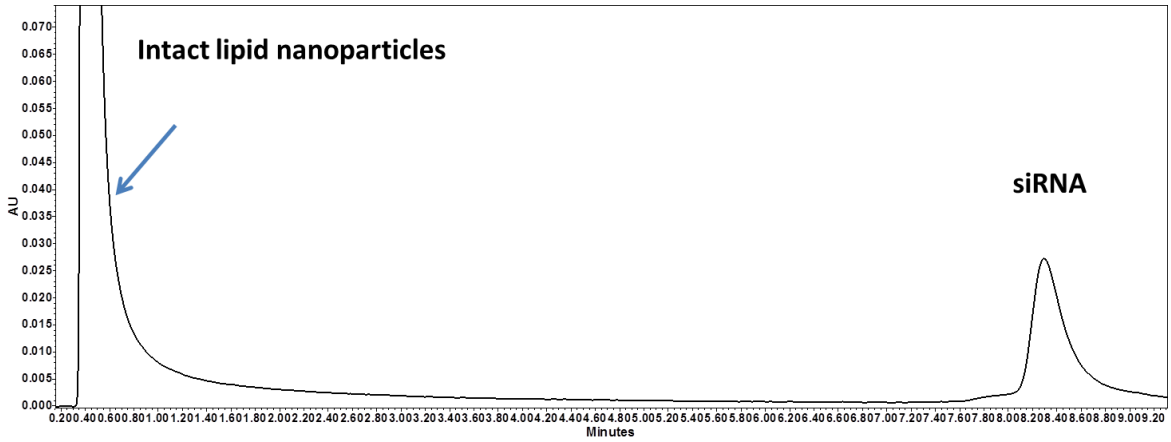

Figure 6.1 Direct analysis of a LNP formulation: chromatographic traces of intact nanoparticles and free siRNA.

Conditions: Proswift Weak Cationic Exchange column (50 x 4.6 mm); Oven temperature: 30 ^{o}C; Mobile phase A consisted of 10 mM tris buffer (pH 7.2) in water, and mobile phase B was a mixture of 10 mM tris buffer and 100 mM NaCl (pH 7.2). The gradient method was run from 65% to 100% B in 10 minutes, followed by an isocratic hold at 100% B for 3 minutes. The flow rate was 0.2 mL/minute and the injection volume was 5 µL, with UV absorbance detection at 210 nm.

Finally, future work in this area should focus on incorporating mass spectrometry as alternative detection to UV absorbance in order to fully characterize the main degradation products observed in the stress testing presented in Chapter 5.

VITAE

Li Li received her Bachelors of Science and Masters of Science degrees in Chemistry from Anhui University in 1992 and University of Sciences and Technology of China in 1995, respectively. After graduation, she moved to the US in 1996, and there she completed her MS degree in Biochemistry from the University of Louisville in 1999. She started her industry career in 2000 and currently she works in the Pharmaceutical Sciences and Clinical Supply - Analytical Sciences group as a Principal Scientist. She is responsible for developing predictive in vitro methodology and designing stability studies for over 20 Merck development candidates ranging from pre-clinical to Phase III. She is also leading the analytical effort at Merck to develop an enhanced understanding of polymer structure-performance relationship for oral and parenteral delivery of a range of development candidates with diverse physical and chemical properties.

In the fall of 2008, Li began her graduate study towards a Ph.D. as a part-time student at Drexel University under the direction of Dr. Joe P. Foley. During her Ph.D. studies at Drexel, she has had portions of her research published in the Journal of Chromatography A. She also completed a second manuscript for submission to the Journal of Chromatography A.